Insights into Imaging

Education and strategies in European radiology

ESGAR 2014 Book of Abstracts / Volume 5, 2014 / Supplement 2 / 2014-04-11

ESGAR 2014 / June 18 – 21 / Salzburg, Austria
25th Annual Meeting and Postgraduate Course

European Society
ESGAR
Gastrointestinal and Abdominal Radiology

JUNE 18 - 21

ESGAR 2014

SALZBURG
AUSTRIA

European Society of Gastrointestinal and Abdominal Radiology

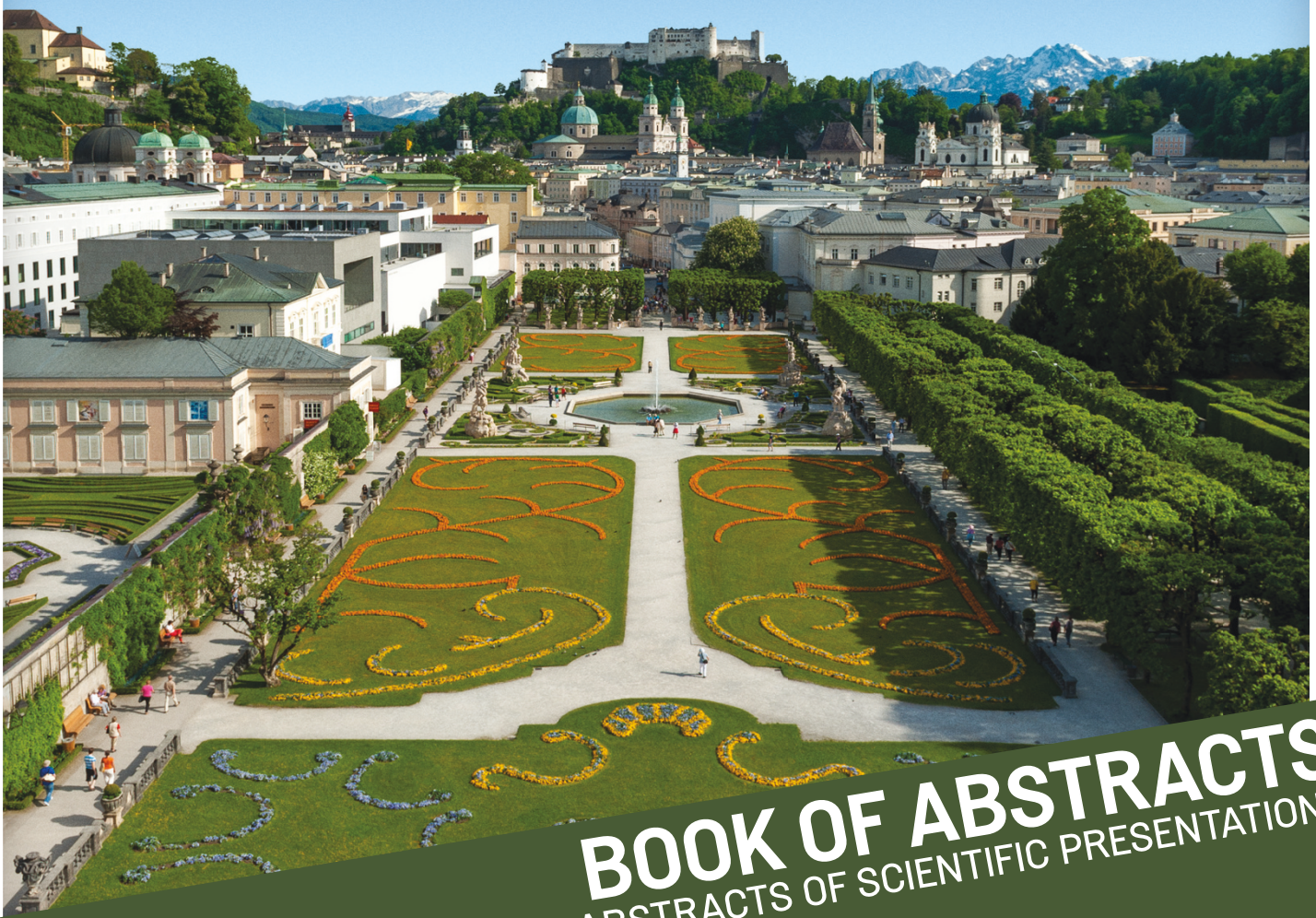

BOOK OF ABSTRACTS

INCLUDES ABSTRACTS OF SCIENTIFIC PRESENTATIONS

IMPORTANT ADDRESSES

ORGANISING SECRETARIAT

Central ESGAR Office
Neutorgasse 9
AT – 1010 Vienna, Austria
Phone: +43 1 535 89 27
Fax: +43 1 535 70 37
E-Mail: office@esgar.org

WEBSITE

www.esgar.org

EXHIBITION MANAGEMENT

MAW – Medizinische Ausstellungsgesellschaft
Freyung 6
AT – 1010 Vienna, Austria
Phone: +43 1 536 63 -34 or -35
Fax: +43 1 535 60 16
E-Mail: maw@media.co.at

CONFERENCE VENUE

Salzburg Congress
Auerspergstraße 6
AT – 5020 Salzburg, Austria

CONFERENCE VENUE

CME CREDITS

The ‘ESGAR - THE EUROPEAN SOCIETY OF GASTRO-INTESTINAL AND ABDOMINAL RADIOLOGY’ (or) ‘ESGAR 2014 - 25th ESGAR Annual Meeting’ is accredited by the European Accreditation Council for Continuing Medical Education (EACCME) to provide the following CME activity for medical specialists. The EACCME is an institution of the European Union of Medical Specialists (UEMS), www.uems.net.

The ‘ESGAR 2014 - 25th ESGAR Annual Meeting’ is designated for a maximum of (or ‘for up to’) 24 hours of European external CME credits. Each medical specialist should claim only those hours of credit that he/she actually spent in the educational activity.

Date of publishing: May 2014

JOINT SESSIONS

EASL EUROPEAN ASSOCIATION FOR THE STUDY OF THE LIVER | ENDORSED EVENT

The Final Programme of ESGAR 2014 is available on the ESGAR website www.esgar.org

DOI: 10.1007/s13244-014-0341-5

TABLE OF CONTENTS

European Society ESGAR Gastrointestinal and Abdominal Radiology

ESGAR EXECUTIVE COMMITTEE

PRESIDENT
L. Martí-Bonmatí (Valencia/ES)

PRESIDENT-ELECT
C. Matos (Brussels/BE)

VICE PRESIDENT
S. Halligan (London/UK)

SECRETARY
A. Palkó (Szeged/HU)

TREASURER
S. Jackson (Plymouth/UK)

PAST PRESIDENT
F. Caseiro Alves (Coimbra/PT)

EDUCATION COMMITTEE
R.G.H. Beets-Tan (Maastricht/NL)

MEMBERSHIP COMMITTEE
T. Helmberger (Munich/DE)

WORKSHOP COMMITTEE
A. Laghi (Latina/IT)

MEETING PRESIDENT
G. Mostbeck (Vienna/AT)

PRE-MEETING PRESIDENT
Y. Menu (Paris/FR)

PRE-PRE-MEETING PRESIDENT
V. Valek (Brno-Bohunice/CZ)

PAST MEETING PRESIDENT
C. Ayuso (Barcelona/ES)

MEMBERS AT LARGE
P. Prassopoulos (Alexandroupolis/GR)
J. Stoker (Amsterdam/NL)
M. Zins (Paris/FR)

ESGAR PROGRAMME COMMITTEE

CHAIRMAN
F. Caseiro Alves (Coimbra/PT)

MEMBERS:
C. Ayuso (Barcelona/ES)
R.G.H. Beets-Tan (Maastricht/NL)
S. Halligan (London/UK)
T. Helmberger (Munich/DE)
S. Jackson (Plymouth/UK)
A. Laghi (Latina/IT)
L. Martí-Bonmatí (Valencia/ES)
C. Matos (Brussels/BE)
Y. Menu (Paris/FR)
G. Mostbeck (Vienna/AT)
A. Palkó (Szeged/HU)
P. Prassopoulos (Alexandroupolis/GR)
J. Stoker (Amsterdam/NL)
V. Valek (Brno-Bohunice/CZ)
M. Zins (Paris/FR)

ESGAR 2014 MEETING PRESIDENT

Prof. Gerhard Mostbeck
Wilhelminenspital
Department of Diagnostic and Interventional Radiology
Montleartstr. 37
AT – 1160 Vienna, Austria

LOCAL ORGANISING COMMITTEE

A. Ba-Ssalamah (Vienna/AT)
G. Böhm (Linz/AT)
K.A. Hausegger (Klagenfurt/AT)
K. Hergan (Salzburg/AT)
W. Jaschke (Innsbruck/AT)
A. Maier (Vienna/AT)
T. Mang (Vienna/AT)
C. Neumann (Vienna/AT)
W. Schima (Vienna/AT)
E. Schober (Vienna/AT)
H. Schöllnast (Graz/AT)
M. Uggowitzer (Leoben/AT)

This edition of the ESGAR 2014 Book of Abstracts was language edited by:

ABSTRACT EDITOR

S. Jackson (Plymouth/UK)

ABSTRACT REVIEWING PANEL

D. Akata (Ankara/TR)
O. Akhan (Ankara/TR)
C. Ayuso (Barcelona/ES)
M.A. Bali (Brussels/BE)
R.G.H. Beets-Tan (Maastricht/NL)
P. Boraschi (Pisa/IT)
R. Bouzas (Vigo/ES)
G. Brancatelli (Palermo/IT)
D.J. Breen (Southampton/UK)
C. Bru (Barcelona/ES)
F. Caseiro Alves (Coimbra/PT)
C. Catalano (Rome/IT)
J. Cazejust (Paris/FR)
N. Courcoutsakis (Alexandroupolis/GR)
E. Delabrousse (Besancon/FR)
R.F. Dondelinger (Liège/BE)
M. D'Onofrio (Verona/IT)
N. Elmas (Izmir/TR)
H. Fenlon (Dublin/IE)
B. Fox (Plymouth/UK)
A.H. Freeman (Cambridge/UK)
A. Furlan (Pittsburgh, PA/US)
S. Gourtsoyianni (London/UK)
L. Guimaraes (Porto/PT)
J.A. Guthrie (Leeds/UK)
S. Halligan (London/UK)
T. Helmberger (Munich/DE)
P. Huppert (Darmstadt/DE)
F. Iafrate (Rome/IT)
S. Jackson (Plymouth/UK)
M. Karcaaltincaba (Ankara/TR)
C. Kay (Bradford/UK)
S.H. Kim (Busan/KR)
H.-U. Laasch (Manchester/UK)
A. Laghi (Latina/IT)
J.S. Lameris (Amsterdam/NL)
E. Leen (London/UK)
P. Lefere (Roeselare/BE)
M. Lewin (Villejuif/FR)
J.H. Lim (Seoul/KR)
D.J. Lomas (Cambridge/UK)
O. Lucidarme (Paris/FR)
M. Maas (Maastricht/NL)
F. Maccioni (Rome/IT)
M. Maher (Wilton/IE)
D.E. Malone (Dublin/IE)
R. Manfredi (Verona/IT)
T. Mang (Vienna/AT)
D. Marin (Durham, NC/US)
B. Marincek (Cleveland, OH/US)
L. Martí-Bonmatí (Valencia/ES)
D.F. Martin (Manchester/UK)
G.F. Maskell (Truro/UK)
C. Matos (Brussels/BE)
Y. Menu (Paris/FR)
G. Morana (Treviso/IT)
M. Morrin (Dublin/IE)
G. Mostbeck (Vienna/AT)
E. Neri (Pisa/IT)
B. Op De Beeck (Edegem/BE)
A. Palkó (Szeged/HU)
P.L. Pereira (Heilbronn/DE)
P. Pokieser (Vienna/AT)
P. Prassopoulos (Alexandroupolis/GR)
M. Puckett (Torquay/UK)
J. Puig Domingo (Sabadell/ES)
C. Ridereau-Zins (Angers/FR)
G.A. Rollandi (Genova/IT)
L.H. Ros Mendoza (Zaragoza/ES)
E.J. Rummeny (Munich/DE)
W. Schima (Vienna/AT)
S. Schmidt Kobbe (Lausanne/CH)
O. Seror (Bondy/FR)
P. Sidhu (London/UK)
S. Skehan (Dublin/IE)
S. Somers (Dundas, ON/CA)
M. Staunton (Cork/IE)
J. Stoker (Amsterdam/NL)
C. Stoupis (Maennedorf/CH)
Z. Tarjan (Stevenage/UK)
S.A. Taylor (London/UK)
S. Terraz (Geneva/CH)
C. Triantopoulou (Athens/GR)
V. Valek (Brno-Bohunice/CZ)
D. Vanbeckevoort (Leuven/BE)
V. Vilgrain (Clichy/FR)
M.-P. Vullierme (Clichy/FR)
D. Weishaupt (Zurich/CH)
S.D. Yarmenitis (Athens/GR)
C.J. Zech (Basel/CH)
M. Zins (Paris/FR)

E-POSTER JURY

D. Akata (Ankara/TR)
O. Akhan (Ankara/TR)
A.J. Aschoff (Kempten/DE)
C. Ayuso (Barcelona/ES)
M.A. Bali (Brussels/BE)
R.G.H. Beets-Tan (Maastricht/NL)
P. Boraschi (Pisa/IT)
R. Bouzas (Vigo/ES)
G. Brancatelli (Palermo/IT)
F. Caseiro Alves (Coimbra/PT)
C. Catalano (Rome/IT)
J. Cazejust (Paris/FR)
N. Courcoutsakis (Alexandroupolis/GR)
L. Crocetti (Pisa/IT)
E. Delabrousse (Besancon/FR)
M.C. Della Pina (Pisa/IT)
R.F. Dondelinger (Liège/BE)
M. D'Onofrio (Verona/IT)
N. Elmas (Izmir/TR)
B. Fox (Plymouth/UK)
A.H. Freeman (Cambridge/UK)
A. Furlan (Pittsburgh, PA/US)
S. Gourtsoyianni (London/UK)
J.A. Guthrie (Leeds/UK)
S. Halligan (London/UK)
T. Helmberger (Munich/DE)
F. Iafrate (Rome/IT)
S. Jackson (Plymouth/UK)
M. Karcaaltincaba (Ankara/TR)
C. Kay (Bradford/UK)
S.H. Kim (Busan/KR)
A. Laghi (Latina/IT)
J.S. Lameris (Amsterdam/NL)
T. Lauenstein (Essen/DE)
P. Lefere (Roeselare/BE)
M. Lewin (Villejuif/FR)
D.J. Lomas (Cambridge/UK)
O. Lucidarme (Paris/FR)
M. Maas (Maastricht/NL)
F. Maccioni (Rome/IT)
A. Madureira (Porto/PT)
M. Maher (Wilton/IE)
D.E. Malone (Dublin/IE)
R. Manfredi (Verona/IT)
T. Mang (Vienna/AT)
D. Marin (Durham, NC/US)
B. Marincek (Cleveland, OH/US)
L. Matí-Bonmatí (Valencia/ES)
D.F. Martin (Manchester/UK)
G.F. Maskell (Truro/UK)
C. Matos (Brussels/BE)
Y. Menu (Paris/FR)
G. Morana (Treviso/IT)
M. Morrin (Dublin/IE)
G. Mostbeck (Vienna/AT)
E. Neri (Pisa/IT)
B. Op de Beeck (Edegem/BE)
A. Palkó (Szeged/HU)
N. Papanikolaou (Heraklion/GR)
P.L. Pereira (Heilbronn/DE)
P. Pokieser (Vienna/AT)
P. Prassopoulos (Alexandroupolis/GR)
M. Puckett (Torquay/UK)
C. Ridereau-Zins (Angers/FR)
L.H. Ros-Mendoza (Zaragoza/ES)
A. Ruiz (Paris/FR)
E.J. Rummeny (Munich/DE)
W. Schima (Vienna/AT)
S. Schmidt Kobbe (Lausanne/CH)
P. Sidhu (London/UK)
S. Skehan (Dublin/IE)
S. Somers (Dundas, ON/CA)
M. Staunton (Cork/IE)
J. Stoker (Amsterdam/NL)
C. Stoupis (Maennedorf/CH)
Z. Tarjan (Stevenage/UK)
S.A. Taylor (London/UK)
C. Triantopoulou (Athens/GR)
V. Valek (Brno-Bohunice/CZ)
D. Vanbeckevoort (Leuven/BE)
J. Venancio (Lisbon/PT)
V. Vilgrain (Clichy/FR)
M.-P. Vullierme (Clichy/FR)
D. Weishaupt (Zurich/CH)
S.D. Yarmenitis (Athens/GR)
C.J. Zech (Basel/CH)
M. Zins (Paris/FR)


European Society
ESGAR
Gastrointestinal and Abdominal Radiology

11:00 - 12:30 **Europa Hall**

Scientific Session 1

Pancreas: ductal adenocarcinoma

SS 1.01

Appraisal of NCCN and ESMO guidelines for the diagnosis and staging of pancreatic adenocarcinoma

Y.M. Purcell[1], A.M. Cahalane[1], S.H. Mcevoy[1], A.G. Carroll[1], E.R. Ryan[1], E. O'Toole[1], M. Staunton[2], D.E. Malone[1]; [1]Dublin/IE, [2]Cork/IE

Purpose: This study was performed to establish the relative validity of these guidelines using evidence-based medicine (EBM) methodology.

Material and Methods: An "Answerable Question" was designed and a literature search was performed using EBM technique. Two sets of guidelines and a single centre's recommendations (not a defined guideline) were retrieved. The National Comprehensive Cancer Network (NCCN) 2014 guidelines and the European Society of Medical Oncology (ESMO) 2012 guidelines were appraised. To assess the methodological rigour and transparency used in developing the guidelines, the Appraisal of Guidelines for Research and Evaluation (AGREE) II instrument was used. The domains were: Scope and Purpose, Stakeholder Involvement, Rigour of Development, Clarity of Presentation, Applicability and Editorial Independence. Three radiologists, under the guidance of the Research and Evaluation Manager of the Irish National Cancer Control Program, compiled a consensus of their results.

Results: The AGREE II scaled domain scores were calculated as follows: (obtained score-minimum possible score)/(maximum possible score - minimum possible score) x 100. The NCCN guidelines scored the highest at 55%. The ESMO guidelines scored 38%. Both guidelines were recommended for use but with modifications. The NCCN guidelines would be improved by clearer search strategy and inclusion of corresponding levels of evidence.

Conclusion: The methodological rigour and transparency of leading guidelines varies as described. Neither guideline is perfect. If guidelines disagree, the NCCN guidelines have the highest validity by EBM criteria.

SS 1.02

Assessment of extra-pancreatic perineural invasion in resectable cancer of pancreatic head with pathomorphological correlation

E. Kasatkina, V. Lyadov, I. Shrainer, S. Bogomazova, E. Mershina, V. Sinitsyn; Moscow/RU

Purpose: As the retroperitoneal soft tissue margin can rarely be re-resected in cases of positive frozen-section biopsy, the aim of study was to find whether CT is capable of detecting extrapancreatic perineural invasion (EPNI) pre-operatively in resectable adenocarcinoma of pancreatic head.

Material and Methods: CT-examinations of 38 patients with resectable PC, who underwent Whipple-procedure were retrospectively evaluated by two independent observers blinded to results of histological reports. Directly after surgery, SMA-margin was marked by operating surgeon for pathohistological evaluation. EPNI was identified as confluent tissue of similar attenuation to primary PC extending along known neural-plexuses pathways. In our study, PLX-II (area along inferior posterior pancreatoduodenal artery, IPDA, and jejunal trunk extending up to superior mesenteric artery plexus) was assessed as this area is more susceptible for EPNI. Two patterns of peripancreatic spread were established: confluent tumor spread (Pattern1) and infiltration (Pattern2) along known pathway.

Results: EPNI was found in 26 patients, all positive cases were correctly diagnosed on preoperative-CT-scans by both observers. Pattern1 was found in 16 patients, Pattern2 in 10 patients. Kappa-value was 0.63, which represents good agreement between two observers. There were no false-negative results, seven false-positive results were present in Pattern2 and histologically were reported as fibrosis/inflammatory cells. Sensitivity of MDCT was 99%, specificity–59%, diagnostic accuracy–81%.

Conclusion: MDCT provides sufficient information to detect PPC-II invasion on pre-operative CT-series in patients with resectable pancreatic head cancer. It might be overestimated when Pattern2 is present.

SS 1.03

4-D imaging with dual energy perfusion-CT of small pancreatic carcinomas

F. Fritz, M. Klauss, W. Stiller, G. Pahn, M. Kieser, T. Hackert, H.U. Kauczor, L. Grenacher; Heidelberg/DE

Purpose: Identification of small and isodense tumors in the pancreatic parenchyma is still a diagnostic challenge; functional imaging techniques may have the potential to overcome today's limitations; to evaluate a feasibility study for dual energy perfusion-CT (DE-CT) in patients with small pancreatic carcinomas.

Material and Methods: 25 patients with pancreatic cancer were examined with a multidetector-CT (Siemens Definition Flash) using a dynamic perfusion protocol of 34 dual-energy acquisitions every 1.5s and a range of 1.5 cm (80 ml of iodinated contrast (370 mg/ml, 5ml/s)). Analysis of the perfusion images were performed with a multimodality workplace and the Body-PCT-tool (MMWP, Siemens Medical Solutions) using the Patlak-model. Color-coded parameter maps have been generated and perfusion, permeability and blood volume values were calculated.

Results: All 25 carcinomas could clearly differentiated from normal tissue in the color-coded parameter maps; n= 5/25 (20%) carcinomas appeared isodense. Using the 80 kV(p)-data mean perfusion, permeability and blood volume of malignant tissue was significantly lower with 27.23 ± 21.89 ml/100 ml/min, 42.96 ± 21.91 x 0.5 ml/100 ml/min and 38.64 ± 20.21 ml/100 ml than healthy tissue with 91,12 ± 19,93 ml/100 ml/min, 74.78 ± 15.88 x 0.5 ml/100 ml/min and 119.52 ± 52.76 ml/100 ml ($p< 0.0001$). Using the weighted-average 120 kV(p)-equivalent perfusion-, permeability- and blood volume-values determined from DE image data standard-deviation is distinctly smaller.

Conclusion: 4D-imaging with DE-CT is feasible in pancreatic carcinomas and could be helpful for defining the carcinomas even though they are not visible in contrast-enhanced CT.

SS 1.04

Pancreatic neuroendocrine tumor (PNET): staging accuracy and diagnostic performance of MDCT for differentiate atypical PNET from pancreatic adenocarcinoma

J.H. Kim, H.W. Eun, J.M. Lee, J.K. Han, B.I. Choi; Seoul/KR

Purpose: Our study investigated staging accuracy of MDCT for pancreatic neuroendocrine tumor (PNET). We also assessed diagnostic performance to differentiate atypical PNET from pancreatic adenocarcinoma.

Material and Methods: Our study consisted of 109 patients with surgically proven PNET (T1=33, T2=37, T3=39, N1=20; NETG1=66, NETG2=31, NEC=12) who underwent preoperative MDCT. Two reviewers independently and retrospectively accessed T-stage, N-metastasis. They evaluated the presence or absence of predefined findings of the PNET on CT. We analyzed the typical finding and relationship between CT findings and tumor grade. Using atypical PNET, they also estimated the possibility of atypical PNET or pancreatic adenocarcinoma (n=29) using a five-point scale. ROC curve analysis, kappa statistics, Fisher's exact test, Chi-square test were used for statistical analysis.

Results: Diagnostic accuracy for T-stage was T1=92%-97%, T2= 91%-93%, T3=86%- 88% with excellent agreement (κ=0.847). Accuracy for N-metastasis was 83%-89% with moderate agreement (κ=0.614). Typical CT findings included well circumscribed, homogeneous enhanced, hypervascular on arterial and venous phase, which were more common in lower grade tumor ($p<0.01$), whereas atypical CT findings (n=31) included ill-defined, heterogeneous enhanced, hypovascular on arterial and venous phase, duct dilation, which were more common in higher grade tumor ($p<0.01$). AUCs for differentiate atypical PNET from pancreatic adenocarcinoma were 0.806 and 0.760 with excellent agreement (κ=0.831). Duct dilatation and homogeneous enhancement were common in the pancreatic adenocarcinoma ($p<0.01$).

Conclusion: Preoperative CT accurately depicts T- and N-stage of PNET. However, sometimes it is hard to differentiate atypical PNET from pancreatic adenocarcinoma.

SS 1.05

Molecular imaging of pancreatic adenocarcinoma: MRI biodistribution study comparing different iron loaded nanoparticles with and without matrix metallopeptidase 9 substrates

A. Strauss[1], S. Dobiasch[1], K. Felix[1], I. Rosenberger[2], J. Kreuter[2], M.C. Franchini[3], J.-P.M. Lellouche[4], B.I. Rivka[4], I. Liron Limor[4], G. Opdenakker[5], J. Vandooren[5], H.U. Kauczor[1], L. Grenacher[1]; [1]Heidelberg/DE, [2]Frankfurt/DE, [3]Bologna/IT, [4]Ramat Gan/IL, [5]Leuven/BE

Purpose: MRI distribution studies were done using MMP9-covered nanoparticles (NPs) targeted for pancreatic adenocarcinoma (PDAC), as a novel approach to cloak the particles and increase their size as a matter to escape the RES-system as far as possible. These NPs were developed as part of the EU funded SaveMe project.

Material and Methods: Galectin-1 was chosen as the target molecule because of its overexpression in PDAC and in its precursor lesions. For targeting the tumor, four peptide-sequences functioning as Galectin-1 ligands have been chosen and linked to five different iron loaded NPs partly covered with MMP-9-substrates. These NPs were tested in nude mice carrying an orthotopic and a subcutaneous pancreatic tumor (Panc-1 or Su86.86). T2w sequences were used in a 1.5 T system with a custom mouse coil. The signal intensities were compared pre- and repetitively after injection of the NPs over a period of 60 min for the orthotopic and the s.c. tumor, as well as for the liver as reference for the RES.

Results: The largest signal drops were 84% 44 min for the liver, 18% 60 min for the orthotopic tumor and 15% 60 min p.i. for the s.c. tumor.

Conclusion: Two of the particles showed a clear tendency of accumulation over time inside the tumor. The best particle showed a clear signal drop in both tumor sites, but only when coupled with MMP-9-substrates showing the efficiency of that approach.

SS 1.06

Dynamic-contrast-enhanced MRI as a biomarker for a new concept of oral vaccination for locally advanced pancreatic cancer

T. Friedrich[1], H. Schmitz-Winnenthal[1], H. Lubenau[2], K. Breiner[3], W. Haefeli[1], P. Beckhove[1], L. Grenacher[1]; [1]Heidelberg/DE, [2]Mannheim/DE, [3]Zürich/CH

Purpose: Acquisition and analysis of dynamic-contrast-enhanced MRI (DCE-MRI) as part of a phase I trial of locally advanced or stage IV pancreatic cancer after oral DNA vaccination targeting VEGF-Receptor-2.

Material and Methods: Randomized, placebo-controlled, double blind dose-escalation study including 45 Patients. DCE-MRI assessed on a 1.5 T MRI on day 0, 38 and 3 months after treatment. Manually drawn regions of interest within the tumor-tissue followed by pixel-by-pixel analysis using a Siemens software package. ROI-modelling was based on Tofts model, K_{trans} regarded as primary endpoint. Besides, tumor staging according to RECIST. Clinical parameters included biomarkers CA 19-9, VEGF-A and collagen IV.

Results: At day 38, mean changes in K_{trans} were -18% versus +2% in the placebo group (36 patients). MRI after 3 months showed mean changes of -18% versus +3% in the placebo group (26 patients).These patients showed significant decrease in k_{trans} values at day 38 ($\alpha<0,05$, Wilcoxon test). MRI data corresponded with increasing VEGF-A and collagen VI while no markable effects could be observed with response to RECIST-criteria.

Conclusion: MRI with DCE-measurement is a promising radiologic tool as a diagnostic biomarker for the evaluation of antivascular therapies in malignant pancreatic tumors. Data suggests that VXM 01 can induce VEGFR 2 specific T-cell response and impacts tumor perfusion.

SS 1.07

Preoperative liver DW-MRI in pancreatic resectable adenocarcinoma

M.-P. Vullierme[1], A.-M. Marion-Audibert[2], A. Rode[3], M. Zins[4], A. Sauvanet[1], V. Vilgrain[1]; [1]Clichy/FR, [2]Ecully/FR, [3]Lyon/FR, [4]Paris/FR

Purpose: To evaluate sensitivity and specificity of preoperative DW-MRI in depicting liver metastasis as well as lymph node metastasis before resection of pancreatic adenocarcinoma.

Material and Methods: Prospective multicentric national study of consecutive patients planned to have a surgical resection of a pancreatic adenocarcinoma, with a negative MDCT for liver metastasis or lymph nodes. DW-MRI (with at least B 0, B 150 and B 800 sequences, and ADC map) was performed as well as gadolinium-enhanced MRI. FDG-PET was also performed when possible. After a multidisciplinary decision, if a liver metastasis was depicted, a biopsy of the lesion was performed. If biopsy was positive for metastasis another treatment other than surgery was planned.

Results: 15 patients out of 127 (11.8%), had liver metastasis (n=14), or N2 lymph node (n=1). DW-MRI per patient sensitivity was 87.5%, specificity 85.3%, PPV 58.3%, NPV 96.7%, and conventional MRI respectively 28.6%; 91.4%; 40%; 86.5%. FDG-PET did not depicted these metastasis. DW-MRI per lesion sensitivity was 95.2%, specificity 84.2%; and conventional MRI, respectively 23.8% and 91.9%. DW-MRI depicted 22 metastasis (75%), not seen with conventional MRI, and 26 not seen with MDCT (100%). Sensitivity of DW MRI was significantly better than MDCT ($p = 0.02$).

Conclusion: DW-MRI changed the therapeutic strategy for 11.8% of our patients with potentially resectable pancreatic adenocarcinoma, thus preventing non-curative pancreatic surgery.

SS 1.08

DWI and pancreatic cancer: comparison of mono-, biexponential and non-Gaussian kurtosis models

N. Kartalis[1], N. Albiin[1], L. Loizou[1], M.A. Fischer[1], M. Del Chiaro[1], C. Ansorge[1], K. Marias[2], N. Papanikolaou[1]; [1]Stockholm/SE, [2]Heraklion/GR

Purpose: To compare three DWI models, namely the two Gaussian, i.e. monoexponential [apparent diffusion coefficient (ADC)] and biexponential fit [true (D) and pseudo-(D*) diffusion coefficient, perfusion fraction (f)] and the non-Gaussian fit {kurtosis (K), corrected diffusion coefficient [D(k)]} for the differentiation of tumorous and non-tumorous tissue in patients with pancreatic adenocarcinoma.

Material and Methods: Fifteen consecutive patients with histopathologically proven disease underwent DWI at 1.5 T with 8 b-values (0, 50, 100, 150, 200, 300, 600 and 1000 s/mm^2). ADC, D, D*, f, K and D(k) were calculated from multiple ROIs on lesions and parenchyma and the differences were compared. ROC curve analysis was performed to determine area under the curve (AUROC) and optimal thresholds.

Results: In all ROIs (n=85), deviation from the Guassian model was noted, while significant deviation was found in 74% of tumorous and in 58% of non-tumorous ROIs. The only parameters that provided with statistically significant differences between tumorous and non-tumorous tissue where mean ADC and D(k) (for both, $p<0.0001$). AUROC for ADC, D, D*, f, K, and D(k) were 0.75, 0.52, 0.61, 0.65, 0.47, and 0.84, respectively. For a threshold D(k) value of 2.34×10^{-3} mm^2/s, the sensitivity and specificity were 74% and 85%, respectively.

Conclusion: Non-Gaussian diffusion modeling is more accurate for the differentiation of pancreatic cancer from surrounding non-cancerous parenchyma, while D(k) provides higher AUROC compared to ADC and biexponential diffusion coefficients.

SS 1.09

Assessment of treatment response in pancreatic ductal adenocarcinomas: RECIST criteria vs. ROI-based and histogram-based apparent diffusion coefficient analysis: preliminary results

S. Pullini[1], S.-L. Chao[2], J. Absil[2], F. Puleo[2], J.-L. Vanlaethem[2], C. Matos[2], M.A. Bali[2]; [1]Udine/IT, [2]Brussels/BE

Purpose: To compare the performance of ROI-based and histogram-based apparent diffusion coefficient (ADC) analysis and of RECIST criteria in the evaluation of treatment response in pancreatic ductal adenocarcinomas (PDC).

Material and Methods: 8 patients with PDC underwent T2- and diffusion-weighted MR (DW-MR) imaging acquired with nine b values (0, 10, 20, 30, 40, 50, 150, 300, 1000 s/mm^2), performed on 1.5T, before and after 4 cycles of chemotherapy. For each PDC: 1) tumour longest diameter on T2-weighted images; 2) tumour volume on DW-MR images; 3) mean ADC obtain from 2 to 3 ROIs (ROI-ADC) drawn on ADC maps; 4) mean, median, 10th, 25th, 50th, 75th and 90th centile of ADC histograms (H-ADC) obtained from the entire tumour volume were calculated. The therapeutic response was based on clinical and biological evaluation. Mann-Whitney test was applied for comparison.

Results: 4/8 (50%) were responders. Tumour diameter decreased more than 30% in only one responder (1/8) ($p>0.05$). DW-MR-based tumour volume reduction was greater than 30% in all responders ($p=0.03$). After treatment, in responders both mean ROI-ADC and median H-ADC increased (3/4) or remained unchanged (1/4). In non-responders, these parameters were unchanged (2/4) or decreased (2/4). Median H-ADC tends to be lower at baseline in responders ($p>0.05$).

Conclusion: Quantitative DW-MR may be useful in monitoring chemotherapy efficacy for PDC.

SS 1.10

CT imaging aspects of early local recurrence of pancreatic adenocarcinoma after pancreaticoduodenectomy: a retrospective study 2004-2013

C. Balaj, C. Sellal, I. Petit, X. Orry, A. Ayav, V. Laurent; Vandoeuvre les Nancy/FR

Purpose: To describe semiology and topography of pancreatic ductal adenocarcinoma early local recurrence after pancreaticoduodenectomy.
Material and Methods: This retrospective study was realised in University Hospital of Nancy (France). Between January 2004 and September 2013, patients who underwent pancreaticoduodenectomy for ductal adenocarcinoma, preoperative CT less than 30 days before surgery and recurrent postoperative CT during 1 year after surgery, were included. After studying postoperative imaging, correlations with clinical, histological data and preoperative imaging were made.
Results: Among 123 patients who underwent pancreaticoduodenectomy, 48 patients had sufficient follow-up imaging and were included. 33 had a local early recurrence (Group 1). 15 had no local recurrence (Group 2). Local recurrence consisted of 2 types of anomalies: tissue nodules on surgical clips (94%), and peri arterial invasion (82%). In preoperative imaging, tumor diameter ($p = 0.02$) and venous borderline resectable tumor ($p < 0.001$) are predictive of local recurrence. Healthy peri tumor parenchyma seems to be correlated with recurrence.
Conclusion: Tissue nodules on surgical clips and peri arterial invasion characterize early local recurrence. This tumor dissemination has probably lymphatic and nervous origin, and is linked to the tumor spread type. Radiologist has an essential role in the therapeutic strategy because of imaging predictive factors and recurrence diagnosis. Moreover, neoadjuvant treatments impact, for downstaging and improving survival, must be evaluated.

11:00 - 12:30 **Mozart**

Scientific Session 2

Imaging HCC and differential diagnosis

SS 2.01

Radio-pathological correlation in HCC treated by transarterial chemoembolisation: comparison between RECIST, mRECIST and EASL criteria

M. Dioguardi Burgio[1], M. Ronot[2], O. Bruno[2], C. Francoz[2], V. Paradis[2], F. Durand[2], L. Castera[2], J. Belghiti[2], V. Vilgrain[2]; [1]Palermo/IT, [2]Clichy/FR

Purpose: To compare the performances of RECIST1.1, mRECIST, and EASL criteria for tumoural necrosis evaluation in a consecutive series of patients treated with transarterial chemoembolisation (TACE) before liver transplantation (LT) for hepatocellular carcinoma (HCC).
Material and Methods: Between 2006 and 2012, all patients treated with at least one session of TACE before LT for HCC were identified. Response to treatment was evaluated by 2 independent readers on the last CT before LT according to RECIST1.1, mRECIST, and EASL criteria. Imaging response was compared to the tumoural necrosis assessed by pathology on the liver explant. Inter-reader agreement for the tumoural response was evaluated by the kappa statistic. Factor associated with a major (>90%) necrosis were tested by multivariate analysis.
Results: Population included 58 patients with 88 HCC treated with 94 TACE sessions. 51 nodules (58%) showed major necrosis. Among them, lesions were classified as complete response according to RECIST1.1, mRECIST and EASL in 2 (4%), 47 (92%) and 47 (92%) for reader 1, respectively, and 1 (2%), 45 (88%) and 45 (88%) for reader 2, respectively. Despite similar performances with mRECIST and EASL, only mRECIST was correlated with major necrosis on multivariate analysis for both readers ($p<0.0001$). Inter-observer agreement was substantial for RECIST1.1 ($k=0.65 +/- 0.08$), mRECIST ($k=0.78 +/- 0.07$), and EASL ($k=0.75 +/- 0.07$).
Conclusion: mRECIST and EASL criteria showed better correlation with major tumoural necrosis than RECIST1.1. mRECIST showed better correlation with tumoural major necrosis and should be used to evaluate response to TACE.

SS 2.02

Quantitative prediction of histological grade of hepatocellular carcinoma by nonlinear compartment model analysis of gadoxetate disodium-enhanced MR imaging

A. Yamada[1], K. Ueda[1], S. Yanagisawa[1], M. Kurozumi[1], Y. Fujinaga[1], K. Maruyama[2], M. Kadoya[1]; [1]Matsumoto/JP, [2]Tokyo/JP

Purpose: A nonlinear compartment model analysis of gadoxetate disodium-enhanced MR imaging can quantify cellular uptake function as intrinsic clearance (CL_{int}) which cannot be evaluated by extracellular MR contrast agents. The purpose of this study was to asses prediction capability of nonlinear compartment model analysis of gadoxetate disodium-enhanced MR imaging for histological grade of hepatocellular carcinoma (HCC).
Material and Methods: Twenty-four consecutive patients with histologically proven HCCs who preoperatively underwent gadoxetate disodium-enhanced MR imaging were included. T1-weighted images with fat suppression at precontrast and 12 postcontrast enhanced phases were obtained using K-space weighted image contrast reconstruction technique. Time-intensity-curves (TICs) of abdominal aorta, main trunk of portal vein and HCC were obtained from region of interests on MR images. Pharmacokinetic parameters including distribution volume (V_d) at extracellular fluid space and CL_{int} of gadoxetate disodium in HCC were determined by applying TICs into nonlinear compartment model. Linear discriminant analysis according to V_d and CL_{int} was performed on histological grade of HCC.
Results: The mean value and its 95% confidence intervals of area under ROC curve in distinguishing moderately and poorly differentiated HCCs from well-differentiated HCCs by linear discriminant analysis were 0.772 and 0.768 to 0.777 for V_d alone, 0.795 and 0.791 to 0.800 for V_d and CL_{int}, respectively.
Conclusion: Separation of moderately and poorly differentiated HCCs from well-differentiated HCCs can be improved by CL_{int} determined from nonlinear compartment model analysis of gadoxetate disodium-enhanced MR imaging.

SS 2.03

withdrawn by the authors

SS 2.04

Spectral CT and volumetric-iodine uptake in hepatocellular carcinoma

E. Bozzi, I. Bargellini, O. Perrone, G. Lorenzoni, F. Turini, C. Bartolozzi; Pisa/IT

Purpose: To assess image quality and diagnostic accuracy of monochromatic imaging from spectral CT and reproducibility of volumetric iodine uptake (VIU) in patients with hepatocellular carcinoma (HCC).
Material and Methods: Forty-three patients with 108 HCC nodules underwent multiphasic CT with spectral imaging in the late arterial phase, to generate conventional 140-kVp polychromatic images (group A), 70-keV monochromatic images (group B) and iodine-based images (group C). Images were compared in terms of tumour-to-liver contrast-to-noise ratio (CNR), image quality (score 1-5), lesion conspicuity (score 1-3) and number of detected HCCs. VIU was calculated in the iodine-based images.
Results: Mean CNR was significantly higher in group C (4.19±2.42) compared to group A (2.17±1.6) and group B (2.79±1.78) (P<0.0001). Mean scores for image quality and lesion conspicuity were 4.72±0.5 and 2.51±0.6, respectively, for group A, 4.74±0.5 and 2.83±0.4 for group B and 4.44±0.7 and 2.83±0.5 for group C; the highest number of HCC nodules were identified in group C (106/108; 98.1%) compared to group A (84.2%) and B (94.4%). Measurement of VIU was fast (mean post-processing time 92±80 seconds) and reproducible (k=0.99), with a mean iodine concentration within the segmented volume of 22.4±6.9 μg/cm^3.
Conclusion: In HCC patients, iodine-based images derived from spectral CT can improve lesion detectability and provide a reproducible quantitative parameter that reflects tumor neoangiogenesis.

SS 2.05

Infiltrative hepatocellular carcinoma: multidetector computed tomography and magnetic resonance imaging with hepatobiliary agent findings

M. Dioguardi Burgio, M. Calamia, A. Anastasi, A. Taibbi, T.V. Bartolotta; Palermo/IT

Purpose: To assess the role of multidetector CT (MDCT) and magnetic resonance imaging (MRI) in the diagnosis of infiltrative hepatocellular carcinoma (iHCC).
Material and Methods: 18 patients (15 male and 3 female; mean age 66 years; range 38-78 years) with histology-proved iHCC, underwent MDCT (n=13) using a 64-slice scanner and/or MRI with hepatobiliary contrast agent (Gd-EOB-DTPA or Gd-BOPTA) (n=11). Two experienced radiologists retrospectively reviewed in consensus CT and MRI findings with respect to lesion location, size, contour, tumor growth pattern, enhancing pattern, lymphadenopathy, direct invasion to adjacent organ and distant metastasis.
Results: 10/18 (56%) iHCCs were larger than 10 cm; 8/18 (44%) tumors involved both lobes; 14/18 (78%) iHCC showed venous invasion (12 portal vein, 1 hepatic vein and 1 both portal and hepatic vein) (p<0.05). 12/18 (67%) patients had at least 1 satellite nodule and 4/18 (22%) had biliary dilatation. Two patients presented with extrahepatic disease. Enhancement during hepatic arterial phase followed by wash-out in portal-venous or late phase was seen in 8/13 (61%) iHCC at CT and in 9/11 (82%) at MRI as “patchy” appearance (p<0.05). 11/11 (100%) iHCCs were hypointense on hepatobiliary phase (p<0.05). 5/5 (100%) iHCCs showed restriction on DWI images (p<0.05).
Conclusion: MDCT and MRI with hepatobiliary contrast agent may suggest the correct diagnosis of iHCC, by showing patchy enhancement on hepatic arterial phase followed by wash-out, vascular invasion, DWI restriction and hypointensity on hepatobiliary phase.

SS 2.06

Prospective validation of liver-imaging reporting and data system in nodules smaller than 2 cm detected in cirrhotic patients

A. Darnell, A. Forner, J. Rimola, M. Reig, J. Bruix, C. Ayuso; Barcelona/ES

Purpose: To evaluate the diagnostic accuracy of liver imaging–reporting and data system (LI-RADS) for hepatic nodules ≤20mm in cirrhotic patients.
Material and Methods: Cirrhotic patients with a new, solitary nodule ≤20mm detected during surveillance were examined by MR and fine-needle biopsy (gold-standard). Nodules without pathological confirmation were followed-up with MRI/6m (median 95 months). A LI-RADS (LR) category was assigned to each nodule.
Results: 159 patients were included. The final diagnosis was: 103 HCC, 3 intrahepatic cholangiocarcinoma (ICC), 1 neuroendocrine metastasis and 52 benign lesions. In 26 patients, the nodule was not detected by MRI. Five lesions were categorized as LR-1 (3.8%), all benign; 12 as LR-2 (9%), 3 (25%) were HCC; 42 as LR-3 (31.6%), 29 (69%) were HCC and 1 was ICC; 25 as LR-4 (18.8%), 24 were HCC and 1 benign lesion; 45 as LR-5 (33.8%), 43 were HCC, 1 a regenerative nodule and 1 a neuroendocrine metastasis; and 4 as other malignancies (3%). LR-5 (definitively HCC) had a sensitivity, specificity, positive and negative predictive value of 41.7%, 96.4%, 95.6% and 47.4%, respectively, for HCC diagnosis. Considering altogether LR-4 and LR-5 as definitively HCC, the figures were 65.1%, 94.6%, 95.7% and 59.6%, respectively.
Conclusion: LR-4 establishes HCC diagnosis with the same accuracy as LR -5. Thus, both categories may be unified to definitely diagnose HCC. In addition, a relevant proportion of LR-2/LR-3 lesions correspond to an HCC.

SS 2.07

Will slow injection of Gd-EOB-DTPA enable to detect more hypervascular hepatocellular carcinoma at the multiple arterial phases?

T.L. Harada, K. Saito, N. Yoshimura, Y. Araki, T. Funatsu, T. Saguchi, M. Kawasaki, K. Sugimoto, S. Akata, K. Tokuuye; Shinjuku-ku/JP

Purpose: To evaluate the detectability of hypervascular hepatocellular carcinoma (HCC) with slow injection protocol of Gd-EOB-DTPA, and to compare with the moderate injection protocol.
Material and Methods: We retrospectively evaluated 68 patients with 107 hypervascular HCCs and 16 hypovascular hepatocellular nodules detected by CT hepatic arteriography (CTHA). We assigned 20 patients with 35 lesions to the slower injection group (1 mL/s, group A) and 48 patients with 88 lesions to the moderate injection group (2 mL/s, group B). A three-dimensional volumetric interpolated breath-hold examination was used with the dynamic study. The monitoring scan technique was used to obtain the optimal arterial phase. We obtained 5 arterial phases during breath-holding. Each lesion was classified into 4 categories.
Results: The respective sensitivity of each phase in group A was 86%, 86%, 79%, 62%, and 51%, whereas the respective sensitivity of each phase in group B was 88%, 94%, 81%, 58%, and 35%. No significant differences were observed between 1st, 2nd and 3rd phase of group A and CTHA, and between 1st and 2nd phase of group B and CTHA.
Conclusion: It showed longer optimal timing in slower injection group than in moderate injection group. The sensitivity of moderate injection group was higher than that of slower injection group, although no significant difference was observed.

SS 2.08

Low-tube-voltage arterial-phase CT of hepatocellular carcinoma: image quality and radiation dose savings

J.L. Wichmann, P. Majenka, W. Kromen, M. Beeres, R.W. Bauer, M.J. Kerl, T. Gruber-Rouh, R. Hammerstingl, T. Vogl, B. Schulz; Frankfurt am Main/DE

Purpose: To intra-individually compare a low-tube-voltage (100 kVp) with a standard 120 kVp CT protocol regarding image quality and radiation dose during arterial phase in patients with hepatocellular carcinoma.
Material and Methods: 68 patients with known hepatocellular carcinoma underwent abdominal dual-energy CT. 100 kVp and mixed 120 kVp images during the arterial phase were compared. Signal measurements in the abdominal aorta, portal vein, carcinoma and non-infiltrated liver parenchyma were compared. DLP of 100 kVp acquisition and the complete dual-energy CT arterial phase were compared. Three readers subjectively evaluated image quality, delineation, image sharpness and noise of both image series using a five-point Likert scale.
Results: Average DLP of 100 kVp acquisition was reduced by nearly half compared to the complete dual-energy CT examination (189.6 vs. 382.9 mGy cm). Signal of the abdominal aorta, portal vein, hepatic parenchyma and carcinoma was significantly higher with low-tube-voltage technique (P < 0.001). Although readers preferred standard 120 kVp over 100 kVp acquisition regarding image quality (4.86 vs. 4.45), delineation (4.84 vs. 4.71), sharpness (4.87 vs. 4.46) and noise (4.88 vs. 4.26), all image series received a score of at least 4 out of 5.
Conclusion: Low-tube-voltage arterial-phase CT at 100 kVp allows for significant radiation dose savings with a high subjective image quality for evaluation of hepatic malignancy and parenchyma in patients with hepatocellular carcinoma.

SS 2.09

Peripheral mass-forming cholangiocarcinoma: dynamic patterns of enhancement at multiphasic computed tomography and magnetic resonance imaging and correlation with clinicopathologic features

M. Ciresa, A.M. De Gaetano, D. Curione, M. Pompili, E. Rinninella, M. Vellone, F.M. Vecchio, L. Bonomo; Rome/IT

Purpose: To evaluate dynamic pattern of enhancement at multiphasic computed tomography (CT) and magnetic resonance imaging (MRI) of peripheral mass-forming cholangiocarcinoma (PMCC) with emphasis on chronic liver disease and differentiation grading.

Material and Methods: Dynamic pattern of enhancement at CT and MRI of 71 histologically confirmed PMCC nodules was defined according to the progression of enhancement throughout the different phases, as follows. (1) Progressive contrast enhancement (CE): the nodule enhances progressively with maximal intensity in delayed phases (typical of PMCC); (2) stable CE: nodule enhancement is unmodified from the arterial to venous phases (atypical pattern of PMCC); (3) washout: intense contrast uptake during the arterial phase followed by contrast washout in delayed phases (typical pattern of hepatocellular carcinoma, HCC).

Results: 60/71 (84.5%) PMCCs showed progressive CE, 8 (11.3%) stable CE and 3 (4.2%) washout pattern. Progressive CE pattern was more frequent in normal hepatic parenchyma (92%), in moderately differentiated (100%) and larger than 3 cm (90%) lesions; stable pattern was more frequent in chronic liver disease (15%), in poorly differentiated (32%) and smaller than 3 cm (22.5%) lesions; washout pattern were observed in chronic liver disease (9%), in 2 poorly differentiated and larger than 3 cm lesions and in 1 well-differentiated and smaller than 3 cm nodule.

Conclusion: 11/71 (15.5%) PMCCs showed atypical dynamic pattern of enhancement; washout pattern in chronic liver disease was a risk of misdiagnosis with HCC.

SS 2.10

Differentiation between primary and secondary liver neoplasms: value of ADC histogram quantification

K. Drevelegas[1], N. Papanikoloau[2], K. Marias[3], K. Nikiforaki[3], M. Kostantinidis[1], I. Stoikou[1], A. Drevelegas[1], L. Papalavrentios[1]; [1]Thessaloniki/GR, [2]Stockholm/SE, [3]Heraklion/GR

Purpose: To investigate the potential of apparent diffusion coefficient (ADC) histogram analysis in differentiation of primary and secondary liver tumors.

Material and Methods: 29 consecutive patients with histopathologically proven focal liver lesions, underwent DWI at 3.0 T (b-values: 0, 1000 s/mm^2). ADC histogram analysis was performed quantifying histogram metrics including; min, max, mean, mode, sd, variance, kurtosis, skewness, 5% (V5), 30% (V30), 70% (V70) and 95% (V95) percentiles, peak position and peak height. 19 patients were diagnosed with liver metastastic tumors while 12 with primary tumors (7 hepatocellular carcinomas and 5 cholangiocarcinomas). The histogram metrics that resulted in statistically significant differences were further evaluated with ROC analysis to define area under the curve and optimal thresholds.

Results: The parameters that provided statistically significant differences between primary and metastatic tumors were 30% percentile (p=0.005), mean (p=0.009), median (p=0.01), peak position (p=0.02). The AUROC of V30 was 0.813, while V30>0.918X10-3) resulted in 75% sensitivity and 76.5% specificity for the differentiation between primary and metastatic lesions.

Conclusion: ADC quantification can be used to differentiate primary from secondary liver neoplasms, while histogram quantification only marginally improve sensitivity and specificity.

11:00 - 12:30 **Karajan**

Scientific Session 3

Diffuse liver disease: MR imaging

SS 3.01

Liver steatosis assessed with preoperative MR imaging: an independent risk factor for severe complications after major hepatic resection

G. D'Assignies[1], C. Fayard[1], H.S. Leitão[2], S. Dokmak[1], F. Fteriche[1], V. Paradis[1], J. Belghiti[1], F. Tubach[3], V. Vilgrain[1], B. Van Beers[1]; [1]Clichy/FR, [2]Coimbra/PT, [3]Paris/FR

Purpose: To assess if liver steatosis determined with MR imaging is an independent risk factor of complications after major liver resection.

Material and Methods: All patients who had liver MR imaging before major liver resection in our institution between January 2001 and December 2011 were included in this retrospective study. Liver fat fraction was assessed with in- and opposed-phase T1-weighted dual echo gradient-echo MR imaging. The association between steatosis and post-operative complications, unadjusted and adjusted for potential confounding factors including age, ASA score, body mass index >25 kg/m^2, diabetes, liver fibrosis > F2 and type of surgery was assessed with univariate and multivariate analyses.

Results: Liver steatosis, defined as liver fat fraction ≥5% at MR imaging, and adjusted for the confounding factors, was associated with severe postoperative complications (Clavien scores ≥ IIIa) (P = 0.04), higher aminotransferase levels (P = 0002; ALT: P = 0.0008), more pulmonary complications (P = 0.02) and longer hospital stay (P = 0.02).

Conclusion: Liver steatosis ≥5% assessed with routine preoperative MR imaging is an independent risk factor of severe postoperative complications after major liver resection.

SS 3.02

Non-invasive differentiation between simple steatosis and steatohepatitis using gadoxetic acid-enhanced MRI in patients with non-alcoholic fatty liver disease: a feasibility study

N. Bastati-Huber[1], D.S. Feier[2], C. Balassy[1], A. Wibmer[1], D. Tamandl[1], H. Einspieler[1], C. Kulinna-Cosentini[1], A. Ba-Ssalamah[1]; [1]Vienna/AT, [2]Cluj-Napoca/RO

Purpose: To distinguish between simple steatosis and non-alcoholic steatohepatitis (NASH) in non-alcoholic fatty liver disease (NAFLD) patients using gadoxetic acid-enhanced MRI.

Material and Methods: We examined 81 patients with suspected NAFLD with gadoxetic acid-enhanced 3-Tesla MRI. Patients were histopathologically classified as simple steatosis or NASH using the SAF score based on the semiquantitative scoring of steatosis, activity and liver fibrosis. The MR images were analyzed using the relative liver enhancement. Univariate and multivariate regression analyses were applied to identify variables associated with relative enhancement measurements and the performance of relative enhancement values was assessed for the differentiation between simple steatosis and NASH using the area under the receiver operating characteristic curve (AUC) analysis.

Results: Testing the relationship between enhancement measurements and histology, relative enhancement values correlated strongly with lobular inflammation (r=-0.59, p=<0.001), ballooning (r=-0.44, p=<0.001), and fibrosis (r=-0.59, p=<0.001), but not with steatosis (r=-0.15, p=0.15). In multivariate analysis, all three histological parameters were independently associated with the relative enhancement. The measurements performed well for the differentiation between simple steatosis and NASH, with an AUC of 0.85, [cutoff=1.24, (sensitivity=97.1%, Specificity =63%)].

Conclusion: Gadoxetic acid-enhanced MRI may be used as a non-invasive diagnostic tool to distinguish between simple steatosis and NASH in NAFLD patients.

SS 3.03

Liver fat quantification by multi-echo chemical shift gradient echo MRI sequences with histological correlation

M. Franca[1], A. Alberich Bayarri[2], L. Martí-Bonmatí[2], J.A. Oliveira[1], J.R. Vizcaino-Vasquez[1], F.E. Costa[1], H. Pessegueiro-Miranda[1]; [1]Porto/PT, [2]Valencia/ES

Purpose: To validate an MR imaging protocol that allows to accurately measure fat within the liver, as parametric imaging biomarker, in a group of patients with different diffuse liver disorders.

Material and Methods: Consecutive patients that have clinically indicated liver biopsy were recruited to perform a 3.0 Tesla MRI examination (multislice MECSh GRE sequence: TR/TE=10/0.99, 1.69, 2.39, 3.09, 3.79, 4.49, 5.19, 5.89, 6.59, 7.29, 7.99, 8.69, msec), end expiratory phase breath-hold acquisition. Quantification for liver fat fraction (FF) was performed with dedicated software (with phase reconstruction and T2* correction) selecting a ROI within the biopsied liver segment. Liver biopsy was used as gold standard for steatosis grading (0-3).
Results: Twenty-five patients followed the inclusion criteria. There were 19 patients with grade 0, 3 with grade 1, and 3 with grade 3 liver steatosis. High significant correlation was obtained between steatosis histological grade and the median of calculated fat fraction (ρ=0.741, p<0.001).
Conclusion: Our preliminary results demonstrate a good correlation between non-invasive fat fraction quantification by MECSh GRE MRI sequence with phase reconstruction and T2* correction, and liver biopsy. If this is validated in larger cohorts, this MRI sequence could be used as a fast, non-invasive and quantitative liver fat imaging biomarker.

SS 3.04

Comparison of the controlled attenuation parameter values and 1H-MR spectroscopy determined liver fat percentages in patients with NAFLD or NASH: interim results

J.H. Runge, A.J. Nederveen, J. Verheij, U. Beuers, J. Stoker; Amsterdam/NL

Purpose: In non-alcoholic fatty liver disease (NAFLD) and non-alcoholic steatohepatitis (NASH) patients, MRI now allows non-invasive, quantitative fat measurement. Due to MRI's costs and relative burden, other methods are sought-after. In this study, we compared the new controlled attenuation parameter (CAP) on the FibroScan® (FS) with ^{1}H-MR spectroscopy (^{1}H-MRS) determined fat-% in patients with clinical suspicion of NAFLD or NASH and liver biopsy.
Material and Methods: Consecutive adult NAFLD/NASH patients were seen within 6 weeks of biopsy for a ≥8 hr fasting FS and ^{1}H-MRS measurement. From March 2013 up to January 2014, 16 subjects were included: one had to be excluded as FS was not possible. ^{1}H-MRS was performed at 3T with a 5-echo STEAM sequence (TE/ΔTE/TR: 10/5/3500ms) in a single, 21s breath hold, allowing for individual T2-correction. CAP-values and fat-% were compared using Spearman's correlation coefficient (rs).
Results: Data of 15/16 subjects were eligible. Median (IQR) age and BMI were 53.5 (49.3-57.3) and 26.8 (26.1-30.5), respectively. Median CAP-value in dB/m was 303 (260-337). Median fat-% was 11.9% (4.2-22.3%). rs between CAP-values and fat-% was 0.91 (95%-CI: 0.73-0.97, P<0.0001).
Conclusion: The CAP-value can quantitatively measure liver fat, showing near perfect correlation with ^{1}H-MR spectroscopy as reference standard. The results thus far appear to support the more widespread use of the CAP-value for liver steatosis assessment, especially as the FibroScan allows simultaneous elasticity measurement.

SS 3.05

Reliability and repeatability of diffusion tensor imaging of the liver

R. Girometti, M. Maieron, G. Lissandrello, L. Cereser, C. Zuiani, M. Bazzocchi; Udine/IT

Purpose: To evaluate the reliability and repeatability of diffusion tensor imaging of the liver (LDTI) quantitative results.
Material and Methods: Ten healthy volunteers (median age 23 years) underwent LDTI on a 3.0 T magnet in two imaging sessions separated by 2 weeks (session-1/-2, respectively). A single-shot Echo-planar sequence with 16 non-collinear diffusion gradient directions and b-values of 0, 1000 sec/mm^2 was used. By averaging multiple measurements, two radiologists in consensus assessed liver apparent diffusion coefficient (ADC) and fraction of anisotropy (FA) values on ADC- and FA-maps at four reference levels, namely: right-upper-level (RUL), right-lower-level (RLL), left-upper-level (LUL) and left-lower-level (LLL), respectively. We then performed: (i) analysis of reliability/repeatability, by calculating the coefficient of variation (CV%) of ADC/FA values on intra- and inter-session basis; (ii) Bland-Altman analysis, to assess the limits of agreement between inter-session measurements.
Results: Intra-session CVs% were 9.51% (session 1) and 9.48% (session 2) for ADC, and 12.93% (session 1) and 11.48% (session 2) for FA, respectively. When comparing RUL, RLL, LUL and LLL on an inter-session basis, we showed CVs% of 2.43%, 4.01%, 4.09% and 3.98% for ADC values, and 5.20%, 4.91%, 7.00% and 5.16% for FA values, respectively. We observed limits of agreement no larger than -0.15 to 0.23 x10^{-3} mm^2/sec (ADC values) and -0.05 to 0.07 (FA values).
Conclusion: LDTI provides reliable and repeatable estimates of liver ADC/FA, with low CV% and close limits of agreement.

SS 3.06

The effect of echo times on the accuracy of susceptibility weighted magnetic resonance imaging in staging liver fibrosis

C. Balassy[1], S. Witoszynskyj[1], D.S. Feier[2], G. Reiter[1], A. Ba-Ssalamah[1]; [1]Vienna/AT, [2]Cluj-Napoca/RO

Purpose: To assess the effect of echo-sampling on the accuracy of magnetic resonance (MR) susceptibility weighted imaging (SWI) to detect and stage liver fibrosis in patients with chronic liver diseases (CLD), using histology as reference standard.
Material and Methods: Sixty-eight consecutive patients were included. Liver fibrosis was evaluated using the Metavir scoring system. MRI was performed on a 3 T unit. Data were collected using echo times (TE), 2.5 ms and 10 ms. Signal intensity (SI) of the liver and spinal muscle was defined and liver-to-muscle signal intensity ratios were calculated. The diagnostic performance of both TE was assessed using sensitivity (Se%), specificity (Sp%) and area under receiver operating characteristics (AUROC) analysis.
Results: Histology resulted F0 (n=13), F1 (n=6), F2 (n=8), F3 (n=12), F4 (n=28). Both 2.5TE LMR and 10TE LMR correlated strongly with liver fibrosis. The diagnostic performance of LMR at 2.5 ms was very good, with an AUROC of 0.85 (Se=90.7%, Sp=76.9%) for stages ≥F1, 0.88 (Se=95.8%, Sp=73.7%) for stages ≥F2, 0.90 (Se=92.5%, Sp=74.1%) for stages ≥F3 and 0.89 (Se=85.7%, Sp=82.1%) for liver cirrhosis diagnosis (F4). Diagnostic accuracy improved further with TE=10ms. MecNemar tests revealed a statistically significant difference between the two parameters regarding the diagnosis of early fibrosis (stages ≥F1, p<0.0001).
Conclusion: SWI is a promising non-invasive tool to detect and stage liver fibrosis in CLD patients, having increased accuracy with higher TE values.

SS 3.07

The feasibility of texture analysis using susceptibility-weighted magnetic resonance imaging in detecting patients with liver cirrhosis

D.S. Feier[1], T. Knogler[2], M.E. Mayerhoefer[2], C. Balassy[2], N. Bastati[2], A. Ba-Ssalamah[2]; [1]Cluj-Napoca/RO, [2]Vienna/AT

Purpose: To establish the feasibility of textural features of liver parenchyma obtained on susceptibility weighted (SWI) MRI which will enable the detection of liver cirrhosis in patients with diffuse chronic liver diseases (CLD).
Material and Methods: Sixty-five patients (mean age, 51.65 years; 60% males) with CLD and histologically proven liver fibrosis were included retrospectively. Fibrosis was evaluated according to the Metavir system and grouped in patients with (F4 Metavir, n=27, 42%) and without (F0-F3 Metavir, n=38, 58%) liver cirrhosis. All patients underwent 2D multislice breath-hold SWI sequence on a 3T MRI unit and the imagines were used for texture analysis. A region of interest (ROI) was manually defined. Texture features derived from the grey-level histogram, the co-occurrence matrix, the autoregressive model, and the wavelet transform were calculated. Fisher coefficients were calculated to determine which texture features were best suited for distinguishing between no-cirrhosis and cirrhotic liver tissue. The classification accuracy was used as the primary outcome measure. Sensitivity and specificity were used as secondary variables.
Results: Six out of ten texture features selected on the basis of Fisher coefficients were derived from grey-level histogram. Of the 65 patients included, 62 (95.38%) were classified correctly by k-NN. Sensitivity was 96.3% and specificity was 94.7%.
Conclusion: Texture features extracted from the grey-level histogram calculated form SWI MRI data are feasible to correctly identify cirrhotic changes in liver parenchyma of patients with CLD.

SS 3.08

Magnetization transfer ratio imaging of the liver: could it play a role in quantifying liver cirrhosis?

M.H. Martens[1], S. Noordzij[1], D.M. Lambregts[1], N. Papanikolaou[2], L.A. Heijnen[1], G. Koek[1], R.G.H. Beets-Tan[1]; [1]Maastricht/NL, [2]Heraklion/GR

Purpose: The diagnosis of liver cirrhosis is an important diagnostic challenge. So far, imaging techniques have not proven successful in quantifying cirrhosis and invasive liver biopsy remains the golden standard. The contrast in magnetization transfer ratio (MTR) imaging is based on the presence of macromolecules. We hypothesize that cirrhosis contains many macromolecules and will show a higher MTR than normal liver parenchyma. Hence, the aim of this study was to evaluate if MTR is able to differentiate between liver cirrhosis and normal liver parenchyma.

Material and Methods: Eighteen patients with proven liver cirrhosis were compared to 5 healthy volunteers. All subjects received a standard liver MRI including one axial slice of the MT sequence at the center of the liver. Regions of interest (ROI) covering the liver parenchyma (excluding large vessels and focal liver lesions) were drawn on the MT-MRI to calculate MTR. Mann-Whitney U test was used to compare the MTR of the liver parenchyma between cirrhosis patients and controls.
Results: ROI size ranged between 19.0 and 173 cm^2. The mean MTR of the cirrhosis group was 53.8% and of the control group was 23.1%. This difference was statistically significant with $p<0.001$.
Conclusion: The magnetization transfer ratio could play a role in the diagnosis of liver cirrhosis. Further research with a larger patient cohort is recommended.

SS 3.09

High field (3T) MR evaluation of cirrhotic patients: comparison of two different injection rates of hepatospecific contrast agent

V. Battaglia[1], A. Grigolini[1], F. Signorini[1], G. D'Ippolito[2], C. Bartolozzi[1]; [1]Pisa/IT, [2]Sao Paulo/BR

Purpose: To evaluate if different injection rates of the hepatospecific contrast agent (Gd-EOB-DTPA) in a selected group of cirrhotic patients determines alterations of liver enhancement in early arterial and arterial phase.
Material and Methods: Eighty cirrhotic patients (M-F: 60:20; mean age: 62 ys; range: 41-82 ys) underwent high-field (3T) MR examination. All patients were within Milan criteria, without signs of portal thrombosis (main branch and segmental branches); hepatic function was preserved. Standard study protocol presupposed a fixed time delay for the acquisition of early arterial and arterial phases after the injection of hepatospecific contrast agent (Gd-EOB-DTPA), administered by automatic injector. In 48/80 patients, the contrast agent injection flow rate was 3 ml/sec (group 1); in 32/80 patients, the injection flow rate was 1.5 ml/sec (group 2). For each MR study, in both early arterial and arterial phase, the parenchymal enhancement values were calculated, by means of evaluation of ER (enhancement ratio); in all cases, a standard (150 mm^2) ROI (region of interest) was positioned in pre-definite segments. Values obtained in the two groups were compared by means of two-tailed Student's T test.
Results: Means (±SD) of parenchymal enhancements on early arterial and arterial phases in 48/80 patients were 0.12 (±0.17) and 0.58 (±0.19); in group 2 were 0.13 (±0.14) and 0.67 (±0.22) ($p>0.01$).
Conclusion: Different injection rates of hepatopecific contrast agent do not influence the parenchymal enhancement in cirrhotic patients in none of arterial phases.

SS 3.10

Interobserver agreement of Gandon- and R2*-methods for liver iron concentration measurement

J.H. Runge, E.M. Akkerman, A.J. Nederveen, J. Stoker; Amsterdam/NL

Purpose: Liver iron concentration (LIC) can be measured with a number of MRI-methods. As thus far no reasonably sized study has been performed comparing the interobserver agreement of the Gandon- and R2*-methods, we aimed to compare these.
Material and Methods: Baseline MRI LIC-measurements performed between January 2009 and December 2012 in our centre were included retrospectively. The Gandon-, and R2*-methods were used to derive LIC in µmol/g and R2* in s^{-1}, respectively. To assess interobserver variability, two readers independently drew regions-of-interest (ROIs). LIC and R2* values of both reades were assessed using intraclass correlation coefficients (ICCs) and Bland-Altman analysis derived repeatability indices.
Results: Gandon and R2* data were acquired in 77 patients. Median (IQR) LIC and R2* for reader 1 were 90 (32.5-220) µmol/g and 44 (105-279) s^{-1}, respectively. ICCs (95%-CI) between reader 1 and 2 for LIC and R2* were 0.995 (0.992-1.000) and 1.0 (1.0-1.0), respectively. Repeatability indices (95%-CI) for LIC and R2* were 5.14% (4.11-6.17%) and 0.81% (0.65-0.97%), respectively.
Conclusion: Interobserver agreement in terms of ICC and repeatability indices for both Gandon and R2* methods were excellent. Given that R2* measurements can be performed in a single breath hold and are sensitive for iron concentrations that are above the Gandon threshold, R2* seems preferable.

SS 3.11

Comparison of serum ferritin and transferrin levels and MRI-determined liver iron concentration

J.H. Runge, E.M. Akkerman, A.J. Nederveen, U. Beuers, J. Stoker; Amsterdam/NL

Purpose: MRI allows accurate, reproducible, non-invasive measurement of the liver iron concentration (LIC) and is preferable over biopsy. Conversely, serum markers assess whole body iron content, can thus serve as screening tools but may be influenced by concurrent inflammation or infection. As the serum marker ferritin is an acute phase protein, it may be raised without reflecting actual increased LIC. Few studies have thus far compared MRI-determined LIC with ferritin and non-acute phase (protein) markers such as transferrin and transferrin-saturation.
Material and Methods: All MRI LIC-measurements performed between January 2009 and December 2012 in our centre were included retrospectively. The Gandon method was applied to derive the mean LIC over three slices. Serum iron, transferrin, transferrin-saturation and ferritin levels respectively were noted when available. Spearman's correlation coefficient (rs) was used to compare the serum levels with the LIC value.
Results: A total of 99 baseline MRI-scans were performed. LIC values could be determined accurately in 82 cases. Ferritin and transferrin correlated substantially with LIC at $r_s=0.72$ ($P<0.0001$, $n=69$) and $r_s=-0.69$ ($P<0.0001$, $n=41$). These correlations did not differ significantly ($P=0.77$). Iron and transferrin-saturation showed lower but significant correlations with LIC.
Conclusion: Correlations between transferrin and ferritin with MRI-determined LIC did not differ significantly. Based on these results, no preference can be given to either ferritin or transferrin to screen for increased liver iron content.

11:00 - 12:30 **Wolf Dietrich**

Scientific Session 4

GI tract malignancy - diagnosis and staging

SS 4.01

Can PET/CT-defined tumour variables predict circumferential resection margin involvement in patients with oesophageal cancer?

K.G. Foley, P. Fielding, W.G. Lewis, A. Karran, D. Chan, P. Blake, S.A. Roberts; Cardiff/UK

Purpose: PET/CT is now a routine staging investigation in oesophageal cancer (OC). The prognosis of patients with OC is poor and evidence regarding the optimum method of treatment is deficient, with different multicentre trials producing conflicting results. Prediction of the circumferential resection margin (CRM) would enable clinicians to select patients requiring neo-adjuvant chemoradiotherapy prior to surgery, as has been successfully demonstrated in rectal cancer. This study aims to assess whether PET/CT tumour defined variables could predict CRM involvement.

Material and Methods: Consecutive patients referred to the SE Wales Upper GI Cancer MDT staged with PET/CT prior to surgical resection between October 2010 and March 2013 were included. Primary outcome was the association of PET/CT defined tumour variables with pathological CRM involvement.

Results: 57 patients staged with PET/CT subsequently underwent surgical resection (47 male, 47 adenocarcinoma). Association was tested using binary logistic regression. SUVmean (median CRM-ve 5.20 vs. CRM+ve 7.35) was significantly and independently associated with CRM involvement (HR 1.172, 95% CI 1.011–1.359, p=0.035). SUV_{max} (p=0.039) and tumour length (TL, p=0.050) were significantly associated with CRM involvement on univariate analysis.

Conclusion: Functional PET/CT staging variables have the potential to predict CRM involvement. This study is the first to demonstrate CRM prediction on PET/CT, and highlights the value staging OC patients with PET/CT, by guiding the clinicians towards the optimum treatment strategy.

SS 4.02

The use of EUS FNA in evaluating proximal mediastinal nodal disease in junctional tumours and the impact on staging and management

F. Dambha[1], S. Varghese[1], E.M. Godfrey[2], A. Metz[1], N. Carroll[2]; [1]London/UK, [2]Cambridge/UK

Purpose: Endoscopic ultrasound (EUS) has improved the staging accuracy of oesophageal cancer and is the most accurate modality in identifying loco-regional and nodal involvement. EUS is able to obtain EUS guided fine needle aspiration (FNA) samples from posterior and inferior mediastinal nodes (Stations 7, 8 and 9). Patient management including treatment pathways and outcome is directly influenced by lymph node involvement. Our aim was to study the impact of EUS-FNA of high thoracic nodal disease in the management of patients with junctional oesophageal cancer.

Material and Methods: Retrospective analysis of all patients who underwent EUS-FNA of high mediastinal nodes during a 9-year period. Review of staging CT, CT-PET, EUS, EUS-FNA data and MDT case notes and pathology. The impact of EUS-FNA on patient staging and treatment pathway was documented.

Results: 168 consecutive patients underwent EUS-FNA of high mediastinal nodes. Adenocarcinoma was identified in 25 samples (14.88%), squamous cell carcinoma in 30 patients (17.86%), lymphoma in 13 samples (7.74%), benign pathology in 53 patients (31.54%) and other pathology in 47 samples (27.98%). Following MDT discussion, patients with junctional oesophageal malignancy and positive EUS-FNA cytology, management was altered in 35 patients (63.64%).

Conclusion: EUS-FNA of high mediastinal nodes in patients with junctional tumours has a direct impact of patient management and appropriate treatment pathways.

SS 4.03

T staging and diffuse type of Lauren's classification as surrogate endpoints of gastric adenocarcinoma N staging by MDCT

R. Mateus Marques, P. Mendonça, P. Santos, N.V. Costa, J. Esteves, M. Oliveira, L. Costa, J. Guedes Da Silva, A.C. Fradique; Lisbon/PT

Purpose: MDCT has some limitations in N staging of gastric adenocarcinoma (GA). The purpose of our study is to evaluate T staging and diffuse type of Lauren's classification as surrogate endpoints (SE) to improve N staging of GA by MDCT.

Material and Methods: Between January 2010 and July 2013, 102 patients were retrospectively evaluated according with following criteria: endoscopic diagnosis of GA, gastrectomy associated with retrieval of at least 15 loco-regional nodes and state-of- the-art MDCT (three cases with complementary MRI) performed less than 60 days before surgery. Staging was performed in consensus by two radiologists, considering two steps. Step one (S1): N staging by imaging (NSI) versus N staging by pathology. Step two (S2): the same with adding one level to NSI in patients with T4 staging by imaging or with diffuse type of Lauren's classification. Absolute agreement and effectiveness analysis of diagnosing stage N2 or higher were compared.

Results: Absolute agreement raised from 49% to 60.7% from S1 to S2 (Chi-square p-value 0.091, not statistically significant). From S1 to S2: sensitivity and NPP raised 0,711 to 0.844 and 0.812 to 0.889 respectively, specificity and PPP lowered 0.982 to 0.883 and 0.970 to 0.905, respectively.

Conclusion: Aforementioned SE are useful to increase absolute agreement of NSI in GA and increased NPP of NSI N2 or higher. With further SE statistically significant results may be possible.

SS 4.04

Accuracy of radiological staging in identifying poor prognostic factors in colon cancer

G. Gossedge, A. Hood, S. Sook-Cheng Chin, L. Saraswat, H. Lambie, R. Hyland, D. Jayne, D.J.M. Tolan; Leeds/UK

Purpose: Within the context of the FOxTROT trial, CT can identify 'poor prognosis' colon cancer patients with a sensitivity of 78% and a specificity of 67%. We aimed to undertake a 'pragmatic' study of the diagnostic accuracy of routine radiological staging in colon cancer following completion of the pilot phase of FOxTROT, at a single institution.

Material and Methods: Consecutive primary colon cancer patients, discussed at MDT between October 2011 and October 2013, had their pre-operative CT images evaluated according to TNM staging, prior to surgery. Following surgery, radiological staging was correlated with histopathological staging (TNM 5) as the reference standard. Patients with synchronous tumours and distant metastases were excluded. Patients were stratified according to 'good' (T2 or less, N0, and absence of extramural venous invasion (EMVI)) or 'poor' prognosis (T3 or more, N1 or more, or presence of EMVI).

Results: Of 172 cases, the sensitivity, specificity, positive and negative predictive values for stratification by CT compared with histological examination were 82% (95% CI: 75-88), 76% (95% CI: 54-90), 95% (95% CI: 90-98) and 42% (95% CI: 27-57), respectively, with a diagnostic odds ratio of 14.73. Accuracy for detecting malignant lymph nodes and EMVI was 68% and 69%, respectively. R0 resections were performed in 92% of cases.

Conclusion: Outside the context of a clinical trial, radiological staging using CT is accurate and feasible and can stratify patients for neo-adjuvant therapies.

SS 4.05

Colon cancer lymph node metastases: where are we going wrong?

R. Wiles, E. Hall, P. Healey; Liverpool/UK

Purpose: Accurately diagnosing lymph node metastases in colon cancer is notoriously difficult. The study aim is to determine our accuracy in nodal staging and, when we overstage, what features of the nodes contribute to this.

Material and Methods: Preoperative CT scans of 50 patients with histologically proven colon cancer were independently reviewed by two radiologists (two cases were later excluded due to non-visualisation of the tumour). Data recorded included: suspected number of involved nodes, short axis length, shape and character of the most suspicious node. Histological findings were compared with the recorded data.

Results: Reader 1 and 2 agreed on lymph node staging in 62.5% of cases. Reader 1 correctly staged 45.8% of cases, overstaged 47.1% and understaged 12.5%. Values for reader 2 were 52.1%, 29.2% and 18.8%, respectively. In 15 cases, one or both reader overcalled when histological N=0. The readers agreed in 10 of these cases (67%). Nodal characteristics in these cases were

reviewed. 96% of overcalled nodes measured >5 mm. 88% had at least one feature of round shape, irregular border or short axis diameter >9 mm. 56% had two of these features and 4% had all three.
Conclusion: In our practice, as with other studies, nodal staging is inaccurate using CT. Overcalling was more common than undercalling nodal metastases, but both occurred. Abnormal nodal shape, outline or size does not accurately predict metastatic involvement.

SS 4.06

Transrectal ultrasound and 3-Tesla magnetic resonance imaging in preoperative staging of rectal cancer: a performance comparison

E. Guidi[1], R. Scandiffio[1], L. Faggioni[1], R. Balestri[1], G. D'Ippolito[2], P. Buccianti[1], C. Bartolozzi[1]; [1]Pisa/IT, [2]Sao Paulo/BR

Purpose: To evaluate the agreement between transrectal ultrasound (TRUS) and magnetic resonance imaging (MRI) in preoperative staging of rectal cancer.
Material and Methods: 50 patients with rectal cancer underwent TRUS and 3-Tesla MRI for preoperative staging. With both imaging techniques were evaluated the following features: lesion site, tumour longitudinal extent, distance between lesion and puborectalis muscle, levator ani muscles infiltration, depth of extramural spread and lymph nodes involvement. The correlation between MRI and ultrasound data was calculated for each parameter using the Spearman rank test and considering statistically significant p-values <0.05.
Results: TRUS and MRI showed a statistically significant correlation for the lesion site (rs = 0.8597, p <0.0001), the tumour longitudinal extent (rs = 0.446, p = 0.0022), the distance between lesion and puborectalis muscle (rs = 0.80, p <0.0001) and the depth of extramural spread (rs = 0.5279, p <0.0001). Moreover, TRUS and MRI were able to demonstrate the levator ani muscles infiltration with an overall agreement of 78% and the lymph nodes involvement with an accordance of 76%. MRI allowed, however, the evaluation of other very important features for the correct staging of rectal cancer, in particular the distance between lesion and mesorectal fascia.
Conclusion: The excellent agreement between MRI and TRUS in preoperative staging of rectal cancer argues in favor of the use of MRI, because it also allows a more comprehensive local assessment.

SS 4.07

Initial staging of locally advanced rectal cancer and regional lymph nodes: comparison of diffusion-weighted MR-imaging with 2-deoxy-2-[18F]fluoro-D-glucose positron emission tomography/computed tomography

M. Cerny, S. Schmidt, J. Prior, D. Hahnloser, R. Meuli, V. Dunet; Lausanne/CH

Purpose: To compare diffusion-weighted MR-imaging (DWI) parameters with 2-deoxy-2-[18F]fluoro-D-glucose positron emission tomography/computed tomography (FDG-PET/CT) in locally advanced primary rectal tumour.
Material and Methods: Seventeen patients with histologically confirmed and locally advanced untreated rectal adenocarcinoma (T3 and T4) were prospectively enrolled from October 2012 to June 2013. All the patients underwent a whole body 1.5T DWI MRI (b0, b1000) and a whole body FDG-PET/CT within the same week. FDG-PET/CT was considered as the standard reference. In consensus, two independent readers measured maximum and mean FDG standardized uptake values (SUV_{max} and SUVmean) of the rectal tumour and of the pathologic regional lymph nodes on PET/CT and compared these values to minimum and mean values of apparent diffusion coefficient (ADCmin and ADCmean), displayed on maps generated from DWI.
Results: Regarding the tumour (n=17), we found a significant negative correlation between SUVmean and the corresponding ADCmean values (Spearman's rho=–0.63, p=0.006) and between ADCmin and SUV_{max} (Spearman's rho=–0.55, p=0.02). Regarding the lymph nodes (n=28), ADCmean showed a significant negative correlation with the corresponding SUVmean values (Spearman's rho=–0.42, p=0.03). There was no significant correlation between ADCmin and SUV max.
Conclusion: Our significant negative correlations between ADC and SUV suggest an association between tumour cellularity and metabolic activity in primary untreated rectal adenocarcinoma. Further studies are needed to determine, if DWI can predict histopathological response of the tumour to neoadjuvant chemoradiation.

SS 4.08

Remaining malignant lymph nodes in good responders after chemoradiotherapy for rectal cancer: where are they located?

L.A. Heijnen[1], D.M.J. Lambregts[1], S.-X. Rao[2], M.H. Martens[1], G.L. Beets[1], R.G.H. Beets-Tan[1], M. Lahaye[1]; [1]Maastricht/NL, [2]Shanghai/CN

Purpose: When considering local excision or 'wait-and-see' after CRT in rectal cancer, nodal status is crucial. In spite of a good tumour response, any remaining N^+-nodes harbour a risk for recurrence. Knowledge on the presence and location of these remaining N^+-nodes may help guide treatment intensification (e.g. boost radiotherapy). Aim of this study was to investigate patterns in the location of remaining N^+-nodes in good responders after CRT.
Material and Methods: 211 locally advanced rectal cancer patients underwent CRT, which resulted in a good response (downstaging to ypT0-2) in 134 patients, who constituted the final study group. For the patients with a ypT0-2N^+ status, a detailed lesion-by-lesion comparison between restaging-MRI and histology was performed on the location of the individual N^+-nodes.
Results: 8/134 patients (6%) had a ypT0-2N^+ status. 47% of the N^+ nodes was located at the same height as the tumour, 53% was located at a distance of 1.2-6.5 cm above the tumour level (of which 40% within <5 cm from the tumour and 60% >5 cm above). In the axial plane, 71% of the nodes was located near (within <1 cm from) the tumour/rectal lumen.
Conclusion: 1. The incidence of remaining N^+-nodes in case of good tumour response is very low. 2. Remaining N^+-nodes are solely located at the same level or proximal to the tumour. 3. The majority of N^+ nodes are located near the tumour/lumen.

SS 4.09

How accurate is MRI in predicting a positive/negative surgical margin in patients with recurrent rectal cancer

D. Mondal, R. Hyland, H. Lambie, N. Scott, P. Sagar, D.J.M. Tolan; Leeds/UK

Purpose: Recurrent rectal cancer has a poor prognosis and curative resection is associated with significant morbidity. MRI detects the site and extent of local recurrence. It may also be able to predict a positive surgical margin, to allow optimal selection of patients for surgical resection. This study assesses whether MRI predicts involvement of the surgical margin in patients with recurrent rectal cancer.
Material and Methods: Patients with recurrent rectal carcinoma being considered for surgery in a national recurrent rectal cancer centre were studied over a 7-month period from January 2013. Radiology was reviewed and data collected including site(s) of recurrence, pelvic structures involved and predicted positive/negative surgical margin. Pathological reports were assessed for correlation.
Results: 51 patients were eligible. 21/50 patients proceeded to surgical resection; one was excluded with no pathology specimen for correlation. In 17/21 patients, radiological prediction of a positive or negative surgical margin was confirmed. In 4/21 patients, radiology and pathology did not match: one patient had a long time interval (5 months) between MRI and surgery; 2/21 patients had post-chemoradiotherapy complete tumour response with fibrosis and scan to surgery interval of >3 months; in 1/21 patients, a positive margin in the surgical specimen was not predicted on MRI. MRI assessment in recurrent rectal cancer has sensitivity 88.2%, specificity 50%, PPV 88.2% and NPV 50%.
Conclusion: MRI can pre-operatively predict margin status in recurrent rectal cancer.

SS 4.10

withdrawn by the authors

11:00 - 12:30 **Papageno**

Scientific Session 5

Imaging of Crohn's disease

SS 5.01

Grading of Crohn's disease activity using CT, MRI, US and scintigraphy: a meta-analysis

C.A.J. Puylaert, J.A.W. Tielbeek, S. Bipat, J. Stoker; Amsterdam/NL

Purpose: To assess the role of computed tomography (CT), magnetic resonance imaging (MRI), ultrasonography (US) and scintigraphy in grading Crohn's disease (CD) activity.

Material and Methods: MEDLINE, EMBASE and Cochrane databases were searched for studies evaluating CT, MRI, US and scintigraphy in grading CD activity as compared to (ileo)-colonoscopy, biopsies or intraoperative findings as the reference test. Two independent reviewers assessed the data. Three-by-three tables (none, mild, frank disease) were constructed for all studies and overall grading accuracy, overgrading and undergrading were calculated/summarized by fixed or random effects models.

Results: Our search yielded 9024 articles, from which 19 articles were determined eligible for inclusion. A total of 549 patients were included. Per-patient data showed overall grading accuracy values for CT, MRI, US and scintigraphy of 86% (95% CI: 75–93%), 84% (95% CI: 67–93%), 44% (95% CI: 28–61%) and 40% (95% CI: 16–70%), respectively. CT and MRI data were pooled and showed similar overall grading accuracy estimates (P=0.8). Per-segment data showed overall grading accuracy values for CT, MRI, US and scintigraphy of 87% (95% CI: 77–93%), 78% (95% CI: 72–82%), 66% (95% CI: 52–78%) and 86% (95% CI: 80–91%), respectively. CT showed similar grading accuracy to MRI (P=0.08) and scintigraphy (P=0.8). Both CT and scintigraphy showed higher grading accuracy than US (P=0.001 and P=0.003, respectively).

Conclusion: CT and MRI showed comparable high accuracy values both in the per-patient and in the per-segment analyses. Results for US and scintigraphy were inconsistent and limited data was available.

SS 5.02

The value of clinical and MR imaging findings as independent predictors of Crohn's disease activity in patients scanned by gadobenate dimeglumine-enhanced MR enterography

E. Quaia, B. Cabibbo, L. De Paoli, A.G. Gennari, M.A. Cova; Trieste/IT

Purpose: To define the best clinical and imaging-independent predictors for active inflammation in patients with Crohn's disease (CD) examined by gadobenate dimeglumine (Gd-BOPTA)-enhanced magnetic resonance (MR) enterography with dynamic scanning.

Material and Methods: Ninety patients (46 M and 44 F; mean age ± SD, 39.4 ± 17.3 years) with a biopsy-proven diagnosis of CD activity index ≥150 (n=34 patients) or <150 (n=56) underwent MR enterography including TSE T2-weighted, FFE T1-weighted, and fat-suppressed THRIVE 3D T1-weighted sequences after Gd-BOPTA injection during arterial (30 s), portal venous (70 s), and delayed phase (3 and 5 min from contrast injection). Two readers analysed the MR images in consensus. Reference standard was the Rutgeerts's modified endoscopic grading system with deep mucosal biospy on the terminal ileal loop. Analysis of covariance (ANCOVA) was performed to assess clinical (CDAI and calprotectin levels) and MR imaging findings as predictors of inflammatory disease activity. A difference with P < .05 was considered statistically significant.

Results: Patients revealed prevalently fibrotic (n=43 patients) or prevalently active CD (n=47). Calprotectin levels (25.6; 2.92-224.01), length of the involved loop (Odds Ratio, OR 25.66; 95% confidence intervals, CIs 4.97-132.32), multiple loop involvement (5.89; 0.65-53.11), and T2 hyperintensity (25.6; 2.92-224.01) were independent predictors of active CD.

Conclusion: Calprotectin levels and different MR imaging findings were predictors of active disease in patients with CD examined by Gd-BOPTA-enhanced MR enterography.

SS 5.03

Monitoring Crohn's disease during anti-TNF-α therapy using MRI enterography: correlation between a magnetic resonance enterography global score and clinical assessment of disease activity

D. Prezzi, G. Bhatnagar, J. Makanyanga, R. Vega, S. Halligan, S.A. Taylor; London/UK

Purpose: To assess the ability of a global MRI score of activity (MEGS) to characterise disease response to anti-TNF-α therapy compared to a combined clinical reference standard.

Material and Methods: Thirty-two Crohn's disease patients (median age 32, male 18) commencing anti-TNF-α therapy with concomitant baseline MR enterography were retrospectively identified. Clinical course was followed for 3 years, patients undergoing at least 2 further MRIs. Scan order was randomised and the MEGS score (a published global activity score based on subjective segmental scoring of activity metrics including mural thickness, enhancement, T2 signal, disease length and extra-enteric complications) was applied by two blinded radiologists. Based on clinical status, CRP and endoscopy reports a gastroenterologist classified patient activity at the time of each MRI into remission, mild, moderate and severe, and into responders versus non responders to therapy. On statistical advice MEGS and clinical scores were compared using Mann-Whitney, Kruskall-Wallis and Spearman's rank.

Results: Mean MEGS significantly decreased among baseline (28.7), first (14.8) and second (12.0) follow up (P=0.039). MEGS decreased significantly between baseline and first follow up in clinical responders (n=25, P=0.014) but not in non-responders (n=7; P=0.805). There was a significant positive correlation between MEGS and clinical activity classification (r=0.499; P<0.001).

Conclusion: MEGS shows good correlation with clinical assessment of disease activity and can categorise response to anti-TNF-α therapy.

SS 5.04

MRI textural analysis in Crohn's disease is associated with histological and MRI disease activity

J. Makanyanga, B. Ganeshan, M. Rodriguez-Justo, G. Bhatnagar, A. Groves, S. Halligan, K. Miles, S.A. Taylor; London/UK

Purpose: Textural analysis (TA) imaging is proposed as an imaging biomarker of histopathological signatures in neoplasia. The purpose was to explore TA of MRI in Crohn's disease (CD) in comparison to validated MRI and histological disease activity scores.

Material and Methods: 16 patients undergoing ileal resection for CD underwent 1.5T MR enterography. A validated MRI CD activity score (CDA) based on mural thickness, T2 signal and enhancement was derived from large ROIs placed in the bowel destined for resection. Small ROIs were also placed corresponding to sites of histological sectioning from which histological acute inflammatory scores (AIS) were derived. TA features were extracted from both ROI sizes on axial single-shot turbo spin-echo (SSTSE) images using TexRAD software, which utilises an image filtration-histogram technique. Univariable regression analysis tested associations between TA and CDA parameters (large ROI) and AIS (small ROI).

Results: Skewness (2 mm filter) was positively associated with AIS (coefficient 4.27, p=0.02). Entropy (large ROI at 2 mm, 3 mm and 4 mm filters) was positively associated with T2 signal [odds ratio (OR) 2.32 to 3.16, p=0.02 to 0.004]. Mean of positive pixels was positively associated with mural thickness (filter 2 mm, OR 0.91, p=0.04) with a negative association to CDA (filters 2 mm, 3 mm and 5 mm), coefficients -0.16 to -1.15, p=0.03 to 0.008.

Conclusion: TA features show variable associations to both MRI and histological CD activity scores and further research is indicated.

SS 5.05

The value of time-intensity curves obtained after microbubble contrast agent injection to discriminate responders from non-responders to anti-inflammatory medication among patients with Crohn's disease

E. Quaia, B. Cabibbo, R. Angileri, M.A. Cova; Trieste/IT

Purpose: To assess the value of time-intensity curves obtained after sulphur hefluoride-filled microbubble contrast agent injection to differentiate responders from non-responders to anti-inflammatory therapy in patients with Crohn's disease.

Material and Methods: Ten patients (6 male and 4 female; mean age ± SD, 50 years ± 6) with a biopsy-proven diagnosis of Crohn's disease involving the terminal ileal loop were included. In each patient the terminal ileal loop was scanned after microbubble injection 1–30 days before and 6 weeks after the

beginning of specific anti-inflammatory treatment. In each patient, the variation (Δ = before – after 6 weeks of therapy) of the area under the time-intensity curve during the wash in, the peak enhancement, and the time to peak enhancement were related to the therapeutic outcome assessed after 12–18 weeks from the beginning of pharmacologic treatment by CDAI and/or endoscopy.

Results: Responders (n=7 patients) vs non-responders (n=3) differed in the Δ of area under time-intensity curve during washin (37669.3 ± 386.39 vs 621.58 ± 374.53 P<.05) and in the peak enhancement (28085.68 ± 444.41 vs 9795.11 ± 345.22, P<.05) while did not differ in the time to peak enhancement (–3.29 ± 1.02 vs -3.01 ± 1.06 secs, P=.15).

Conclusion: The Δ of the area under time-intensity curve during washin and peak enhancement after microbubble injection may differentiate responders from non-responders in patients with Crohn's disease.

SS 5.06

Interobserver agreement of MEGS in serial MR enterography for Crohn's disease

D. Prezzi, G. Bhatnagar, J. Makanyanga, R. Vega, S. Halligan, S.A. Taylor; London/UK

Purpose: To assess interobserver agreement of MEGS, a global MR enterography activity scoring system in Crohn's patients receiving anti-TNF-alpha therapy.

Material and Methods: Thirty two Crohn's disease patients (median age 32, male 18) receiving anti-TNF-α therapy and serial MR enterography follow up (mean 3 MR's over 3 years) were retrospectively identified. Ninety-four MR's were scored independently and in random order by two radiologists, blinded to clinical data, using MEGS, a previously published subjective activity scoring system. Small bowel and colonic segmental mural thickness, T2 signal, enhancement/enhancement pattern, mesenteric oedema and colonic haustral loss were scored in each of nine segments; segmental scores were adjusted for disease length; a global score was derived including scores for the presence of lymphadenopathy, comb sign, fistulae and abscesses. On statistical advice, interobserver agreement was assessed using the 95% Bland-Altman limits of agreement (BA LoL) and intra-class correlation coefficient for continuous data.

Results: MEGS values ranged from 0 to 163. The mean difference between observers' scores was +1.1 (BA LoL -14 to +16) with intra-class correlation coefficient of 0.98 (95% CI 0.97 to 0.99). Agreement was superior in patients with quiescent disease or mild activity (MEGS ≤15) (BA LoL, -7 to +7).

Conclusion: MEGS demonstrates good interobserver agreement even in patients with mild activity and subtle changes on MRI when agreement may be expected to deteriorate.

SS 5.07

Diffusion MRI in Crohn's disease as marker of global activity: comparison with fecal calprotectin

D. Pendse, J. Makanyanga, A. Plumb, D. Atkinson, S. Halligan, S.A. Taylor; London/UK

Purpose: To evaluate diffusion-weighted imaging (DWI) as a measure of global Crohn's disease activity against a reference standard of faecal calprotectin (fC).

Material and Methods: 69 patients (age, sex) with cdisease underwent MR enterography including axial DWI (b0, 50, 100, 300, 600, 800) on either 1.5T or 3.0T platforms, providing a same-day stool sample for fC assay. Enteric signal intensity on high B value DWI images was scored (0-normal 1-probably normal, 2 probably abnormal 3-definitely abnormal by 2 radiologists in consensus. The extent of any DWI abnormally was then classified into small bowel alone (<10 cm or >10 cm), colon alone or both small bowel and colon. fC was compared according to DWI signal intensity and disease extent using Wilcoxon rank sum and Kruskal Wallis analysis of variance.

Results: Mean fC score was 398 ug/g (range 0-1970 ug/g), and raised (>120 ug/g) in 44/69 patients. In patients scored probably or definitely abnormal on DWI, fC was significantly higher than in those scored normal or probably normal (492±422 ug/g vs 159±257 ug/g, p<0.0001). DWI had sensitivity 84%, specificity 52% for raised fC. There was a significant difference in fC according to DWI defined disease extent, being lowest in isolated small bowel disease <10 cm and highest in patients with both colonic and small bowel involvement.

Conclusion: Qualitative assessment of diffusion MRI is sensitive to the severity and extent of Crohn's disease activity against a global reference standard of calprotectin.

SS 5.08

Diffusion MRI in ileal Crohn's disease: ADC value may discriminate between grades of disease activity

D. Pendse, A. Plumb, J. Makanyanga, D. Atkinson, S. Halligan, S.A. Taylor; London/UK

Purpose: To investigate the performance of apparent diffusion coefficient (ADC) in assessment of disease activity severity in patients with ileal Crohn's disease.

Material and Methods: 33 patients (age 18-67) with active ileal Crohn's disease underwent MRE using a standard protocol following 1l of 2.5% mannitol on 1.5T (N=18) and 3.0T (N=15) systems. Axial fat-saturated EPI diffusion weighted imaging (DWI) was performed using B values B=0, 50, 100, 300, 600, 800 s/mm^2. ADC was quantified in the ileum independently by two radiologists via regions of interest placed at the site of maximum DWI abnormality and averaged between the two. A MR-enterography global score (MEGS) evaluating ileal mural thickness, T2 signal, enhancement, enhancement pattern, disease length and extra-enteric complications, previously validated against endoscopic biopsy and calprotectin was used as a reference standard. Data were correlated using Spearman rank.

Results: ADC (mean 1642, range 1015-2793 x10^{-6} mm^2/s) was inversely correlated to MEGS (Spearman's rho=-0.34, P=0.05). Mean ADC was not significantly different between 1.5T (1679±496 x10^{-6} mm^2/s) and 3.0T (1596±414 x10^{-6} mm^2/s). In patients mild disease (MEGS <10), mean ADC (1801±537 x10^{-6} mm^2/s) was significantly higher than in those with moderate/severe disease (MEGS ≥10) (ADC=1473±278 x10^{-6} mm^2/s) p=0.0359.

Conclusion: DWI has previously been shown to discriminate between normal and inflamed bowel but may be able to differentiate grades of activity within Crohn's affected bowel.

SS 5.09

Development of a new tool to assess Crohn's disease magnetic resonance inflammation severity

M. Zappa[1], Y. Bouhnik[1], V. Abitbol[2], M. Lewin[3], M. Boudiaf[2], J. Cosnes[2], V. Vilgrain[1], J.-Y. Mary[2]; [1]Clichy/FR, [2]Paris/FR, [3]Villejuif/FR

Purpose: To develop a small bowel CD magnetic resonance index of inflammation severity (CDMR-IS).

Material and Methods: Thirteen centres participated in this prospective transversal study. Selected MR-DVDs (6 per centre) were blinded and allocated to others centres. A combined reading was conducted by a pair of radiologist and gastroenterologist in each centre. Total length and number of 20 cm-diseased segments were noted. In each segment, following data were recorded: wall thickness, T2 wall hypersignal, T1 degree of intensity and pattern of enhancement, deep ulceration, comb sign, sclerolipomatosis, lymph nodes, fatty infiltration, fistula and abscess. For each MR examination, global inflammation severity (GIS) was evaluated qualitatively using a linear analog scale. To construct the CDMR-IS, multivariate linear mixed model was used with forward selection through likelihood ratio test.

Results: 438 readings were analysed. Mean of GIS was 20.7. The independent predictors of the GIS were the number of segments (n) with the following independent predictors : T1 mild to moderate intensity of enhancement (MM), T1 severe intensity of enhancement (S), deep ulceration (DU), comb sign (CS), any fistula (F), and abscess (A). This leads to build the formula: CDMR-IS=2*n MMT1+3*nST1+nDU+nCS+3*nF+4*Na.

Conclusion: The CDMR-IS is a standardized index to evaluate the severity of inflammation in patients with small bowel CD. Further studies are mandatory for validation of CDMR-IS in new patients, and to study its sensitivity to change after anti-inflammatory treatment.

SS 5.10

Correlation between morphological expansion and impairment of motility in inflammatory small bowel lesions in patients with Crohn's disease: preliminary data

S. Bickelhaupt, M. Wurnig, A. Boss, M.A. Patak; Zurich/CH

Purpose: The aim of this study is to investigate if alterations of motility in inflamed small-bowel segments correlate with length, wall-thickness and prelesionary dilatation of inflammatory small bowel lesions in patients suffering from Crohn's disease assessed with MRI.

Material and Methods: This retrospective, IRB approved study included 25 patients (12 males, 13 females, 18-77y) with inflammatory lesions examined using magnetic resonance imaging enterography (MRE). Cine MRE was performed using a coronal 2D steady-state free precession sequence (TR 2.9, TE 1.25, matrix 224x160, slice-thickness 10 mm, number-of- time-points 90)

on a 1.5 T MRI scanner. Small bowel motility was examined using a dedicated MR-motility assessment software (Motasso). Motility patterns (contraction frequency, relative occlusion rate and mean diameter) were assessed in correlation to wall thickness, length and prelesionary dilatation of the lesions. Statistical analysis was performed by calculation of the Pearson's-Correlation coefficient.

Results: The length of the inflammatory segments, the wall thickening and prelesionary dilatation did not correlate with the frequency of the contractions (r=0.17, p=0.477; r=0.316, p=0.123; r=0.161, p=0.441) or the impairment of luminal occlusion (r=0.274, p=0.184; r=0.199, p=.0339; r=0.015, p=0.945) and only the prelesionary dilatation (r=0.410, p=0.042) correlated to the mean luminal diameter of the segment.

Conclusion: The degree of motility impairment within inflammatory small bowel lesions does not significantly correlate with the extent of the lesion. This could indicate that motility changes have a segmental pattern, independent of length and wall thickness.

SS 5.11

Changes in global small bowel motility in response to inflammation in Crohn's disease

G. Bhatnagar, J. Makanyanga, D. Atkinson, D. Pendse, A. Menys, S.A. Taylor; London/UK

Purpose: To investigate whether small bowel motility is inhibited by the burden of inflammatory activity in Crohn's disease (CD).

Material and Methods: 71 CD patients (median age 33, range 16-78) prospectively underwent enteric MRI with motility assessment (1L 2% Mannitol prep; 1.5T Siemens (TrueFISP, TR=3.85 ms, TE=1.93 ms,) or 3T Philips Achieva (Philips: BTFE, TR=1.96, TE=0.98); slice thickness 10 mm, temporal resolution 1 image/s). Sequential motility blocks encompassed the whole small bowel volume. Motion analysis employing a modified 2D optic-flow technique to register the dynamic series and generate deformation fields generated 3 parameters for the whole small bowel volume; average global motility (A.U), global variance (A.U) and contraction rate (CPM). Global disease activity was assessed by same day faecal calprotectin (fC), and correlated using Spearman's Rank correlation.

Results: Mean fC score 398 µg/g (0-1970 µg/g) with correlations as follows: mean global motility score 0.3A.U (range 0.15-0.5), Spearman's Rho 0.02, P=0.88. Mean global variance score 0.012A.U range (0.001-0.338), Spearman's Rho 0.36, P=0.026. Mean contraction rate 5CPM (range 0-8), Spearman's Rho 0.02, P=0.84.

Conclusion: Global motility is not inhibited by inflammatory activity in CD contrasting previous published pilot data. However, a small but significant negative correlation between fC and variance in the motility score suggests inflammatory burden may derange motility coordination, possibly reducing the magnitude of normal intrinsic regional variation.

11:00 - 12:30 **Europa Hall**

Scientific Session 6

Pancreas: various neoplasms and inflammation

SS 6.01

Correlation between MDCT features of endocrine tumors of the pancreas and their behavior

F. Lombardo, G.A. Zamboni, M.C. Ambrosetti, R. Pozzi Mucelli; Verona/IT

Purpose: To correlate the CT features of endocrine tumors of the pancreas with their behaviour.

Material and Methods: We reviewed the multiphasic MDCTs performed on 36 patients (17 M, 19 F; mean age 52.5 years) with 38 endocrine tumors (1 patient had 3 tumors). Associations between tumor size, vascularity, homogeneity, growth type, presence of metastases and vascular invasion at CT were evaluated with Fisher's and t tests. Tumor size, hypervascularity, growth pattern and homogeneity were compared with the proliferative index (Ki-67) from the pathology reports.

Results: Mean tumor diameter was 4.26 cm (0.8-14cm). 27 tumors were hypervascular in the late arterial phase, 11 were not. 20 tumors were inhomogeneous and 18 homogeneous. 29 tumors had expansive growth and 9 infiltrative. 8 patients had liver metastases at CT, and 28 did not. There was no significant difference in tumor diameter between patients with or without liver metastases. Infiltrative growth pattern at CT was significantly associated with the presence of liver metastases (p=0.0089). No association was observed between tumor size, vascularity or homogeneity and presence of liver metastases (p=n.s.). Tumor hypervascularity was significantly associated with Ki-67 <10%. No association was seen between Ki-67 and tumor size, growth pattern or homogeneity.

Conclusion: Tumor hypervascularity at CT is associated with low proliferation index. Infiltrative growth margins are associated with presence of liver metastases. These features appear to be more predictive of tumor behaviour than tumor size.

SS 6.02

MRI of pancreatic neuroendocrine tumors: added value of diffusion-weighted imaging

M. D'Onofrio[1], R. De Robertis[1], P. Tinazzi Martini[1], S. Crosara[1], S. Canestrini[1], M. Pregarz[2], R. Pozzi Mucelli[1]; [1]Verona/IT, [2]Peschiera del Garda/IT

Purpose: To evaluate MR features of neuroendocrine pancreatic tumors, comparing conventional sequences with DW sequences.

Material and Methods: MR examinations of 39 patients with histology-proven pancreatic neuroendocrine tumors were retrospectively evaluated. Both a qualitative analysis (appearance, site, main pancreatic duct dilation, signal intensity) and a quantitative analysis (dimensions, degree of main pancreatic duct dilation, ADC value) were performed.

Results: 69% of lesions were solid, mainly located in the pancreatic head (46%). Mean dimension was 31 mm; mean main pancreatic duct dilation was 7 mm. 79% of lesions did not determine ductal dilation. 74% of lesion were hypointense on T1-weighted images, 56% were hypointense on T1-weighted fat-suppressed images, 57% were hyperintense on T2-weighted fat-suppressed images; 59% of lesions were isointense in pancreatic phase images, 48% were hyperintense during the portal phase. Regarding DWI, 78% of lesions were hyperintense in b=800 images; the majority of T2-isointense lesions showed instead hyperintensity in b=800 images; the majority of isointense pancreatic-phase lesions were hyperintense in b=800 images. Mean ADC value was $1.38\pm0.2\times10^{-3}$ mm^2/s.

Conclusion: DWI depicts a higher number of lesions in comparison with T2-weighted fat-suppressed and pancreatic-phase images, being therefore more sensitive for the identification of pancreatic neuroendocrine tumors.

SS 6.03

Patterns of contrast accumulation for differential diagnosis pancreatic solid tumors with homogeneous contrast enhancement at MDCT

N.Y. Makeeva-Malinovskaya, G.G. Karmazanovsky; Moscow/RU

Purpose: To evaluate the capabilities of contrast-enhanced MDCT for the differential diagnosis of pancreatic solid tumors with homogeneous accumulation of contrast agent.

Material and Methods: Contrast-enhanced MDCT has been done for 74 patients with solid pancreatic tumors. Delta was calculated as difference of the density of tumor and pancreas for all phases of the examination. The calculation formula for the Delta is: T(p)-P(p), for p= {p1,p2,p3,p4}, T – the absolute value of the relative density of the tumor, P – the absolute value of the relative density of the pancreas, p1-pre contrast phase, p2-arterial phase, p3-portal phase, p4 - delayed phase.
Results: 24 patterns of Delta were identified, top eight patterns amount 73% of patients (n=54). All tumors were segmented into two classes by accumulation of contrast agents in tumor versus pancreatic parenchyma in the arterial phase: 1. "Adenocarcinoma" - accumulation in tumor is lower than in pancreatic parenchyma. 2. "Not adenocarcinoma" - accumulation in tumor is higher than in pancreatic parenchyma. "Adenocarcinoma" were detected for 65% of patients (n=35). Morphological types of the tumors: adenocarcinoma 85.7% (n=30), neuroendocrine neoplasms 8.6% (n=3), solid pseudopapillary tumor (SPT) 5.7% (n=2). "Not adenocarcinoma" were detected for 35% patients (n=19). Morphological types were: adenocarcinoma 5% (n=1), neuroendocrine neoplasms 80% (n=15), SPT 5% (n=1), metastasis of renal cancer 10% (n=2).
Conclusion: Applicability for pancreatic solid tumors differentiation by MDCT: sensitivity 88%, specificity 80%, accuracy 90%.

SS 6.04

MRI features of the solid pseudopapillary neoplasm of the pancreas

A. Ventriglia, E. Boninsegna, S. Mehrabi, R. Manfredi, R. Pozzi Mucelli; Verona/IT

Purpose: To evaluate the magnetic resonance imaging (MRI) findings of the solid-pseudopapillary neoplasm (SPN) of the pancreas.
Material and Methods: From January 2006 to June 2012, 41 patients with SPN of the pancreas were retrospectively evaluated. Inclusion criteria were the execution of an MR examination and a tumor resection with an histopathological evaluation at our Institution. Exclusion criteria were the execution of a CT or an ultrasonography (15/41) and the execution of imaging examinations at other centers (10/41). The quantitative analysis included: maximum size of the lesion, wall thickness and maximum diameter of the main pancreatic duct (MPD); the qualitative analysis evaluated: location (head/body-tail), shape (round/oval/lobulated), margins (regular/irregular), and signal intensity on T1 and T2-weighted images compared to the surrounding pancreas (hypo-, iso-, or hyperintense and homogeneous or heterogeneous), appearance of MPD and the secondary ducts and the presence of metastases.
Results: The population comprised 16 women (median age: 30y) with a median tumor size of 41 mm, a median wall thickness of 2.1 mm and median diameter of the MPD of 1.8 mm. 9/16 were at the head; 7/16 on the body/tail: respectively 8/16 round, 6/16 oval and 2/16 lobulated. On T1-weighted images 8/16 appeared homogeneously hypointense, 6/16 heterogeneously hypointense and 2/16 heterogeneously hyperintense. On T2-weighted appeared images 1/16 homogeneously hyperintense and 15/16 heterogeneously hyperintense. No metastasis were detected at time of diagnosis.
Conclusion: MR imaging features help the diagnosis of SPN.

SS 6.05

Acoustic radiation force impulse imaging of focal pancreatic lesions

M. D'Onofrio, R. De Robertis, C. Poli, S. Crosara, S. Canestrini, G. Puntel, E. Demozzi, R. Pozzi Mucelli; Verona/IT

Purpose: To evaluate the application of acoustic radiation force impulse (ARFI) elastosonography with virtual touch tissue quantification for the characterization of focal pancreatic lesions.
Material and Methods: 120 patients with pancreatic lesion (64/120 solid; 36/120 cystic) were prospectively enrolled. 5 measurements were performed on each lesion with virtual touch tissue quantification. Different shear wave speed cut-off were chosen to identify ductal adenocarcinomas. Lesions with >1 measurement (analysis method 1) or >2 measurements (analysis method 2) above each cut-off were calculated. Sensitivity, specificity, positive and negative predictive values and accuracy of both methods were calculated. The evaluation of cystic lesions aimed to differentiate serous (benign) from mucinous (potentially malignant) lesions. The non-numerical value "XXXX/0" identifies serum. To identify mucinous content, two analysis methods were chosen: >2 measurements with numerical result (analysis method 3) or prevalence of numerical values upon all measurements (analysis method 4).
Results: Analysis method 1 with a 2.00 m/s cut-off has the highest accuracy for adenocarcinoma identification (78%); 100% specificity and positive predictive value are obtained with a 4.00 m/s cut-off. Sensitivity, specificity, positive and negative predictive values, and accuracy for cystic lesions are respectively: 69%, 54.2%, 64.5%, 59.1%, 62.3% for analysis method 3 and 48.3%, 83.3%, 77.8%, 57.1%, 64.1% for analysis method 4.
Conclusion: ARFI imaging with virtual touch tissue quantification can have a role in the non-invasive characterization of pancreatic lesions.

SS 6.06

Can MRI differentiate mucinous cystoadenomas from cystoadenocarcinomas of the pancreas?

V. Di Paola, F. Castelli, S. Mehrabi, R. Manfredi, R. Pozzi Mucelli; Verona/IT

Purpose: To identify MRI-findings to differentiate mucinus cystoadenomas (MCAs) from mucinus cystoadenocarcinomas (MCACs) of the pancreas to a better surgical planning and prognostic definition.
Material and Methods: 16 Patients were retrospectively included (14F, 2M; mean-age 58), 9 with hystolpathological diagnosis of MCA and 7 of MCAC of the pancreas. In each group we evaluated: size; number of cysts; presence of mucin, presence of mural nodules; presence and enhancement of septa; wall thickness. T-Student-Test for parametric variables and Fisher-test for non-parametric variables were calculated for the two groups; Cohen's-k was calculated to establish the degree of correlation of each feature with lesion malignancy.
Results: The mean size of MCAs and MCACs were respectively 5.5 and 10.5 cm ($p < 0.05$); the mean number of cysts was 2.7 in MCAs and 9.75 in MCACs ($p< 0.05$). Mucin was seen in 1/9 MCA and in 6/7 MCACs ($p<0.05$). Mural nodules were seen in 0/9 MCA and in 6/7 MCACs ($p<0.001$); septa were seen in 7/9 MCAs and in 6/7 MCACs($p>0.05$); among these the septa-enhancement was seen in 1/7 MCA and in 6/6 MCACs ($p<0.05$). The mean septa-thickness was 2.7 cm in MCAs and 8.6 in MCACs ($p<0.001$); the mean wall-thickness was 3.4 cm in MCAs and 9 cm in MCACs ($p<0.05$). The concordance was higher for mural nodules (0.871), septa-enhancement (0.847), septa-thickness and wall-thickness >5 mm (1 and 0.746 respectively), presence of mucin and number of cysts >4 (both 0.746).
Conclusion: MRI features which better allow to differenziate MCAs from MCACs are: mural nodules, enhancement and thickeness of septa >5 mm.

SS 6.07

The value of diffusion-weighted MR imaging for differentiating malignant from benign intraductal papillary mucinous neoplasm of the pancreas

S.-Y. Choi, K.M. Jang, S.H. Kim, J.H. Min, S.J. Lee, D. Choi; Seoul/KR

Purpose: To evaluate whether diffusion-weighted imaging (DWI) adds diagnostic accuracy for differentiating malignant from benign intraductal papillary mucinous neoplasms (IPMN) of the pancreas in comparison with contrast-enhanced MR imaging with MR cholangiopancreatography (MRCP).
Material and Methods: A total of 61 patients with surgically resected IPMNs (19 malignant and 42 benign) who underwent gadoxetic acid-enhanced and DW MR imaging and MRCP were included. Two blinded observers evaluated the two image sets, i.e., conventional MR with MRCP images vs. and combined conventional MR with MRCP and DW MR images, and scored their confidence for malignancy of IPMNs. Qualitative analyses of the IPMNs were also conducted. Diagnostic performance, accuracy, sensitivity, specificity, PPV, and NPV were evaluated and Fisher's exact test was used to compare groups.
Results: The diagnostic performance (area under ROC curve [Az]) with respect to predicting malignant IPMNs improved significantly after additional review of DW images for both observers ($P < 0.05$). The diagnostic accuracy, sensitivity, specificity, PPV, and NPV of combined conventional and DW MR images were higher than those of conventional MR images alone. The presence of diffusion restriction was more often in malignant IPMNs (78.9%) than in benign IPMNs (16.7%, $P < 0.001$) with excellent interobserver agreement ($\kappa = 0.965$).
Conclusion: Adding DW imaging to conventional MR imaging improves diagnostic accuracy with increased specificity for differentiating malignant from benign IPMNs of the pancreas compared with conventional MR imaging alone.

SS 6.08

Utility of DWI sequences in autoimmune pancreatitis before and after steroid therapy

B. Pedrinolla, A. Cybulski, R. Negrelli, S. Mehrabi, R. Manfredi, R. Pozzi Mucelli; Verona/IT

Purpose: To evaluate the utility of diffusion weighted (DWI) sequences in autoimmune pancreatitis (AIP) and to identify typical values of apparent diffusion coefficients (ADC) before and after steroid therapy.

Material and Methods: Between February 2010 and April 2013, we evaluated retrospectively 35 MRI examination with DWI sequences of 25 patients with diagnosis of AIP (19 men, 6 women, mean age 45.7 years). 10/25 patients performed MRI before and after steroid therapy, 3/25 only before and 12/25 only after therapy. Two radiologists separately analyzed each exam, evaluating the signal intensity of the affected parenchyma on T1 and DWI sequences and measuring ADC values (b value 1000 mm^2/s).
Results: In the acute phase AIP appeared hypointense on T1 in 13/13 (100%) and hyperintense in 11/13 (84.6%) patients, with an ADC value of $1.12\pm0.19x10^{-3}$ mm^2/s; after steroid treatment the signal intensity remained hypointense on T1 in 16/22 (72.7%) and decreased on DWI in 17/22 patients (77.3%) with an ADC of $1.44\pm0.16x10^{-3}$ mm^2/s, statistically different from the acute phase value (p=0.0002).
Conclusion: AIP appears hypointense on T1 sequences, hyperintense on DWI and shows a low-ADC value. After steroid treatment, signal intensity in T1 remains low in the most of the cases, but signal intensity on DWI decreases and ADC value increases, reflecting disease activity. DWI and ADC are qualitative and quantitative complementary parameters in evaluation of the response to treatment in course of AIP.

SS 6.09
US-guided fine needle agobiopsy of 1009 focal pancreatic lesions: accuracy and complications
R. De Robertis, M. D'Onofrio, E. Demozzi, E. Martone, S. Crosara, S. Canestrini, R. Pozzi Mucelli; Verona/IT

Purpose: To assess accuracy and short-term complication rate of ultrasound-guided fine-needle aspiration cytologic sampling of focal pancreatic lesions.
Material and Methods: We reviewed 1009 consecutive US-guided fine-needle aspiration cytologic sampling procedures for focal pancreatic lesions from January 2004 to december 2013. The procedures were performed with a 20- or 21-gauge needle. The onsite cytopathologist evaluated the appropriateness of the sample and made a diagnosis. We reviewed the final diagnosis and the radiologic and medical records of all patients for onset of complications during or within 7 days of the procedure.
Results: Sampling was diagnostic in 95.9% of cases. 41/1009 samples were nondiagnostic. In 7/1009 procedures (0.7%) abdominal fluid was found within 72 h after the procedure, mainly after nondiagnostic sample. No major complications occurred.
Conclusion: Ultrasound-guided cytologic sampling is safe and accurate for diagnosis and planning of management of focal pancreatic lesions. With a cytologist on site, the rate of acquisition of samples adequate for diagnosis is high, reducing the need for patient recall.

SS 6.10
Low-tube-voltage CT during the pancreatic parenchymal phase: image quality and radiation dose savings
J.L. Wichmann, P. Majenka, W. Kromen, M. Beeres, R.W. Bauer, M.J. Kerl, T. Gruber-Rouh, R. Hammerstingl, T. Vogl, B. Schulz; Frankfurt am Main/DE

Purpose: To intra-individually compare low-tube-voltage (100 kVp) with standard 120 kVp CT acquisition regarding image quality and radiation dose during the pancreatic parenchymal phase.
Material and Methods: 72 patients with suspected pancreatic pathology underwent abdominal dual-energy CT. 100 kVp and mixed 120 kVp images during the pancreatic parenchymal phase were compared. Signal measurements in the abdominal aorta, peripancreatic fat, pancreatic pathologies and parenchyma were compared. DLP of 100 kVp acquisition and the complete dual-energy CT examination were compared. Three readers subjectively evaluated image quality, delineation, image sharpness and noise of both image series using a five-point Likert scale.
Results: Average DLP of 100 kVp acquisition was 41% lower compared to the complete dual-energy CT examination (356.3 vs. 608.7 mGy cm). Signal of the abdominal aorta, pancreatic parenchyma and pathologies was significantly higher with low-tube-voltage technique ($P < 0.001$). Although readers preferred standard 120 kVp over 100 kVp acquisition regarding image quality (4.94 vs. 4.51), delineation (4.89 vs. 4.72), sharpness (4.91 vs. 4.52) and noise (4.92 vs. 4.22), all image series received a score of at least 4 out 5.
Conclusion: Low-tube-voltage CT at 100 kVp enables significant radiation dose savings while maintaining adequate subjective image quality for examination during the pancreatic parenchymal phase.

11:00 - 12:30 **Mozart**

Scientific Session 7
Focal liver lesions - non-cirrhotic patient

SS 7.01
To compare the per-lesion sensitivity of detection of focal hepatic lesions before and after administration of hepatocyte specific gadolinium chelate (gadobenate dimeglumine) using diffusion-weighted imaging
K. Ganesan, B. Nanda; Mumbai/IN

Purpose: To compare the lesion-to-liver signal intensity ratio on DW images acquired before and after intravenous administration of hepatocyte specific gadolinium chelates.
Material and Methods: 93 patients underwent MR imaging at 3 T for the evaluation of focal hepatic lesions. In these patients, we assessed 93 focal hepatic lesions: 39 HCC, 21 hemangioma, 10 metastasis, 7 cholangiocarcinoma and 16 other focal liver lesions including the following (cysts, FNH, combined neoplasms and granulomas). All patients underwent free breathing DW imaging (b=0 and b=500) before and 5-minutes after intravenous administration of gadobenate dimeglumine (Gd-BOPTA, MultiHance).
Results: Statistical comparison was performed using paired two-sided student t-tests and p=0.05 as threshold for significance. In our study, there was no significant difference in the signal intensity of the lesion at b0 and b500 sec/mm^2 values before and after contrast administration. However, the signal intensity values of liver at b0 and b500 sec/mm^2 following contrast adminsitration were significantly decreased ($p<0.001$). Similarly the mean ADC and mean ADC ratios of the lesion to liver were decreased significantly ($p<0.001$) after contrast administration compared to the precontrast values. This study demonstrated increased conspicuity of the focal liver lesions on the post-contrast DW images.
Conclusion: In this study, we see a trend that supports our hypothesis that DW imaging following intravenous administration of hepatocyte specific gadolinium-based contrast is more sensitive in detecting focal liver lesions vis-a-vis precontrast DW imaging.

SS 7.02
Hypertrophic scar in small focal nodular hyperplasia evaluated with hepatospecific MR contrast media (Gadoxetic acid): a diagnostic challenge?
A. Colleoni, L. Romanini, P. Tessitore, M. Orsatti, F. Laffranchi, L. Grazioli, R. Maroldi; Brescia/IT

Purpose: The differential diagnosis of small FNH (<3cm) with hypertrophic scar, hypointense in the portal and delayed phase after hepatospecific MR contrast media (Gd-EOB-DTPA) could be difficult, especially in oncologic patients. The enhancement pattern of small FNH with hypertrophic scar was therefore evaluated.
Material and Methods: In this retrospective review from 2007 to 2013, we selected 19 liver lesions, of more than 300 nodules characterized as FNH by MR, smaller than 3 cm with hypertrophic scar (>50% of lesion volume). T2w, DWI and not-enhanced T1w signals, the enhancement pattern after Gd-EOB-DTPA in the dynamic study and in the hepatospecific phase (20') of central scar and parenchymal component were evaluated.
Results: The scar was hyperintense on T2w and hypointense on not-enhanced T1w sequences in 84% of cases, showed intense arterial enhancement in 79% of cases, venous washout in 67%, hypointensity at the equilibrium and hepato-biliary phases in all the cases. The thin, peripheral, parenchymal component around the scar was isointense on T2w (74%) and T1w (53%); hyperintense in all dynamic phases, with typical "rim-like" pattern in the hepatospecific phase (100%).
Conclusion: The hypointensity of the hypertrophic scar during the dynamic study with Gd-EOB-DTPA could be misinterpreted, the hyperintensity of the parenchymal rim in hepatobiliary phase has to be the feature to characterize these small FNHs.

SS 7.03
DCE-MRI for differentiation between focal nodular hyperplasia and hepatocellular adenoma
N. Jerjir[1], S. Quenet[2], M. Haspeslagh[1], K. Coenegrachts[1]; [1]Bruges/BE, [2]La Ciotat/FR

Purpose: To analyze (semi-)quantitative parameters of DCE-MRI of focal nodular hyperplasia (FNH) and hepatocellular adenoma (HCA) as an additional tool for differentiation.

Material and Methods: Eight patients with FNH and four with HCA (>2cm) underwent DCE-MRI using breath-hold T1w gradient echo sequence with keyhole imaging and profile sharing after injection of 0.1 ml/kg body weight Gd-BOPTA (Multihance) followed by 20 ml saline injection at 3 ml/s. Rigid liver registration was used. New software was used (OleaSphereTM, Olea Medical SA, La Ciotat, France) in which identical ROIs were placed in parametric maps of K_{trans} and V_e for each lesion. This resulted in quantification of K_{trans} and V_e using the extended Tofts model. Also, the time intensity curves (TICs) were classified in different types. K_{trans} and V_e data were analyzed with independent t-test.
Results: The means of K_{trans} and V_e of both groups were not significantly different (t=0.711, p=0.493 and t=-1.316, p=0.218, respectively). Seven of eight FNH-TICs and three of four HCA-TICs could be classified as type 1 curve, one of four HCA-TICs as type 2 curve and one of eight FNH-TICs was undefined.
Conclusion: No significant difference between the two lesion types could be found based on analysis of K_{trans} and V_e. The relative frequence of type 2 curve in HCA might help as an additional tool for differentiating HCA from FNH.

SS 7.04

Subtyping of hepatocellular adenomas using Gd-EOB-DTPA: a qualitative and quantitative analysis

S. Kreimeyer, T. Longerich, M. Kieser, L. Grenacher; Heidelberg/DE

Purpose: To evaluate if a differentiation between subtypes of hepatocellular adenomas is possible using a hepato-biliary specific contrast agent (Gd-EOB-DTPA) in MRI.
Material and Methods: 11 patients with 39 lesions with histologically proven hepatocellular adenomas were evaluated. 34 were inflammatic adenomas (IHCA) and 5 HNF1α adenomas. No β-catenin mutated adenoma was found. We performed a standard protocol following the guidelines of the international consensus conference of Gd-EOB-DTPA using a 1.5T scanner (Somatom Avanto, Siemens). Beside a qualitative analysis of all sequences, we measured quantitative SI-ratio (signal-intensity ratio: $((SI_{LE} - SI_{LVE}) / SI_{LVE}) * 100$) and LLC-ratio (liver to lesion contrast: $(SI_{LE} - SI_{LVE}) / SI_M$).
Results: Qualitative analysis shows that the best sequences for a differentiation of HNF1α adenomas from IHCA were T1w precontrast (p=0.03), portalvenous phase (p<0.0001) as well as the arterial phase (p=0.002). All adenomas were hypointense in the hepatocyte specific phase (15 min). The quantitative analysis of SI-ratio and of LLC-ratio also show statistically significant differences in T1w precontrast (SI: p=0.039 / LLC: p=0.049) and in portalvenous phase (SI: p=0.002 / LLC: p=0.002) images.
Conclusion: Subtyping of hepatocellular adenomas using Gd-EOB-DTPA is possible based on the qualitative and quantitative analysis of the T1w precontrast and portalvenous phase. Beside the SI-ratio and liver to lesion contrast ratio the arterial phase gives additional qualitative information for the differentiation.

SS 7.05

Preoperative assessment of colorectal liver metastases after chemotherapy: can diffusion-weighted MR imaging improve the diagnostic performance of Gd-EOB-DTPA-enhanced MRI at 3T?

F. Donati, P. Boraschi, L. Urbani, R. Gigoni, G. Gherarducci, F. Pacciardi, G. Masi, F. Falaschi, C. Bartolozzi; Pisa/IT

Purpose: To assess whether diffusion-weighted MR imaging (DW-MRI) with b-multiple SE-EPI could improve the diagnostic performance of Gd-EOB-DTPA-enhanced MRI in the preoperative assessment of colorectal liver metastases in patients previously undergone chemotherapy.
Material and Methods: Twenty patients with colorectal cancer and focal liver lesions underwent MR imaging at 3T-device (GE DISCOVERY MR750; GE Healthcare) after preoperative chemotherapy. Three images sets were separately reviewed by two observers in conference: 1, DW-MRI using a spin-echo echo-planar sequence with multiple b values (150,500,1000,1500 sec/mm²); 2, Gd-EOB-DTPA Lava-flex sequence including both dynamic and hepato-biliary phase; 3, combined DW-MRI and Gd-EOB-DTPA images. The MRI findings were correlated with surgery and histopathology, which was our gold standard. Only clear benign lesions at intraoperative ultrasound remained unresected. Statistical analysis was performed on a per-lesion basis.
Results: A total of 146 hepatic lesions were detected; of these, 106 were metastases (72.6%), whereas the remaining 40 (27.4%) were characterized as benign lesions (cysts and hemangiomas). Image set 1 correctly identified 92 out of 106 metastases (sensitivity 86.7%, specificity 50%, diagnostic accuracy 76.7%), image set 2 correctly detected 98/106 metastases (sensitivity 92.4%, specificity 70%, diagnostic accuracy 86.3%), and image set 3 correctly diagnosed 104/106 metastases (sensitivity 98.1%, specificity 95%, diagnostic accuracy 97.2%). Differences were statistically significant (p<0.001).
Conclusion: DW-MRI with b-multiple SE-EPI significantly increases the diagnostic performance of Gd-EOB-DTPA-enhanced 3T MRI in the preoperative assessment of colorectal liver metastases.

SS 7.06

Diffusion-weighted imaging in combination with Gd-EOB-DTPA-enhanced magnetic resonance imaging for detecting liver metastases: a meta-analysis

Y. Liu, L. Li, Z. Huang, H. Tang, B. Song; Chengdu/CN

Purpose: A meta-analysis of diffusion-weighted imaging in combination with Gd-EOB-DTPA-enhanced magnetic resonance imaging (MRI) for detecting liver metastases.
Material and Methods: MEDLINE, EMBASE, and Cochrane Library databases were searched for studies published from January 2001 to December 2013 evaluating the diagnostic performance of Gd-EOB-DTPA-enhanced MRI combined with DWI in detecting liver metastases. Sensitivity and specificity estimates, positive likelihood ratios and negative likelihood ratios, and constructed summary receiver operating characteristic curves were calculated on per-lesion bases.
Results: Across 6 studies (291 patients, 1167 hepatic metastases), the pooled sensitivity of Gd-EOB-DTPA-enhanced MRI combined with DWI was 0.96 (95% CI, 0.95-0.97), and the pooled specificity was 0.88 (95% CI, 0.83-0.91). Overall, the positive likelihood ratio was 11.07 (95% CI, 2.98-41.06), and the negative likelihood ratio was 0.05 (95% CI, 0.02-0.13). Gd-EOB-DTPA-enhanced MRI alone for the diagnosis of liver metastases also were performed in the all studies, the sensitivity and specificity of Gd-EOB-DTPA-enhanced MRI alone were 0.87 (95% CI, 0.84-0.89) and 0.82 (95% CI, 0.77-0.86).
Conclusion: The combination of DWI and Gd-EOB-DTPA-enhanced MRI yielded a better overall detection rate, higher sensitivity and specificity for detecting liver metastases compared with Gd-EOB-DTPA-enhanced MRI alone. Additional DWI may be able to reduce oversight of lesions in Gd-EOB-DTPA-enhanced MRI, especially in the detection of small size lesions (<1cm).

SS 7.07

Characterization of fortuitously discovered liver lesions with ultrasound quantitative supersonic shear wave elastography

M. Ronot[1], S. Di Renzo[1], B. Gregoli[1], S. Lambert[1], R. Duran[2], V. Vilgrain[1]; [1]Clichy/FR, [2]Lausanne/CH

Purpose: To prospectively assess the stiffness of fortuitously discovered FLL using supersonic shear wave elastography (SWE).
Material and Methods: Between June 2011 and May 2012, all FLL fortuitously discovered during an ultrasound (US) examination were prospectively included. For each lesion, quantitative elastography images was acquired. The largest possible region of interest was placed in the lesion to quantitatively assess its stiffness, measured in kPa. Characterization of the lesion relied either on a combination of MR imaging and/or contrast-enhanced US features, or on biopsy. Tumor stiffness was analyzed using ANOVA and non-parametric Mann-Whitney tests.
Results: 105 lesions were successfully evaluated in 73 patients (61 women, 84%) with a mean age of 44.8 (range: 20-75). The mean stiffness was 33.3±12.7 kPa for the 60 focal nodular hyperplasia (FNH), 19.7±9.8 kPa for the 17 hepatocellular adenomas (HCA), 17.1±7 kPa for the 20 hemangiomas, 11.3±4.3 kPa for the 5 focal fatty sparing, 34.1±7.3 kPa for the 2 cholangiocarcinomas, and 19.6 kPa for one hepatocellular carcinoma (p<0.0001). There was no difference between the benign and the malignant group (p=0.64). The stiffness of FNHs was significantly higher than that of HCAs (p<0.0001). The stiffness of the telangiectatic/inflammatory HCAs was significantly higher than that of the steatotic HCAs (p=0.014). The AUROC for differentiating FNH from other lesions was 0.86±0.04.
Conclusion: SWE provides additional information for the characterization of FFL, and helps in differentiating FNH from HCAs, and in subtyping HCAs.

SS 7.08

Should all patients undergo MRI scan in addition to CT in the pre-operative staging of colorectal liver metastases?

M.G. Wiggans[1], G. Shahtahmassebi[2], S. Aroori[1], M.J. Bowles[1], S.A. Jackson[1], D.A. Stell[1]; [1]Plymouth/UK, [2]Nottingham/UK

Purpose: The aim of this study was to measure the accuracy of CT and MRI scans in detecting colorectal liver metastases (CRLM) and to determine if patients staged with MRI in addition to CT have a longer liver recurrence-free survival than those staged with CT alone in a UK tertiary referral centre performing routine intra-operative ultrasound.

Material and Methods: A retrospective analysis of patients undergoing liver resection for CRLM was performed. Patients staged preoperatively with CT or with additional MRI were included and those with additional PET imaging were excluded from survival analysis. Timing and site of tumour recurrence were recorded.
Results: During a seven-year period 303 patients underwent resection for CRLM of whom 47 (15.5%) were staged with CT alone and 36 (11.9%) with additional MRI. The overall accuracy of CT (63%) and MRI (61.9%) was similar in the detection of tumour nodules (P=0.905). There was no difference in the intra-hepatic recurrence rate between groups with 13/47 and 8/36 cases, respectively (P=0.737). There was no difference in the disease free survival curves between groups (P=0.487).
Conclusion: These results suggest that MRI should not be a mandatory imaging modality in patients with CRLM, particularly in publically funded healthcare systems, due to the cost and delay outweighing the potential benefit of improved sensitivity. MRI should be reserved for selected problematic cases and performed only after discussion at a hepatopancreaticobiliary multidisciplinary team meeting.

SS 7.09

CT texture analysis in colorectal liver metastases: a better way than conventional size measurements to assess response to chemotherapy?

S.-X. Rao[1], D.M.J. Lambregts[1], R. Schnerr[1], F. Albarello[2], R.G. Riedl[1], C. Dejong[1], L.A. Heijnen[1], M.H. Martens[1], W.H. Backes[1], G.L. Beets[1], M.-S. Zeng[3], R.G.H. Beets-Tan[1]; [1]Maastricht/NL, [2]Ferrara/IT, [3]Shanghai/CN

Purpose: To compare the potential of CT texture analysis, CT tumor volumetry and unidimensional (RECIST) measurements for response assessment of colorectal liver metastases undergoing preoperative chemotherapy.
Material and Methods: Twenty-one patients with known colorectal liver metastases who underwent CT (portal phase) both before and after preoperative chemotherapy were included. Texture analysis of the largest metastatic lesion was performed. Mean intensity (M), entropy (E) and uniformity (U) were calculated with no filtration (nf) and using different filter values (fine=0.5, medium=1.5, coarse=2.5). Total tumor volume (cm^3) of all metastatic lesions and the largest lesion diameters (RECIST 1.1) were determined. Pre-, post-chemotherapy and the relative change (Δ%) of texture parameters, volume and RECIST-diameters were compared between good responders (n=9; tumor regression grade 1-2) and poor responders (n=12; TRG 3-5). ROC-analyses were performed to establish diagnostic performance for the significant parameters.
Results: Pre-chemotherapy texture parameters were not significantly different between good and poor responders. Post-treatment E_{nf}, U_{nf} as well as the $\Delta\%\text{-}E_{nf,0.5,1.5}$ and $U_{nf,0.5,1.5}$ were significantly different between good and poor responders (p=0.003-0.04), with AUCs ranging between 0.73 and 0.88. Δvolume was significantly different between good and poor responders (p=0.047, AUC=0.77). No significant differences were found for pre- and post-chemotherapy volumetry and RECIST-diameters.
Conclusion: CT texture analyses hold promise to assess pathologic response to chemotherapy in patients with colorectal liver metastases. Results outperform volumetric tumor measurements. Unidimensional tumor measurements according to RECIST are not helpful.

SS 7.10

Whole liver CT texture analysis: effect of the presence of metastatic disease on the remaining liver parenchyma

S.-X. Rao[1], D.M.J. Lambregts[1], W. Van Ommen[1], R. Schnerr[1], L.A. Heijnen[1], M.H. Martens[1], W.H. Backes[1], R.A. Vliegen[2], M.-S. Zeng[3], G.L. Beets[1], R.G.H. Beets-Tan[1]; [1]Maastricht/NL, [2]Heerlen/NL, [3]Shanghai/CN

Purpose: To evaluate the potential of whole-liver CT texture analysis of apparently disease-free liver parenchyma for discriminating between colorectal cancer (CRC) patients with and without hepatic metastases.
Material and Methods: The primary staging CT-examinations of 29 CRC-patients were analysed. Three subgroups were assessed: patients without metastases (n=15), with synchronous metastases (n=10) and with metachronous metastases within 2 years (n=4). Whole-liver texture analysis was performed by manual delineation of the non-diseased liver (excluding metastases/benign liver lesions) on portal-phase images. Mean grey-level intensity (M), entropy (E) and uniformity (U) were derived with no filtration and different filter values (fine=0.5, medium=1.5 and coarse=2.5).
Results: Mean $E_{1.5}$ and $E_{2.5}$ in patients with synchronous metastases were significantly higher compared with the non-metastatic patients (p=0.01-0.02). Mean $U_{1.5}$ and $U_{2.5}$ were significantly lower in the synchronous metastases group (p=0.02-0.04). Texture parameters for the metachronous metastases group were not significantly different from the non-metastatic group (p>0.05), although – similar to the synchronous metastases group – there was a trend towards increased $E_{1.5}$, $E_{2.5}$ and decreased $U_{1.5}$, $U_{2.5}$ values. AUCs for the diagnosis of synchronous metastatic disease based on $E_{1.5,2.5}$ and $U_{1.5,2.5}$ ranged between 0.74 and 0.78.
Conclusion: Texture analysis of apparently non-diseased liver holds promise to differentiate between patients with and without metastatic liver disease from CRC. Further research is required to determine its potential role for the early detection of metachronous/occult liver disease.

SS 7.11

DWI of focal liver lesions: IVIM model with different combination of 11 b values

G. Morana[1], G. Scattolin[2], R. Zanato[2], F. De Leo[1]; [1]Treviso/IT, [2]Padua/IT

Purpose: To investigate different parameters with IVIM model in liver lesions: apparent diffusion coefficient (ADC), perfusion fraction (f), diffusion and pseudodiffusion coefficient (D and D*). To calculate the optimal b values to be utilized in their analysis.
Material and Methods: 96 patients undergoing MR with DWI with diagnosis of HCC (n=28), colorectal carcinoma metastasis (CCM) (n=24) or FNH (n=44). DWI sequence was EPI (TR/TE=4361/54 ms) with 11 b-values. Using MatLab, the estimations of D, D* e f were carried out for different combination of b-values. Statistics Analysis: scatter plot; 2 sample t test; Kruskal-Wallis test.
Results: ADC and D values were not significantly different between lesions. D* and f were not significantly different between HCC and FNH, whereas were significantly higher than in CCM ($p< 0.05$). With lesser b values D* shows a significant ($p< 0.05$) decrease in HCC, not in FNH and in CCM, thus losing the difference between the above groups. f does not show a significant decrease in the above groups. D does not change. f in background liver parenchyma were not significantly different between HCC (21%), FNH (22%), CCM (20%).
Conclusion: IVIM data are dependent of b values being utilized. The D* and f values are useful for the characterization of hyper (HCC; FNH) and hypovascular lesions (CCM). A standardization of techniques is necessary in order to compare results between different studies.

11:00 - 12:30 **Karajan**

Scientific Session 8

GI tract malignancy - treatment response

SS 8.01

Accuracy of MDCT in predicting pathologic response to neoadjuvant chemotherapy in advanced gastric cancer: preliminary results

N. Cioffi Squitieri, C. Pozzessere, S. Guerrini, C. Vindigni, F.G. Mazzei, F. Roviello, M.A. Mazzei, L. Volterrani; Siena/IT

Purpose: To investigate the accuracy of MDCT in predicting pathologic response to neoadjuvant chemotherapy in advanced gastric cancer (AGC).
Material and Methods: 18 consecutive patients (10 male, mean age 61,3 y) with resectable AGC, clinical stage >/= T2 N1, who had been treated with neoadjuvant chemotherapy and gastric resection with D2 lymph nodal dissection, were prospectively enrolled in this study. Pre and post-chemotherapy abdominal CT were analysed by two radiologists in consensus, measuring the Dmax and depth invasion of the primary gastric lesion. Lymph nodal status were also evaluated, according to the III Japanese Classification of Gastric Carcinoma, using two dimensional criteria: a) the measurement of the short axis, with a cut-off of 5 mm for station in group 1, and 8 mm for station in group 2 and 3, and b) the calculation of the reduction rate between the two CT examinations. The sensitivity, specificity, and overall accuracy for both T and N staging of AGC were calculated.
Results: The overall accuracy of MDCT in the T staging was 77.7% (14/18). Regarding the N staging, the dimensional criteria based on the evaluation of reduction rate was more accurate in comparison with the other one.
Conclusion: MDCT may be an accurate tool in the prediction of pathologic response following neoadjuvant chemotherapy in patients with resectable AGC, in spite of the problems related to fibrous changes after chemotherapy.

SS 8.02

Tumour volumetry on diffusion-weighted MRI for identification of complete tumour responders to preoperative chemoradiotherapy in rectal cancer: a multicenter validation study

D.M.J. Lambregts[1], S.-X. Rao[2], S. Sassen[3], M.H. Martens[1], L.A. Heijnen[1], M. Sosef[3], G.L. Beets[1], R.A. Vliegen[3], R.G.H. Beets-Tan[1]; [1]Maastricht/NL, [2]Shanghai/CN, [3]Heerlen/NL

Purpose: Retrospective studies have shown that DWI tumour volumetry can help identify rectal cancer patients with a complete tumour response after neoadjuvant chemoradiotherapy (CRT). This study aims to prospectively validate the diagnostic value of these previous retrospectively determined DWI volume-thresholds in a larger,multicentric patient cohort.
Material and Methods: 119 patients underwent rectal cancer treatment including a long course of CRT. Patients underwent standard T2W-MRI and DWI at 1.5T pre- and post-CRT. An experienced reader determined pre-CRT and post-CRT tumour volumes (cm^3) on T2W-MRI and b1000-1100 DWI by means of free-hand ROI delineation on each tumour containing slice. Tumour volume reduction rates (Δvolume) were calculated. Previously determined T2W and DWI threshold values for pre-volume, post-volume and Δvolume were tested to prospectively assess their diagnostic value in differentiating patients with a complete tumour response.
Results: Twenty-one patients had a complete response. AUCs for the pre-/post-/Δ-volumes were 0.73/0.80/0.69 for T2W-MRI and 0.75/0.86/0.78 for DWI. Using predefined thresholds, sensitivity/specificity for T2W-MRI were 62%/74% for pre-volumetry, 52%/92% for post-volumetry and 38%/86% for Δvolume. For DWI-volumetry sensitivity/specificity were 62%/77% for pre-volumetry, 62%/91% for post-volumetry and 71%/80% for Δvolume.
Conclusion: Previously determined DWI volume thresholds can be reproduced with good results in a prospective and multicenter setting. Post-CRT DWI volumetry provides the best result for discriminating complete responders with an AUC of 0.86 and, prospectively tested, sensitivity of 62% and specificity of 91%.

SS 8.03

Correlation between tumor reduction rate MRI-volumetry and response to preoperative chemo-radiotherapy in locally advanced rectal cancer

E. Guidi[1], R. Scandiffio[1], L. Faggioni[1], G. D'Ippolito[2], E. Neri[1], C. Bartolozzi[1]; [1]Pisa/IT, [2]Sao Paulo/BR

Purpose: To compare tumor volume reduction rate (TVRR) measured by magnetic resonance after preoperative chemo-radiotherapy (CRT) and tumor regression grade (TRG) in locally advanced rectal cancer.
Material and Methods: 20 patients with locally advanced rectal cancer (cT3-T4) underwent preoperative CRT, followed by total mesorectal excision (TME). Tumor volume was measured on 3D MR sequences (CUBE) obtained before and after CRT and tumor volume reduction rate was determined using the equation TVRR (%) = (pre-CRT tumor volume - post-CRT tumor volume) x 100/pre-CRT tumor volume. It was evaluated the downstaging (defined as ypT0-T2) of tumor mass and calculated the correlation between TVRR and TRG proposed by Dworak using the Spearman rank test.
Results: The mean TVRR was 77.3% (range, 26.4-99.3%); TVRR was > 60% in 18 cases (90%) and in 8 of these patients (44.4 %) it was > 80%. Downstaging of tumor lesions was obtained in 15 patients (75%). In 4 cases, there was a complete tumor regression (TRG4) at histological examination and in the same patients there was also a TVRR > 80% measured by MRI-volumetry. Finally has been demonstrated a statistically significant correlation between TVRR and TRG (rs = 0.5466, p = 0.0126).
Conclusion: The TVRR after preoperative CRT correlates with histopathologic downstaging and TGR of locally advanced rectal cancer. The MRI-volumetry is a prognostic factor to estimate the tumor response to preoperative CRT.

SS 8.04

Comparison of MRI and histopathological response to chemoradiotherapy in locally advanced rectal cancer: a prospective audit

M. West, R. Wiles, C. Barben, D. White; Liverpool/UK

Purpose: We aim to compare MRI T-staging (ymrT) and tumor regression grading (mrTRG) at week 9 post-neoadjuvant chemoradiotherapy (NACRT) with histopathological T-staging (ypT) and TRG to assess changes in agreement between MRI (conventional vs. high resolution) and histopathology staging.
Material and Methods: 96 patients underwent standardised NACRT and surgery (median week 10, IQR 9-11) in a prospective audit. Between August 2011 and June 2013 (1st period) conventional MRI sequences were used. High-resolution MRI was used after July 2013 (2nd period). MRI parameters were categorized as ymrT favourable (T0-2) or unfavourable (T3-4) or mrTRG favourable (1-3) or unfavourable (4,5). Comparison with histopathology ypT (favourable (T0-2) or unfavourable (T3-4)) and TRG (favourable (3-4) or unfavourable (0-2)) was undertaken.
Results: 86 patients had evaluable imaging and pathology (1st period - 61 and 2nd period - 25). When considering the relationship between ymrT and ypT in the 1st period, 20% of patients were understaged and 30% overstaged; agreement was fair (Kappa 0.29, 95%CI 0.06-0.53). 29 patients had a favourable TRG and 32 had unfavourable TRG, with poor agreement (Kappa 0.11, 95%CI 0.07-0.29). In the 2nd period, 2% of patients were understaged and 5% overstaged; agreement was very good (Kappa 0.89, 95% CI 0.82-0.99). 17 patients had a favourable TRG and 8 had unfavourable TRG, with very good agreement (Kappa 0.91, 95% CI 0.88-1.00).
Conclusion: Histopathological outcomes can be accurately predicted by using high-resolution sequences.

SS 8.05

Locally advanced rectal cancer: value of ADC mapping with different b-value in prediction of lymph-nodes response after neoadjuvant chemoradiation therapy

P.P. Arcuri[1], S. Roccia[1], A. Pingitore[2], S. Aidala[1], G. Fodero[1]; [1]Catanzaro/IT, [2]London/UK

Purpose: To evaluate the diagnostic performance of quantitative apparent diffusion coefficient (ADC) measurements, using different b-values (b600,1000,1400) in the assessment of the therapeutic response to chemo-radiation therapy (CRT) in each lymph nodes of patients with locally advanced rectal cancer, by analyzing post-CRT values of ADC, in relation to tumor regression grade obtained by histopathologic evaluation.
Material and Methods: Thirty-two patients with locally advanced rectal cancer affected by lymph nodes in the mesorectum, all followed by surgery, who underwent pre and post-CRT MR imaging were retrospectively studied. Histological validation of nodes was obtained. Imaging consisted of T2, DWI (b=600, 1000, 1400), and 3DT1. The signal intensity on DWI was analyzed and

the mean apparent diffusion coefficient (ADC) for each node (ADCnode) and the ADC of each node relative to the mean tumor ADC (ADCrel) were measured.
Results: Pre-CRT DWI with b value=1000 detected 15% more nodes than DWI with b value=600 and 24% more than DWI with b value=1400. Post-CTR, for DWI with b value=1000, sensitivity/specificity for differentiating between benign and malignant lymph nodes were 68%/72% for ADCnode and 71%/74% for ADCrel. For DWI b=600, sensitivity/specificity were 64%/66%, for ADCnode and 67%/71% for ADCrel. For DWI b=1400, sensitivity/specificity were 59%/63% for ADCnode and 62%/68% for ADCrel.
Conclusion: DWI with b=1000 showed higher sensibility in lymph nodes detection in primary rectal staging cancer. After CRT, however, DWI with b=1000 showed major specificity (72/74%) than b=600 (66/71%) and 1400 (63/68%), it is not reliable for differentiating between benign and malignant lymph nodes.

SS 8.06

withdrawn by the authors

SS 8.07

Response evaluation in locally advanced rectal cancer: influence of different region of interest methods on tumor ADC measurements

I. Blazic, R. Maksimovic, G. Lilic, M. Kratovac Dunjic, R. Milenkovic, Z. Krivokapic, D. Saranovic; Belgrade/RS

Purpose: To determine diagnostic performance of different region of interest (ROI) methods in tumor apparent diffusion coefficient (ADC) measurements for assessment of complete tumor response (CR) after chemoradiotherapy (CRT) in patients with locally advanced rectal cancer (LARC).
Material and Methods: Forty patients with LARC treated with neoadjuvant CRT followed by surgery were retrospectively included. For ADC measurements we applied three ROI methods: three circular ROI method (3ROI), single slice method (SS) and whole tumor volume method (WTV) before and after CRT. Parameters of diagnostic performance in detection of CR were assessed for every method in comparison with histopathologic findings as standard of reference. Receiver operating characteristic (ROC) curves were generated to compare performance of different ROI methods.
Results: All parameters of diagnostic performance was higher for SS and WTV compared with 3ROI method. Areas under the ROC curves for identification of CR that was based on preCRT ADC, postCRT ADC and ΔADC were 0.53, 0.54 and 0.68 for 3ROI method, versus 0.64, 0.82 and 0.85 for SS method (p=0.17, 0.02, 0.07) and 0.77, 0.83 and 0.86 for WTV method (p=0.11, 0.01, 0.04).
Conclusion: The WTV and SS methods provided high diagnostic performance for the assessment of CR and is significantly more accurate than is 3ROI method. SS was equally as accurate as WTV method for preCRT ADC, postCRT ADC and ΔADC in identifying CR to CRT in patients with LARC.

SS 8.08

Texture analysis as imaging biomarker of tumoral response to neoadjuvant chemoradiotherapy in rectal cancer patients studied with 3T MR

C.N. De Cecco[1], M. Ciolina[2], B. Ganeshan[3], M. Rengo[1], F. Meinel[4], A. Laghi[1]; [1]Latina/IT, [2]Rome/IT, [3]London/UK, [4]Munich/DE

Purpose: To determine whether texture features of rectal cancer on T2-weighted MR images can predict tumoral response in patients treated with neoadjuvant chemoradiotherapy (CRT).
Material and Methods: We prospectively enrolled 15 consecutive patients with rectal cancer, who underwent pre- and post-treatment 3T MRI. Texture analysis was performed using a commercial research software algorithm on unenhanced axial T2-weigthed images by manually delineating a region-of-interest around the tumor outline. The technique selectively filters and extracts textures at different texture scales followed by quantification of the histogram using kurtosis, skewness and mean value of positive pixels (MPP). After CRT, all patients underwent complete surgical resection and the surgical specimen served as the gold standard.
Results: Six patients showed pathological complete response (pCR), 4 partial response (PR) and five patients were non-responders (NR). Baseline kurtosis was significantly lower in the pCR sub-group in comparison with PR+NR (p=.01). Post-treatment kurtosis without filtration was significantly higher in pCR in comparison with PR+NR (p=.045). The change in kurtosis over treatment was significantly lower in PR+NR compared to pCR (p=.038). At baseline, the area under the ROC curves (AUC), to discriminate between pCR and PR+NR, was significantly higher for kurtosis (0.907, p<0.001) compared to all others parameters. The optimal cutoff value for baseline kurtosis was ≤0.19 (sensitivity 100%, specificity 77.8%).
Conclusion: Texture parameters derived from T2w images of rectal cancer have the potential to act as imaging biomarkers of tumoral response to neoadjuvant chemoradiotherapy.

SS 8.09

Timing of surgery following neoadjuvant chemoradiotherapy in rectal cancer: are we operating too early?

M. West[1], R. Wiles[1], C. Barben[1], D. White[1], G. Kemp[1], M.P. Grocott[2], S. Jack[2], G. Brown[3]; [1]Liverpool/UK, [2]Southampon/UK, [3]Surrey/UK

Purpose: In rectal cancer, the standard of care after completing chemoradiotherapy (NACRT) is surgery; however, a large variation exists with regards to timing for surgery. We aim to assess the association of MRI at 9 and 14 weeks post-NACRT with histopathological outcomes.
Material and Methods: We prospectively studied 39 consecutive patients (27 male) with T3-4/N+ resection margin threatened rectal cancer who completed standardized NACRT. All patients had a MRI at week-9 and 14 post-NACRT, followed by surgery at week-15. Two readers, at two different cancer centres independently assessed images in a blind fashion. MRI parameters were categorized as ymrT (favourable (T0-2) or unfavourable (T3-4); mrTRG (favourable (1-3) or unfavourable (4, 5)) and volume reduction (favourable (>80%), indeterminate (60-80%), unfavourable (<60%)). Results were compared with histopathology ypT (favourable (T0-2) or unfavourable (T3-4)) and TRG (favourable (3-4) or unfavourable (0-2)).
Results: All patients had evaluable imaging and pathology. Interobserver agreement was very good for all MR variables (Kappa >0.85). ymrT is significantly associated with ypT (p=0.002 vs. 0.003) and TRG at both 9 and 14-weeks (p=0.010 vs. 0.010, respectively). mrTRG is significantly associated only with ypT (p=0.008) and TRG at week 14 (p=0.004). Volume reduction is significantly associated with ypT (p=0.003) and TRG (p=0.003) at week-14.
Conclusion: Following NACRT, further downstaging and volume reduction is observed at week-14. The consequences for survival and postoperative morbidity warrant further investigation.

SS 8.10

Diffusion-weighted MR imaging in local recurrence of rectal cancer for clinical application

Z. Zhou, W. Cao; Guangzhou/CN

Purpose: To evaluate the application value of magnetic resonance (MRI) diffusion-weighted imaging (DWI) in the assessment of locally recurrent rectal cancer.
Material and Methods: Totally 325 postoperative rectal cancer patients underwent MRI examination including axial, coronal, sagittal T2WI and axial DWI sequence (b=0, 1000 s/mm^2). Eighty-nine patients with postoperative pelvic abnormalities were enrolled. Two radiologists (R1,R2) used two methods (standard T2WI sequence, DWI sequence and T2WI sequence) to read the images of patients, and to assess the value of DWI sequence in diagnostic performance of local recurrence.
Results: Of the patients with abnormalities, 32.58% (29/89) had local recurrence. High accuracy achieved by two radiologists was 85.39% and 80.90%, respectively, for determining local recurrence by standard T2WI sequence, while it was improved to 91.01% and 87.64%, respectively ($P < 0.05$) using DWI and T2WI sequence. Area under the ROC curve (AUC) of two radiologists using DWI and T2WI sequence was larger than that using the standard T2WI sequence. (R1: 0.907vs0.856, R2: 0.882vs0.823). Inter-observer agreement of two physicians for standard MRI was good (κ=0.674) while it was excellent (κ=0.831) combined with DWI.
Conclusion: Standard T2W sequencing has a high diagnostic accuracy for locally recurrent rectal cancer, and when combined with DWI sequence it improves diagnostic accuracy.

11:00 - 12:30 **Wolf Dietrich**

Scientific Session 9

Appendicitis and other emergency conditions

SS 9.01

Appendicitis CT score: a measure for predicting appendiceal perforation and surgical outcome

B.M.H. Lai, C.Y. Chu, B.S.T. Leung, V.K.P. Fung, T.H.T. Sung, D.T.F. Lee, J.L.S. Khoo; Chai Wan/HK

Purpose: To assess the usefulness of "Appendicitis CT score" as a tool for predicting appendiceal perforation at surgery and surgical outcome.
Material and Methods: Retrospective study on CTs performed for acute appendicitis between May 2011 and January 2012 were assessed for composite CT score (appendiceal wall defect, presence of phlegmon, abscess, extraluminal gas and extraluminal appendicolith). Correlation with presence of appendiceal perforation at surgery and surgical outcomes including need for conversion to open, operative time and duration of hospital stay.
Results: 84 patients were included in this study. About 35% of the subjects had perforated appendix on surgical-pathological examination. Significantly higher CT scores were seen for the group with perforated appendix as compared to the non-perforated group (2.52 vs. 0.51, p<0.001). Higher CT scores were also seen when comparing the open surgery vs. laparoscopic surgery groups (2.78 vs. 1.01, p<0.001). No subject with CT score "0" had perforated appendix. All with CT score >3 had perforated appendix. Regression analysis showed an increase in 1 CT score was associated with increased odds perforated appendix (OR: 7.44, p<0.001), conversion to open surgery (OR: 3.02, p=0.002), increased operative time (14.4 minutes, p<0.001) and increased length of hospital stay (0.84 days, p=0.003).
Conclusion: Appendicitis CT score is a sensitive tool for predicting perforation in acute appendicitis, need for open surgery, OT duration and length of hospital stay and can aid the surgeon in deciding on the operative approach and allow better estimation of surgical outcome.

SS 9.02

Usefulness of dual-energy computed tomography in patients of clinically suspected acute appendicitis

Y.H. Lee, A.L. Im, H.A. Lee, K.H. Yoon; Iksan/KR

Purpose: To determine whether virtual non-enhanced (VNE) images derived from dual energy computed tomography (DECT) replaces true non-enhanced (TNE) images in patients of clinically suspected acute appendicitis.
Material and Methods: 145 patients (57 men, 88 women) who were suspected acute appendicitis underwent CT imaging using dual-energy technique. CT parameters were 80/100 kVp and 140 kVp, auto mAs. Two radiologists independently reviewed the VNE set (VNE and portal phase enhanced images), and TNE set (TNE and Portal phase enhanced images), 4 weeks later. Sensitivities and specificities in each session and radiation doses were calculated. Image quality, noise and artifacts were rated. In addition, calcifications such as appendicoliths or urinary stones, were compared.
Results: 110 patients were histopathologically comfirmed to acute appendicitis. In VNE data set, sensitivity and specificity of each readers were 95% and 94% in reader 1, and 97% and 100% in reader 2. In TNE set, those of each readers were 99% and 95% in reader 1, and 97% and 100% in reader 2. Small appendicoliths were obscured on VNE images. Mean image quality and noise were 3.67 and 3.30 which means general acceptance of VNE images as replacement for TNE images.
Conclusion: Image quality and diagnostic performance of VNE images were not significantly inferior to those of TNE images. Skipping TNE images can reduce CT radiation dose in patients of suspected acute appendicitis.

SS 9.03

Comparison of imaging strategies with conditional versus immediate contrast-enhanced CT in patients suspected of having appendicitis

J.J. Atema[1], S.L. Gans[1], M. Leeuwenburgh[1], A. Van Randen[1], W. Laméris[1], H.W. Van Es[2], J.P. Van Heesewijk[2], B. Van Ramhorst[2], W.H. Bouma[3], W. Ten Hove[3], M.S. Van Leeuwen[4], E.M. Van Keulen[5], M.G. Dijkgraaf[1], P.M. Bossuyt[1], M.A. Boermeester[1], J. Stoker[1]; [1]Amsterdam/NL, [2]Nieuwegein/NL, [3]Apeldoorn/NL, [4]Utrecht/NL, [5]Hilversum/NL

Purpose: Both ultrasound (US) and computed tomography (CT) are used in diagnosing acute appendicitis, with higher accuracy for CT. A conditional CT strategy (i.e. initial ultrasound and CT in negative or inconclusive US) can be used to reduce costs and radiation exposure. The aim of this study was to compare imaging strategies with conditional and immediate CT in patients suspected of acute appendicitis.
Material and Methods: Adult patients clinically suspected for acute appendicitis underwent both US and CT. A final diagnosis was assigned to all patients based on clinical, surgical findings, pathology results, and follow-up. Results of ultrasound and CT were evaluated blinded and independently from each other. Estimates of sensitivity, specificity and predictive values were calculated.
Results: 422 patients were included (251 patients (60%) had appendicitis). In 199 patients (47%) US was inconclusive or negative. Conditional CT imaging correctly identified 241 of 251 patients with appendicitis (sensitivity 96%, 95%CI 92-98%) versus 238 of 251 correctly identified patients with immediate CT imaging (sensitivity 95%, 95%CI 91-97%) (p=0.250). Conditional CT imaging had lower PPV (86% versus 92%) and showed lower specificity (77% (95%CI 70-83%) versus 87% (95% CI 81-91%); p=<0.001).
Conclusion: In patients suspected of having acute appendicitis, a conditional CT strategy is able to correctly identify as many patients with appendicitis as an immediate CT strategy. However, conditional CT imaging results in more false positives.

SS 9.04

Ultrasound scan in diagnosing acute appendicitis

Y. Nakhuda[1], Z. Al-Ani[2], A. Tokala[1], I. Harris[1]; [1]Preston/UK, [2]Manchester/UK

Purpose: To assess the accuracy of ultrasound scan (USS) in the assessment of patients presenting acutely with suspected appendicitis. The influence of USS findings on patient's management in terms of reimaging, conservative treatment or surgical intervention.
Material and Methods: Retrospective study within the settings of a teaching hospital and included patients investigated with USS for suspected acute appendicitis over a period of 10 months. All the USS were performed by specialist gastrointestinal radiologists. Patients who were managed conservatively were followed up for a minimum of 5 months. Ethical approval obtained.
Results: A total of 142 patients had an USS for suspected acute appendicitis. USS showed no evidence of appendicitis in 58% (USS negative group) while suggested acute appendicitis in 29% (USS positive group). In 10% of patients, USS findings were equivocal (USS equivocal group). An alternative diagnosis was suggested by USS in 3%. The specificity and sensitivity for diagnosing acute appendicitis using USS were 96.4% and 92.5%, respectively, with 95% confidence interval. Final outcomes for these 3 groups will be highlighted.
Conclusion: USS is highly sensitive and specific in the hands of gastrointestinal radiologists for assessment of suspected acute appendicitis and recommending management in terms of surgery vs conservative approach. When USS is equivocal, an integrated approach between radiologists and surgeons is necessary.

SS 9.05

Mandatory imaging cuts costs and reduces unnecessary surgery in the diagnostic work-up of patients suspected for appendicitis

M.J. Lahaye[1], D.M.J. Lambregts[1], E. Mutsaers[1], V.C. Cappendijk[2], B. Essers[1], S. Breukink[1], G.L. Beets[1], R.G.H. Beets-Tan[1]; [1]Maastricht/NL, [2]'s-Hertogenbosch/NL

Purpose: In 2010, new Dutch guidelines have been implemented recommending the use of US or CT to confirm or refute clinically suspected appendicitis before (laparoscopic) surgery. For equivocal cases with US, additional imaging (CT/MRI) is recommended. This study aimed to see whether this is an effective and cost-effective strategy to reduce the number of unnecessary surgical procedures (appendicectomy).

Material and Methods: This retrospective study included all consecutive patients with clinically suspected appendicitis at our hospital from 2008 to 2009 (before guidelines) and 2011 to 2012 (after guidelines). Use of imaging (none versus US, CT and/or MRI) and its findings were recorded. Also all medical costs, surgical and histopathological findings - where available - were recorded. Primary study endpoint was the number of appendicectomies before and after guideline implementation.
Results: 1556 patients were included; 756 were collected before and 800 after the implementation of the guidelines. During the pre-implementation period, 36.3% of the patients received imaging. Post-implementation, 97.4% of the patients received imaging before surgery. The percentage of an 'appendicectomy' before the guidelines was 23.2%. After implementation, this average percentage dropped significantly to 6.2% ($p<0.001$). The average cost-per-patient dropped from 2481.55 to 1887.56 euros.
Conclusion: Use of pre-operative imaging in patients with suspected clinically appendicitis result in a significant reduction in the percentage of negative appendectomies. This study suggests that the implementation of imaging in the work-up of these patients could be an effective and cost-effective strategy to reduce the number of unnecessary surgeries.

SS 9.06

iPad-based primary 2D reading of CT angiography examinations of patients with suspected acute gastrointestinal bleeding: performance comparison with a conventional workstation

P. Scalise[1], L. Faggioni[1], E. Neri[1], I. Bargellini[1], F. Calcagni[1], G. D'Ippolito[2], C. Bartolozzi[1]; [1]Pisa/IT, [2]Sao Paulo/BR

Purpose: To evaluate the iPad effectiveness for 2D reading of CT-angiography (CTA) studies performed for suspected acute gastrointestinal bleeding.
Material and Methods: Twenty-five CTA examinations of patients with suspected acute gastrointestinal bleeding either confirmed (20/25, 80%) or ruled out (5/25, 20%) by digital subtraction angiography (DSA) were retrospectively reviewed by four independent readers. Two readers evaluated source axial CTA images on a commercial workstation (Advantage Windows 4.5, General Electric, Milwaukee, WI), whereas the others assessed the same images on a Retina DisplayTM iPad (64GB model, Apple Inc, Cupertino, CA). All CTA images were wirelessly transferred on the iPad in JPEG lossless-format using the BonjourTM protocol. The time needed to complete reading of every CTA examination on the iPad and the workstation, detection of arterial blush, and suspected bleeding arteries as assessed on both devices were recorded.
Results: The time needed to complete reading of every CTA study was significantly shorter on the iPad than on the workstation (171±84 vs 227±91 seconds, respectively; $p<0.002$). Sensitivity and specificity for arterial blush detection were 85% and 60% for the workstation and 90% and 80% for the iPad, respectively. Inter-reader agreement for workstations and iPads was good (Cohen $k=0.70$) and very good ($k=0.88$), respectively. Agreement of workstation and iPad vs DSA on bleeding arteries was very good ($k=0.82$ and 0.89, respectively).
Conclusion: iPad-based preliminary 2D reading of CT angiography studies of patients with suspected acute gastrointestinal bleeding is feasible and significantly faster compared with a conventional workstation.

SS 9.07

Large bowel obstruction: diagnostic performance of MDCT and added value of multiplanar reformations

A. Bonnard, C. Delavaud, I. Boulay-Coletta, M. Zins; Paris/FR

Purpose: To assess the diagnostic accuracy of MDCT and the usefulness of multiplanar reconstructions (MPR) in large bowel obstruction.
Material and Methods: This retrospective study was approved by our institutional review board. 100 MDCT were performed on 98 consecutive patients (average age: 69 (30-97)) admitted for suspected large bowel obstruction. CT Images were retrospectively, randomly and individually analyzed by three radiologists (two senior abdominal radiologists -S1,S2- and one junior radiologist -J-) during two different sessions where only axial images or additional MPR images were made available. The readers classified each examination into two categories: mechanical obstruction or pseudo-obstruction. When mechanical, the cause of the obstruction was specified. A global diagnostic performance rate was assessed.
Results: 77 patients had a mechanical colonic obstruction. Sensitivity of MDCT for diagnosis of mechanical obstruction was respectively 100% (77/77), 97.4% (75/77) and 96.1% (74/77) for readers S1, S2 and J with axial images only and 100% (77/77), 98.7% (76/77) and 100% (77/77) with the addition of MPR images respectively. With axial images only, global performance rate was significantly higher in senior abdominal radiologist's group (S1+S2) compared to the junior radiologist (95% vs. 89%; p-value=0.049). MPR review significantly improved the global performance rates for all readers.
Conclusion: MDCT is an accurate diagnostic examination for the diagnosis of large bowel obstruction. MPR improves the diagnostic performance of MDCT.

SS 9.08

Misty mesentery on CT: role of CT in the evaluation of indeterminate mesenteric stranding and enlarged lymph nodes with proposed algorithm for risk stratification and follow up.

C. Smith, F. Dambha, Y.M. Wong, E.M. Godfrey, S. Whitley, N. Carroll; Cambridge/UK

Purpose: Mesenteric abnormalities are a frequent finding on abdominal CT which exist outside of the context of a known neoplastic or systemic inflammatory disease. Whilst there are several databases published reporting the various underlying pathologies, none has developed an algorithm to enable systematic risk stratification for reporting radiologists to recommend a management and follow up pathway.
Material and Methods: We searched our reporting database for comments on mesenteric pathology over 10 years. We reviewed the images and graded the mesenteric findings using various criteria; e.g. density of stranding, lymph nodes dimensions and morphology. We added to this to non-imaging findings such as systemic symptoms and biochemical markers. This grading was correlated with the outcome found through electronic patient records and follow-up imaging. We have created a diagnostic algorithm which provides follow up recommendations.
Results: The majority of mesenteric abnormalities will represent benign aetiology. Only 15% had significant pathology; lymphoma or metastatic cancer the most common of these. The remaining patients had no follow up or stable or resolving findings on repeat CT. Our algorithm provides a practical tool which objectively graded risk and triaged patients into appropriate management pathways.
Conclusion: The majority of patients will have a benign aetiology underlying the mesenteric findings, however significant pathology can be overlooked. Our algorithm provides a useful tool which grades risk and guides radiologists towards appropriate follow up recommendations.

SS 9.09

Straight to surgery! When contrast-enhanced ultrasound can spare blunt abdominal trauma patients the delay of an emergency preoperative CT scan

D.D. Cokkinos, E. Antypa, P. Tserotas, K. Melaki, C. Iosifidis, D. Kriketou, T. Kolios, E. Tavernaraki, P.N. Piperopoulos; Athens/GR

Purpose: To study the ability of contrast-enhanced ultrasound (CEUS) for imaging blunt abdominal trauma (BAT) under emergency conditions. To assess its capacity to recognise the need for immediate surgery without the delay of a CT scan.
Material and Methods: 89 patients (50 men-39 women, aged 17-84 years) were imaged on an emergency basis with CEUS due to BAT. Findings of 39 patients were confirmed by CT.
Results: CEUS detected 56 solid abdominal organ (spleen, liver, kidneys, adrenals) injuries in 53 patients (3 patients had injuries in 2 organs). 6 of these patients were diagnosed with life-threatening spleen (5) or liver (1) rupture. They were successfully operated upon immediately with no preoperative CT performed. All patients were subsequently discharged from the Hospital with no complications.
Conclusion: Emergency CEUS detected solid abdominal organ injures in all affected BAT patients. Immediate surgery was performed when needed, with no delay for preoperative CT.

SS 9.10

Relative accuracy of computed tomography (CT) of the acute abdomen: a prospective observational cohort study

J. Witherspoon, K.G. Foley, A. Aslanyan, L. Davies, C. Thomas, A. Karran, S.A. Roberts, W.G. Lewis; Cardiff/UK

Purpose: Computed tomographic (CT) examination prior to emergency laparotomy has become almost ubiquitous in contemporary UK NHS practice, but there is relatively little data available regarding the accuracy of CT in this context. The aim of this study was to determine the strength of agreement between pre-operative CT diagnosis and the gold standard, operative findings.

Material and Methods: Analysis of prospectively collected data was performed for patients undergoing emergency laparotomy who had undergone pre-operative CT over a calendar year in a university teaching hospital. The CT diagnosis was compared with operative findings and histopathological diagnoses by means of the weighted Kappa statistic [Kw range 0 (no agreement) to 1 (perfect agreement)].
Results: 215 of 310 patients [69.4%, median age 68 (18-93) yr, 106 male], underwent pre-emergency laparotomy CT. Overall sensitivity, specificity, PPV and NPV were 93.4, 98.0, 93.3 and 98.3%, respectively. Overall Kw was 0.866 (95% CI 0.808-0.924, p<0.001). However, with regard to foregut, midgut and hindgut pathology, Kw varied from 0.668 (Upper GI 0.470-0.866, p<0.001), 0.802 (small bowel, 0.688-0.916, p=0.001), and 0.765 (Lower GI 0.645-0.855, p<0.001).
Conclusion: Overall CT accuracy was in the excellent category, but varied with regard to the anatomical site of the pathology, and was most accurate for mid-gut related diagnoses rather than upper and lower GI diagnoses.

11:00 - 12:30 **Europa Hall**

Scientific Session 10
Liver intervention and treatment response

SS 10.01
Cone-beam computed tomography angiography for determination of tumor-feeding vessels during chemoembolization of liver tumors: comparison of conventional and dedicated-software analysis
M. Ronot[1], M. Abdel Rehim[1], A. Hakime[2], V. Kuoch[2], M. Roux[1], M. Chiaradia[3], V. Vilgrain[1], T. De Baere[2], F. Deschamps[2]; [1]Clichy/FR, [2]Villejuif/FR, [3]Creteil/FR

Purpose: To compare the ability of a dedicated software and conventional CBCT analysis to identify tumoral feeders of a series of hypervascular liver tumors treated with TACE.
Material and Methods: Between January 2010 and 2011, 66 hypervascular liver tumors from patients who underwent TACE with arterial CBCT were gathered. Data were analyzed by 6 interventional radiologists blinded to each other analyses. Readers were asked to perform (1) conventional analysis using post-processing tools, (2) computer-aided analysis using FlightPlan for liver (raw-FPFL), and (3) review of this computer aided analysis (reviewed-FPFL). Analyses were compared to a "Reference Reading" established by two study supervisors in consensus. Sensitivities, positive predictive values (PPV), and false positive ratios (FPR) were compared using Mac-Nemar Khi-square and exact Fisher tests. Analysis durations were compared using a non-parametric Mann-Whitney U test.
Results: A total of 179 feeding vessels were identified in the 'Reference Reading'. The sensitivity of raw-FPFL was significantly higher than that of both reviewed-FPFL and conventional analyses (90.9% vs. 83.2% and 82.1%, p<0.0001), with lower PPV (82.9% vs. 91.2% and 90.6%, respectively (p<0.0001), higher FPR (17.1% vs. 9.4% and 8.8%, respectively (p<0.0001), and higher inter-reader agreement (92% vs. 80 and 79%, respectively, p<0.0001). The conventional analysis was significantly longer than that of both raw- and reviewed-FPFL (<0.0001).
Conclusion: The software enabled a fast, accurate and sensitive detection of tumor feeders.

SS 10.02
Reduction of streak artefact from needle at CT-guided biopsy
K.P. Murphy[1], S. Mcwilliams[1], S. Golestaneh[1], A.-M. Mcgarrigle[1], K.N. O'Regan[1], R.S. Arellano[2], M.M. Maher[1], O.J. O'Connor[1]; [1]Cork/IE, [2]Boston, MA/US

Purpose: CT-guided core needle biopsy (CNB) can be impaired due to streak artefact obscuring needle tip visualization.
Material and Methods: Eight biopsy needles in two sizes from two manufacturers with and without stylets were imaged in a CT phantom using 64-slice CT reconstructed with ASIR and FBP (n=16). CNB-related streak artefact was quantified with profile analysis using ImageJ and Microsoft Excel. Hounsfield unit (HU) differences between the maximum HU at the needle tip and the minimum HU in the streak artefact beyond were compared for each variable. Image acceptability and streak artefact were qualitatively assessed on each phantom image after randomization and on 40 CT CNB procedures with and without the central stylet by three blinded reviewers. Statistical analysis (Mann-Whitney U-test, Kappa and T-test) was performed using SPSS (p-value <0.05 considered statistically significant).
Results: Artefact was significantly less without the stylet than with the stylet in situ (median 1145HU versus 3390HU, p<0.001) for all needles and for 19G needles versus 17G needles (median 1334HU vs 2780HU, respectively; p=0.006). There was no difference based on manufacturer (p=0.906), or reconstruction algorithm (p=0.524). Qualitative analysis of 40 cases demonstrated moderate (0.44) and substantial (0.65) agreement regarding needle tip visualisation and streak artefact, respectively, confirming significantly improved needle visibility and reduced streak artifact after stylet removal.
Conclusion: Streak artefact and needle tip visualisation can be improved on CT by confirming needle position after stylet removal.

SS 10.03
withdrawn by the authors

SS 10.04

A 1-year pilot study in the development a daycase 'drop in' paracentesis service

S. Byott, M. Donnelly, C. Mitchell, A. Craig, S. D'Souza; Preston/UK

Purpose: Ascitic drainage is a common procedure, undertaken in a range of settings, with many patients requiring multiple drainages. Various guidelines (British Society Gastroenterlogy, 2006) detail the clinical considerations of ascitic drainage, but few propose methodology to optimise the service for patients. Our aim is to develop a safe and effective 'drop-in' ascitic drainage service with a focus on quality and patient experience.
Material and Methods: A daycase ascitic drainage service was implemented locally alongside multidisciplinary partners following a local protocol. The service has been piloted from November 2012 to November 2013. 111 drains have been placed in 55 patients. 13 patients have also completed a patient satisfaction questionnaire.
Results: 111 drains have been placed in 55 patients with a median drainage quantity of 3.5 l. No significant complications were encountered. Patient feedback were positive, with patients commenting on the ease of access and effective communication from the staff. Feedback from referrers confirms that the service has been a 'great improvement' and has streamlined the patient pathway, saving time, resources and easing bed pressure in a busy acute hospital.
Conclusion: Daycase drop-in ascitic drainage service is a viable option in managing symptomatic ascites. Ultrasound-guided drainage by an interventional radiologist is a safe procedure with a low-complication rate, and if combined with a convenient, accessible referral route, can lead to better patient outcome and higher levels of patient satisfaction.

SS 10.05

withdrawn by the authors

SS 10.06

Triple transcatheter arterial chemoembolisation in intermediate stage hepatocellular carcinoma: 8-year assessment of survival in 77 consecutive patients

I.J. Walton, L. Vine, U. Warshow, S.A. Jackson; Plymouth/UK

Purpose: The objective of our study was to describe the patient profiles, overall survival and treatment-related adverse events in patients with predominantly intermediate stage hepatocellular carcinoma (HCC) treated with conventional transcatheter arterial chemoembolization (TACE) using doxorubicin, cisplatin, and mitomycin C.
Material and Methods: Seventy-seven patients underwent 226 TACE cycles using standardized lipiodol triple-agent chemotherapy between 2005 and 2013. Forty-six patients received TACE alone with ten receiving TACE as "bridging" to liver transplantation and six patients undergoing curative resection after TACE downstaging. One patient had TACE post recurrence after resection. Eight patients received combination therapy with radiofrequency ablation (RFA) and TACE.
Results: Median survival time was 25.3 mths (95% CI 18.2-32.6 mth). Ten patients underwent liver transplantation after TACE, and survival in these patients was significantly longer than those who did not receive transplantion (Logrank test $p \leq 0.001$). Improved survival was seen in the non-transplant patients receiving TACE with adjunctive RFA than in those receiving TACE with the no RFA out to 48 months (Logrank test $p = 0.02$). Complications occurred in 16 patients (10%) with no mortality within 30 days.
Conclusion: Our conventional TACE protocol confers an overall survival benefit compared to other published protocols, and is effective as a bridging therapy towards liver transplantation, and downstaging prior to resection. Furthermore, the conventional TACE protocol was safe with low complications and acceptable patient tolerability.

SS 10.07

Microwave ablation of native hepatocellular carcinomas: evaluation of therapeutic efficacy and safety

V. Battaglia, S. Mazzeo, C. Cappelli, R. Cervelli, B. Pontillo Contillo, C. Bartolozzi; Pisa/IT

Purpose: To evaluate the therapeutic efficacy and safety of microwave (MW) ablation of native hepatocellular carcinomas (HCCs) in patients, excluded from orthotopic liver transplantation (OLT).
Material and Methods: Between June 2012 and September 2013, 49 native HCCs (mean diameter ± SD: 24.8 mm ± 9.1 mm; range 12-62 mm) in 44 cirrhotic patients (M:F: 33:11; age 59.5 yo; range 49-87 yo) were treated by means of MW ablation (Amica, Hospital Service®). All procedures were performed by means of Ultrasound (US) guidance (MyLabTwice, Esaote®, Genova, Italia); patients were in deep sedation. For each ablation procedure, we did registered parameters such as current, WATT and time, number of accesses necessary for treatment, peri and post-procedural complicacies. All patients did undergo a tri-phasic MDCT examination 1 month after treatment to assess response to treatment, evaluated by mRECIST.
Results: Mean treatment time was 6 minutes (range: 2-16 minutes), mean supplied watt: 35W (range 25-60W), accesses number: 51. In 3/44 patients, a haematoma was observed at the end of the procedure; 1/44 patient had a hypertensive crisis during the procedure. At MDCT, 6/49 (12.3%) nodules did show a partial response (PR); 43/49 (87.7%) a complete response (CR). Response to treatment did not correlate to lesion dimension. In 4/6 nodules with PR, a second treatment was performed by means of radiofrequency ablation (1) and MW (3).
Conclusion: MW ablation is a safe, fast and effective approach for the treatment of HCCs nodules.

SS 10.08

HCC treated by TACE with iodized oil: is one-month follow-up with MDCT predictive of treatment efficacy? A correlation with longer follow-up

G.A. Zamboni, M.C. Ambrosetti, F. Lombardo, A. Contro, G. Mansueto, R. Pozzi Mucelli; Verona/IT

Purpose: Patients with HCC treated with TACE with oil are routinely studied one month post-procedure to assess its success. The purpose of this study is to compare the results of one-month follow-up MDCT with those of further follow-up, to confirm the clinical value of routine one-month follow-up.
Material and Methods: We reviewed the 64-row MDCTs performed 4 weeks after TACE with iodized oil (Lipiodol, Guerbet) on 29 patients with HCC (26M, 3F; mean age 67 years). Unenhanced, arterial, portal-venous and equilibrium phase images were available for all patients. Up to 2 nodules were analyzed per patient, and complete treatment of each nodule was diagnosed based on the absence of residual enhancement. The results of this CT were compared with those of subsequent contrast-enhanced imaging (MDCT, MRI or CEUS), with a lesion-by-lesion analysis. Sensitivity, specificity, PPV and NPV for the one-month follow up were calculated by means of Fisher's test, using the later follow-up as a gold standard.
Results: A total of 40 nodules were analyzed (mean diameter 27mm). Further follow-up was at an average of 6 months after TACE (2-26 months). When the nodule was diagnosed as completely treated at one-month follow-up MDCT, this had 100% sensitivity, 80% specificity, 94% PPV and 100% NPV compared with subsequent follow-up imaging.
Conclusion: Contrast-enhanced multiphasic CT is commonly used for the follow-up of HCC after TACE. The results at one-month follow-up are confirmed by later imaging.

SS 10.09

Potentialities of functional magnetic resonance imaging in evaluation of effectiveness of stereotactic radiotherapy of malignant liver tumours

I. Nemiro, O. Utehina, G. Boka, V. Boka; Riga/LV

Purpose: To evaluate diffusion-weighted (DW)-MRI in liver stereotactic body radiotherapy (SBRT) for 16 patients with 24 malignant lesions.
Material and Methods: Pre/post-treatment (2.5 and 4.8 months) DW-MRI was performed. Gross and Internal Tumor Volumes (GTV, ITV) were contoured. GTV-DW location and volume in respect to GTV and ITV, DW-MRI signal intensity (SI) and ADC values of tumor and liver parenchyma were analyzed.
Results: GTV-DW was always located inside initial ITV. Maximum absolute reduction of ITV volume by 36 cm^3 could be achieved using DW-MRI GTV. Lesions demonstrated high DW-MRI SI and reduced ADC values $0.83\pm0.16x10^{-3}$ mm^2 ($1.2\pm0.15x10^{-3}mm^2$ for parenchyma). During first follow-up, 13 lesions have shown low DW-MRI SI and relatively high ADC values ($1.5\pm0.03x10^{-3}mm^2$). In 4 lesions having high SI and low ADC values, tissue reduction was > 50%, in 6 tumors < 50%, correlated with volume reduction. One tumor demonstrated increase >50%, which correlated with increase of volume, peripheral part demonstrated ADC values decrease to $0.93x10^{-3}mm^2$, confirming prolonged tumor growth. Parenchymal SBRT reactions had increased DW-MRI SI and lower ADC values ($1.54\pm0.13x10^{-3}mm^2$). During second follow-up, residual tumors demonstrated reduced DW-MRI SI and raised ADC values to $1.15\pm0.02x10^{-3}mm^2$. Parenchymal SBRT reactions reduced in size with persistent DW-MRI SI and ADC values.
Conclusion: DW-MRI is promising method for treatment volume determination in liver SBRT and for evaluation of residual tumor activity and parenchymal changes.

SS 10.10

Assessment of response to chemotherapy in patients with liver metastases from colorectal cancer: value of diffusion-weighted MR imaging

T. Zahel, E.J. Rummeny, K. Holzapfel; Munich/DE

Purpose: To evaluate diffusion-weighted MR imaging (DWI) in assessing response to chemotherapy in patients with liver metastases from colorectal cancer.

Material and Methods: Thirty-three patients with liver metastases from colorectal cancer underwent MR imaging (1.5 T, Magnetom Avanto, Siemens) before and after 8 weeks of systemic chemotherapy. The MR imaging protocol comprised DWI using a single-shot echo-planar imaging sequence (b values 50, 300 und 600 s/mm²) combined with navigator echo technique. ADC (apparent diffusion coefficient)-values of metastases were calculated before and after chemotherapy. Regions of interest entailed (a) the whole lesion and (b) the periphery of lesions. Response of metastases to chemotherapy was assessed using the Response Evaluation Criteria in Solid Tumors (version 1.0).

Results: One-hundred-four metastases (72 responding and 32 non-responding) were analyzed using DWI. Responding (1.28 vs. 1.41) and non-responding lesions (1.40 vs.1.46) had higher ADC-values after chemotherapy using whole tumor regions of interest; the increase was statistically significant only for responding lesions ($p<0.001$; nonresponding lesions $p=0.21$). ADC-values in the periphery of metastases showed a significant increase in responding (1.01 vs. 1.20; $p< 0.05$) but not in nonresponding lesions (1.07 vs.1.16; $p=0.46$).

Conclusion: Following chemotherapy, responding lesions showed a significant increase of ADC-values when measured as a whole tumor region of interest and also when the periphery of lesions was analyzed. Nonresponding lesions did not show a significant difference of ADC-values before and after chemotherapy.

11:00 - 12:30 **Mozart**

Scientific Session 11
Diffuse liver disease: LTX, CT and US

SS 11.01

Biliary complications following liver transplantation: assessment with MR cholangiography and MR imaging at 3T-device

P. Boraschi, F. Donati, R. Gigoni, F. Filipponi, F. Falaschi, C. Bartolozzi; Pisa/IT

Purpose: To assess the diagnostic value of MR cholangiography (MRC) and MR imaging at 3T-device when evaluating biliary complications in liver transplant recipients.

Material and Methods: One hundred and six transplant subjects with suspected biliary complications (abnormal liver function tests and/or biliary ductal dilation at ultrasound) underwent MRI at 3T-device (GE-DISCOVERY MR750; GE Healthcare). After acquisition of T1w and T2w images, MRC was performed through thin-slab 3D-FRFSE and thick-slab SSFSE T2w sequences. DW-MRI of the liver was also performed using an axial respiratory-triggered spin-echo echo-planar sequence with multiple b-values (150, 500, 1000, 1500 sec/mm²) in all diffusion directions. All MR images were blindly evaluated by two experienced observers in conference to determine the presence of biliary complications, whose final diagnosis was based on direct cholangiography, surgery and integrating clinical follow-up with ultrasound and/or MR findings.

Results: In twenty-two patients, no biliary abnormality was observed. The remaining 84 subjects were affected by one or more of the following complications: ischemic-type biliary lesions (n=38), anastomotic strictures (n=18), ampullary dysfunction (n=16), anastomotic leakage (n=2), stones, sludge and casts (n=32). The sensitivity, specificity, PPV, NPV and diagnostic accuracy of the reviewers for the detection of all types of biliary complications were 99%, 91%, 98%, 95% and 97%, respectively.

Conclusion: In liver transplant recipients, MRC and MR imaging at 3T-device are extremely reliable for detecting biliary complications and should be recommended before planning any therapeutic interventions.

SS 11.02

Feasibility of three-dimensional virtual surgical planning in living liver donors

J.H. Yoon, J.M. Lee, J.H. Jun, K.-S. Suh, J.K. Han, B.I. Choi; Seoul/KR

Purpose: To determine the accuracy and reproducibility of a semiautomatic liver analysis program for liver volumetry and vascular analysis in estimating graft volume in living liver donors.

Material and Methods: This retrospective study was approved by our institutional review board and informed consent was waived. A total of 105 liver donor candidates (M:F=73:32, age: 18-61 years) who underwent preoperative liver CT were enrolled. Volumes of the whole liver (V_T), four hepatic segments, and predicted volume of the hepatic graft (Vpred) were obtained using a semiautomatic analysis program by radiologists and a conventional volumetry program by surgeons. Intraobserver and interobserver agreements of V_T and V_{pred} were assessed using intraclass correlation coefficients (ICCs). V_{pred} was also compared to the actual graft weight (W_{act}) and the analysis time was recorded. In addition, possible vascular complications were assessed using the surgical planning function of the software.

Results: The mean processing time of hepatic volumetry, segmentation and surgical planning using software (175.9±46.6 seconds) was significantly shorter than manual volumetry (916.6±52.8 seconds). V_T and Vpred showed significant intra-and inter-observer agreements and Vpred showed strong correlation with W_{act} ($r=0.83$-0.86, $P<0.0001$) albeit with a tendency toward overestimation. Furthermore, image review using the liver analysis program detected 4 of 5 vascular complications (80%).

Conclusion: Semiautomatic liver analysis software provided good accuracy and excellent reproducibility to estimate liver volume in a short time and it was useful for predicting vascular complications.

SS 11.03

Pattern of HCC recurrence after liver transplantation: time to modify the current follow-up imaging modalities?

M. Dioguardi Burgio[1], M. Ronot[2], D. Fuks[2], F. Cauchy[2], F. Dondero[2], V. Paradis[2], F. Durand[2], J. Belghiti[2], V. Vilgrain[2]; [1]Palermo/IT, [2]Clichy/FR

Purpose: To analyse the imaging characteristics of hepatocellular carcinoma (HCC) recurrence following liver transplantation (LT) in order to determine whether the current follow-up imaging modalities are relevant in the detection of these recurrences.

Material and Methods: Among 336 cirrhotic patients undergoing LT between 2000 and 2011, 25 (7.4%) experienced HCC recurrence. Their pre-LT characteristics, long-term outcome and imaging characteristics of recurrences were retrospectively analysed.

Results: All patients were males [median age 54 (41-64) years]. Before LT, 13 (52%) patients had lesions outside the Milan criteria. Median time to HCC recurrence was 13.8 (1-75) months following LT and 8 (32%) patients experienced recurrence >24 months after LT. Recurrences were detected using routine US follow-up in only 7 (28%) patients, and CT/MRI imaging in 18 (72%) of the patients including 5 (20%) based on alpha-fetoprotein elevation. The most frequently involved organs were the lungs in 13 (52%) cases and the bones in 9 (36%) cases. Recurrent HCC involved >1 organ in 11 (44%) patients. Recurrences were limited to the liver in one (4%) patient, were exclusively extrahepatic in 18 (72%) patients and were both intrahepatic and extrahepatic in 6 (24%) patients.

Conclusion: Routine US examination alone failed to detect most HCC recurrences. Because HCC recurrence may occur even in patients with favourable prognostic factors, is mainly extra-hepatic, may be delayed, and is rarely identified using US examination, we suggest performing regular whole-body imaging during follow-up visits 2 years or more after LT.

SS 11.04

Withdrawn by the authors

SS 11.05

Critically appraised topic: comparison of conventional and contrast-enhanced ultrasound for screening of vascular complications after orthotopic liver transplantation

J.F. Pekelharing, A.J. Van Der Molen; Leiden/NL

Purpose: Can contrast-enhanced ultrasound (CEUS) in addition to color Doppler ultrasound (CDUS) facilitate evaluation of hepatic artery patency or vascular complications in the early phase after orthotopic liver transplantation (OLTx)? A critical appraisal.

Material and Methods: The literature was systematically searched (PubMed). All initial 115 records were evaluated by one author resulting in 8 relevant articles. These were critically appraised using evidence-based methods, subtracting information about test characteristics of CEUS compared to a golden standard (CTA, angiography, surgery and/or follow up).

Results: All appraised studies show a sensitivity of CEUS of 100%, a specificity of CEUS of 92-100% and negative predictive value of CEUS of 100%. CEUS is a useful noninvasive technique for detection of vascular complications, it helps improve flow visualization in the hepatic arteries and portal veins, and can differentiate thrombosis from a patent artery. CEUS decreases scanning time and the level of observer confidence increases considerably. CEUS has a sensitivity and specificity for detection of hepatic artery thrombosis similar to CTA, but CEUS is available at bedside in the ICU.

Conclusion: CEUS has excellent test characteristics and offers substantial benefits for both patient and clinical team in terms of time, cost and potential risks compared to CDUS. CEUS can be used as a primary test in the evaluation of vascular complications in the early phase after OLTx.

SS 11.06

Acoustic structure quantification using probability density function of echo amplitude for the assessment of hepatic steatosis in living liver donors

J.Y. Son[1], J.Y. Lee[1], E.S. Lee[1], I. Joo[1], S.K. Jang[2], B.Y. Hur[1], C.J. Lee[1], K.G. Kim[2], J.K. Han[1], B.I. Choi[1]; [1]Seoul/KR, [2]Gyeonggi-do/KR

Purpose: To investigate the diagnostic accuracy of acoustic structure quantification (ASQ) for the assessment of hepatic steatosis (HS) in living liver donors, with magnetic resonance spectroscopy (MRS) as the reference standard.

Material and Methods: This study was prospectively designed. A total of 91 candidates for liver donation (mean age, 41.02±14.01 years old; M:F, 62:29) underwent ASQ and MRS. In all patients, ASQ parameters of mode, average, standard deviation and ratio were obtained from right hepatic lobe. Statistical analyses were performed.

Results: According to MRS values, 10 of 91 patients (11.0%) were categorized into normal group; 55 patients (60.4%), mild HS group; and 26 patients (28.6%), substantial HS group. All ASQ parameters showed significant correlation with liver fat concentration of MRS (rho, -0.455 to -0.715, all $P < 0.001$). Multiple linear regression test revealed that the average and ratio of Cm2 values (red) were independently significant ($P < 0.001$). The area under curve (AUC) of the average of Cm2 values (red) for the diagnosis of substantial HS was 0.987 with sensitivity of 100% and specificity of 89.06% with a cut-off value of 107.67. The AUC of the ratio of Cm2 values (red) was 0.999 with sensitivity of 96.3% and specificity of 100% with a cut-off value of 0.1.

Conclusion: ASQ may be a very promising quantitative parameter for the diagnosis of substantial HS in living liver donors.

SS 11.07

Geographic fatty liver deposition in oncologic patient at gray-scale US: role of contrast-enhanced sonography

T.V. Bartolotta, A. Taibbi, M. Dioguardi Burgio, M. Midiri; Palermo/IT

Purpose: To assess the role of contrast-enhanced US (CEUS) in the detection of liver metastases in cancer patients with geographic liver fatty deposition at grey-scale US.

Material and Methods: 36 consecutive patients (23 women, 13 men; age 33-80 years, mean: 58 years) with breast (n=17), colorectal (n=13) and other (n=6) cancer with geographic liver fatty deposition but without any detectable focal liver lesion at gray-scale US, underwent CEUS after the administration of SonoVue®. Two readers reviewed CEUS scans and reported by consensus the presence, size and location of any detected lesion. All patients underwent MRI with hepatocellular specific contrast agent as a confirmatory study.

Results: in comparison with US, CEUS detected seven metastases (size: 5-14 mm, mean: 8.4 mm) in four of 36 (11.1%) patients ($p<0.05$). In the same four patients, MRI confirmed all the CEUS-detected metastases and revealed five additional lesions: four further metastases (4-15 mm, mean: 10.2 mm) and one cyst: (4 mm). In a fifth patient MRI detected two additional benign lesions (one hemangioma and one cyst 6 mm in size each one), whereas in a sixth patient CEUS misdiagnosed geographic fatty change as three metastases. Sensitivity, specificity, PPV, NPV values and accuracy of CEUS considering MRI as gold standard were 80%, 96.8%, 80%, 96.8% and 94.4% respectively.

Conclusion: CEUS improves the detection of liver metastases in cancer patients with geographic liver fatty deposition at grey-scale US.

SS 11.08

Quantification of liver fibrosis in human specimens using grating-based phase contrast computed tomography

A.A. Fingerle[1], M. Willner[2], J. Herzen[3], P.B. Noël[1], E. Drecoll[1], C. Braun[1], F. Fischer[1], E.J. Rummeny[1], F. Pfeiffer[2]; [1]Munchen/DE, [2]Garching/DE, [3]Geesthacht/DE

Purpose: To evaluate the potential of grating-based phase contrast computed tomography (gbPCCT) for the quantification of liver fibrosis in human specimens and to correlate with histological diagnosis.

Material and Methods: IRB approval was obtained. Thirty human liver specimens with varying degrees of fibrosis were prospectively collected during autopsy at the institute of forensic medicine. Tissue samples were fixed in 4% formalin solution and imaged using a Talbot-Lau interferometer with a rotating-anode X-ray tube and a photon-counting detector. Phase-contrast and attenuation-contrast image sets were visually graded according to fibrotic stage using a 5-point scale. Additionally, a software-based method was used for quantfication using thresholds. Specimens were then sliced and stained for histological diagnosis including classification of fibrosis. Results of visual and software-based staging of the severity of fibrosis were compared to histology.

Results: In phase-contrast images, strands of fibrous tissue show high signal intensity and delineate from surrounding liver tissue. When the extent of fibrosis was addressed visually or software-based using a threshold, the results showed strong correlation ($r = 0.84$) with the histological grading. On the contrary, attenuation-contrast images did not allow quantification of liver fibrosis.

Conclusion: Grating-based phase contrast computed tomography allows ex vivo quantification of liver fibrosis in human specimens. In a clinical setup, a gbPCCT scanner may have the potential to improve diagnostics and therapy monitoring of chronic liver disease.

SS 11.09

Comparison between ElastPQ and Fibroscan for evaluation of fibrosis in chronic liver diseases

M.-A. Van Caulaert, N. Michoux, Y. Horsmans, P. Starkel, E. Danse; Brussels/BE

Purpose: Shear wave ElastPQ (PhilipsHealthcare) is a new technique investigating the elasticity of liver tissue. However, its interest, compared to already validated Fibroscan (Echosens) remains to be fully evaluated. Therefore, we sought to compare ElastPQ to Fibroscan in liver fibrosis.

Material and Methods: 132 patients underwent liver elasticity assessment using both ElastPQ and Fibroscan on the same day. 70 patients, who fulfilled the validity criteria for Fibroscan, were included in the analysis and divided into 4 groups. 33 hepatitis C (HCV) patients, 12 hepatitis B (HBV), 5 non-alcoholic steatohepatitis (NASH) patients and 20 patients with other diseases. Inter-technique agreement on fibrosis gradation was assessed with Cohen's weighted kappa. Inter-technique agreement on elasticity measurement (in kPa) was studied with Bland-Altman plot.

Results: Inter-technique agreement for fibrosis gradation was almost perfect in HCV-related and "other chronic liver disease" group. Results were poorly concordant in the HBV and NASH groups. Bland-Altman plot showed that fibroscan slightly overestimates elasticity measurements compared to ElastPQ (regardless of patients group) without influencing the statification.

Conclusion: This study sought to compare ElastPQ and Fibroscan in 4 subgroups of patients. Our preliminary results, although based on a small number of patients, seem to indicate that ElastPQ cannot be considered as a suitable alternative for fibrosis assessment in HBV-related cirrhosis and NASH. However, it revealed accurate concerning HCV-related cirrhosis and "other causes"-related cirrhosis.

SS 11.10

Multiple arterial phase dynamic CT for evaluation of liver tissue perfusion characteristics: correlation with perfusion CT

J.M. Lee, D.H. Lee, J.H. Yoon, B.I. Choi; Seoul/KR

Purpose: To determine the feasibility of multiphasic dynamic CT including multiple arterial phases for evaluation of liver tissue perfusion characteristics using the maximum slope model in humans compared with perfusion CT (PCT) as the standard of reference.

Material and Methods: PCT was performed in 23 patients with chronic liver diseases using Xenetix 370. Five-phase, dynamic CT including unenhanced, triple-arterial phases including information regarding the peak aortic and splenic enhancement and the portal phase were selected in order to obtain perfusion parameters of liver parenchyma using a maximum slope method. Those selected CT datasets and the whole PCT data sets were analyzed using dedicated perfusion software (VPCT body; Siemens Healthcare) for estimating the perfusion parameters. Comparison between the perfusion parameters calculated from the multiphasic dynamic CT datasets and those of PCT was made using the intraclass correlation coefficient.

Results: All of the perfusion parameters of patient liver parenchyma including ALP, PVP, and HBPi obtained by five-phase images in the 23 patients did not differ significantly compared with those of PCT. They showed very high agreement with PCT (ICCs > 0.80, P-value < 0.01) in both the validation and the evaluation groups.

Conclusion: It was feasible to obtain perfusion parameters of the liver using multiphasic dynamic CT scans, and the perfusion parameters using the dynamic CT scans were comparable to those of perfusion CT.

11:00 - 12:30 **Karajan**

Scientific Session 12
CT Colonography

SS 12.01

National survey of CT colonography practice in Ireland

A.E. Smyth, C.F. Healy, E. Aherne, P. Macmathuna, M.M. Morrin, H. Fenlon; Dublin/IE

Purpose: To review the status of CT colonography (CTC) practice in the Republic of Ireland and to assess changes in clinical practice with the introduction of CTC.

Material and Methods: A questionnaire was sent to all adult radiology departments in the Republic of Ireland with a CT scanner.

Results: The questionnaire was sent to 45 hospitals, 27 responded (60%), 21 of these are performing CTC, 6 are not. The median time since the introduction of CTC is 5 years (IQR 3.6-8 years). The median number of CTC examinations performed per department per year is 90 (IQR 50-169). 76% of hospitals reported that most patients are symptomatic. 81% use dual positioning routinely; 38% use IV contrast in ≥90%; 76% use faecal tagging and 57% use Buscopan in most cases and 76% use a CO_2 insufflator. There are 51 consultant radiologists in the 21 hospitals reading CTC (average 2.4 per hospital); 73% have attended a formal CTC course. 51% of consultants report >50 CTC examinations per year. 67% reported a reduction in use of Barium enema since CTC introduction. 67% reported that limited access to the CT scanner was the major limiting factor to increasing numbers of CTC.

Conclusion: CT colonography is increasingly available throughout Ireland and is replacing barium enema in most centres. A high proportion of reporting radiologists have formal training and studies are largely performed according to ESGAR guidelines.

SS 12.02

Eye-tracking at endoluminal CT colonography: differences between false-positives diagnosed by experienced and novice readers

A. Plumb[1], E. Helbren[1], P. Phillips[2], T. Fanshawe[3], S. Mallett[3], D. Boone[4], A. Gale[5], D. Manning[2], D. Altman[3], S.A. Taylor[1], S. Halligan[1]; [1]London/UK, [2]Lancaster/UK, [3]Oxford/UK, [4]Colchester/UK, [5]Loughborough/UK

Purpose: To describe the characteristics of false-positive lesions diagnosed by experienced and novice readers at endoluminal CT colonography (CTC).

Material and Methods: 25 novice and 17 experienced (>200 cases) radiologists each viewed 15 endoluminal CTC videos with simultaneous monitoring of eye movements with an eye-tracker. Readers signaled when they suspected a polyp with a mouse click. False-positives were defined as mouse clicks that occurred when no polyp was visible, with the reference standard being a composite of 3 expert radiologists and unblinded colonoscopy. Features provoking at least 3 readers to make a false-positive diagnosis were further interrogated by an experienced colonographer, who compared reader eye positions at the time of their mouse click with the endoluminal CTC video. The true nature of the perceived endoluminal abnormality was determined by 2D correlation.

Results: Overall, 22 different features provoked more than 3 false-positive mouse clicks (mean=15 FP clicks/feature). 95% of these features were either diverticula (7 instances: 67 FP clicks), faecal residue (8 instances: 133 FP clicks) or artefacts (6 instances: 103 FPs). Experienced readers were significantly less likely than novices to generate false-positive clicks for diverticula (p=0.03). There was no significant difference in false-positives between experienced and novice readers for faecal residue or artefacts.

Conclusion: Diverticula, faecal residue and artefacts commonly provoke false-positive diagnoses at endoluminal CTC. Experienced readers seem more capable than novices at distinguishing diverticula from polyps.

SS 12.03

Impact of post-hysterectomy changes on distal colonic morphology and endoscopy: quantitative assessment at CTC with endoscopic performance correlation

C.N. Weber[1], H.M. Zafar[1], M.S. Levine[1], B. Geiger[2], A.S. Lev-Toaff[1]; [1]Philadelphia, PA/US, [2]Princeton, NJ/US

Purpose: The aim of this study is to quantitatively assess distal colonic morphology using novel software, and evaluating differences by hysterectomy status which may contribute to higher rates of incomplete/difficult endoscopic exams in post-hysterectomy women.

Material and Methods: CTC datasets from 73 women (37 post-hysterectomy/36 control) were compared. Inclusion criteria: incomplete endoscopy. Exclusion criteria: severe diverticulosis, large uterine fibroids, colonic resection, colonic masses. Length, volume, tortuosity (number of high curvature points (hcp)), compactness (boxed volume containing centerline divided by centerline length) of the rectum, sigmoid and combined rectosigmoid were assessed. Height of the sigmoid apex (HSA) relative to the lumbosacral junction was assessed. Each dataset was quantified twice by a single reader on separate occasions. Groups were compared using student's t-test. Relative risk associated with post-hysterectomy status and failure to clear the sigmoid at endoscopy was calculated.
Results: Post-hysterectomy women had lower HSA (29.7 vs 57.4 mm, p=0.002), and more tortuous (5.30 vs 4.42 hcp, p=0.012), compact (3362.1 vs 4028.7 mm^2, p=0.001), shorter (652.0 vs 703.2 mm, p=0.026), and smaller (0.418 vs 0.542 L, p=0.002) rectosigmoid colons. There was increased relative risk of 2.068 (p=0.043) for failure to clear the sigmoid at endoscopy (45.9% vs 22.2%).
Conclusion: Post-hysterectomy women had lower HSA and more tortuous and compact distal colons, possibly from absence of the uterus and pelvic supports. Despite shorter lengths, there was increased failure rate to clear the sigmoid at endoscopy. Smaller volumes suggest adhesions may limit distensibility.

SS 12.04

CT colonography: terminal digit preference biases polyp measurements by radiologists, endoscopists and pathologists

A. Plumb, K. Wooldrage, W. Atkin, S. Halligan; London/UK

Purpose: To determine if (a) radiologists, (b) endoscopists and (c) pathologists exhibit bias when measuring polyps via "rounding" to the nearest 5 mm.
Material and Methods: Polyp diameters measured at CT colonography (CTC), endoscopy and histopathology were collated from the English bowel cancer screening programme (BCSP) and two randomised trials. Log-normal models were fitted to estimate the expected number of polyps at 1 mm increments. The difference between the expected and observed number of polyps was calculated for each terminal digit (1 mm, 11 mm, 21 mm…;2 mm, 12 mm, 22 mm…). Following statistical advice, significance testing was not performed due to over-dispersion.
Results: In the BCSP, at CTC the number of polyps with sizes ending in zero was 75% greater than expected (217 observed, 123.7 expected) and there was a 33% excess of polyps ending in 5 mm (284 observed, 213.1 expected). Similar patterns were demonstrated at endoscopy for polyps with sizes ending in zero (145% greater than expected) and 5 mm (44% excess), and at histopathology for polyps with sizes ending in zero (152% excess). An identical phenomenon was observed in the randomised trials for CTC (155% over-representation of terminal digit zero), endoscopy (285% over-representation) and histopathology (232% over-representation), with similar but lesser effects for sizes ending in 5 mm.
Conclusion: Radiologists, endoscopists and pathologists exhibit terminal digit preference bias when measuring polyps. This may influence trial data, referrals for further testing, polyp surveillance regimes and comparisons between tests.

SS 12.05

Full purgation bowel preparation versus faecal tagging alone prior to CTC: does it really make a difference?

G. Ayub, A. Lowe, C. Kay, A. Williams; Bradford/UK

Purpose: To see if there was a significant difference in the quality of CT-colonography produced between patients prescribed bowel clearance preparation containing laxative to those not containing laxative. In addition, to also get patient feedback on bowel preparation experience.
Material and Methods: Retrospective study was performed looking at 300 CTC investigations. This included 138 investigations in which full preparation (FP) was prescribed (3-day regime with laxative), and 162 investigations in which minimum preparation (MP) was prescribed (2-day regime without laxative). Both preparations also involved a low-residue diet and gastrografin for faecal tagging. CTC investigations were analysed for degree of bowel clearance and bowel insufflation, graded as either poor, moderate or good. Questionnaires were given to patients attending for the investigation to get feedback on bowel preparation experience.
Results: There was no significant difference in the quality of CTC produced with respect to bowel clearance (p=0.23) and bowel insufflation (p=0.81) between the two regimes. 45 patient feedback questionnaires (21 had laxative and 24 did not) showed a statistically insignificant (p>0.05) increase in faecal incontinence, urgency, diarrhoea, nausea and disturbed sleep in patients taking a laxative.
Conclusion: In conclusion, high-quality diagnostic CTC can be obtained without the need for laxative in bowel preparations, also the MP regime is of benefit as it is a shorter regime with reasonably fewer symptoms, and therefore, more manageable for the patient.

SS 12.06

The effect of computer-aided detection markers on visual search and reader performance in CT colonography

E. Helbren[1], A. Plumb[1], T. Fanshawe[2], P. Phillips[3], S. Mallett[2], D. Boone[4], A. Gale[5], D. Altman[2], S.A. Taylor[1], D. Manning[3], S. Halligan[1]; [1]London/UK, [2]Oxford/UK, [3]Lancaster/UK, [4]Colchester/UK, [5]Loughborough/UK

Purpose: To identify the effect of computer-aided detection (CAD) on visual search and performance in CT colonography (CTC) and to identify differences between novice and experienced readers.
Material and Methods: 15 videos were recorded from CTC fly-through examinations, each containing a single polyp. Two versions of each video were generated, with without a CAD prompt. Videos were viewed in a randomised order by 42 readers (17 experienced [>200 cases] and 25 novices [<100 cases]). Visual search was monitored via eye-tracking. Both CAD markers and polyps were treated as regions of interest in data processing. Statistical analysis using multilevel modelling was applied to allow for the cross-classified data structure.
Results: CAD drew readers' attention to polyp location faster, leading to quicker identification times. For example median 'time to first pursuit' was 0.48s (IQR: 0.27-0.87s) with CAD versus 0.58s (IQR: 0.35-1.06s) without. CAD also held readers' visual attention on the polyp for longer. A significant increase in the number of correct polyp identifications across all readers was seen when using CAD (74% without-CAD, 87% with-CAD).
Conclusion: CAD marks significantly alter the visual search patterns of readers viewing endoluminal CTC by all quantitative metrics we measured. CAD exerted a larger effect on novice readers.

SS 12.07

Diagnostic accuracy of low-dose CT colonography using adaptive statistical iterative reconstruction

D. Bellini, D. Caruso, M. Rengo, T. Biondi, A. Laghi; Latina/IT

Purpose: The purpose of this study was to evaluate the diagnostic accuracy and image quality of CT colonography (CTC) using a low-dose acquisition protocol with adaptive statistical iterative reconstruction (ASIR).
Material and Methods: From our dataset, 60 cases of CTC were selected, 30 acquired using a low-dose protocol reconstructed with ASIR (Group I, 100 kV, 50-100 mAs, 50%DR) and 30 acquired using a standard CTC protocol reconstructed with FBP (Group II, 120 kVs, 50-100 mAs). Prevalence of polyps, quality of bowel preparations and colon distension are homogenous between two groups. Two expert radiologists, blinded to the scanning techniques, reported the examinations and assessed image quality. Per patient sensitivity, specificity, negative predictive value and positive predictive value were evaluated for each group. Comparative analyses of image quality score, diagnostic confidence and interpretation time were also performed.
Results: Diagnostic accuracy is similar between two groups (Group I: Se 92%, Sp 95%; Group II: Se 93%, Sp 94%). Radiation dose is significantly lower in group I (2.5 mSv vs 5.6 mSv, mean values). Reporting time and diagnostic confidence are similar between two groups (P> 0.05).
Conclusion: ASiR showed similar diagnostic performance with good image quality compared with FBP reconstruction. Our study confirmed feasibility of low-dose CTC with iterative reconstruction as a promising screening tool.

SS 12.08

Polyp classification error at endoluminal CT colonography: characteristics of polyps viewed but incorrectly dismissed by radiologists

A. Plumb[1], E. Helbren[1], P. Phillips[2], T. Fanshawe[3], S. Mallett[3], D. Boone[4], A. Gale[5], D. Manning[2], D. Altman[3], S.A. Taylor[1], S. Halligan[1]; [1]London/UK, [2]Lancaster/UK, [3]Oxford/UK, [4]Colchester/UK, [5]Loughborough/UK

Purpose: To describe (a) the morphology of polyps viewed by radiologists at endoluminal CT colonography (CTC) but dismissed incorrectly, and (b) eye movements during such errors.
Material and Methods: 42 radiologists each viewed 15 endoluminal CTC videos while eye movements were monitored using an eye-tracker. Classification errors were deemed to occur when readers looked at a polyp but

did not confirm it genuine via a mouse click. “Difficult-to-classify” polyps were defined as those with >15% classification error; others were considered “easy”. Polyp diameter, height, subjective conspicuity and proportion of time looked at by radiologists were compared between “easy” and “difficult” polyps using the Mann-Whitney U test for numerical data and ordinal logistic regression for ordinal data.

Results: “Difficult” polyps were significantly smaller than “easy” polyps (mean diameter 5.4 mm versus 8.4 mm, p=0.01) and subjectively less conspicuous (median conspicuity score 4 versus 2, p=0.032). Expert readers spent less time viewing “difficult” polyps during classification errors; 30.2% of the time “difficult” polyps were on screen was spent viewing them vs 54.0% for “easy” polyps (p=0.009), irrespective of whether or not CAD was available (26.8% vs 54.8% without CAD, p=0.0043; 22.3% vs 49.8% with CAD, p=0.024).

Conclusion: Small, inconspicuous polyps are prone to misclassification despite attracting reader gaze. Such classification errors are made rapidly, implying swift decisions are frequently incorrect, even with CAD. Efforts to improve CTC polyp detection should focus on classification decisions rather than detection alone.

SS 12.09

Computer-assisted polyp matching between optical colonoscopy and CT colonography: a phantom study

S. Halligan, H. Roth, T. Hampshire, E. Helbren, M. Hu, R. Vega, D. Hawkes; London/UK

Purpose: To register endoluminal images obtained during colonoscopy with those reconstructed from prior CT colonography (CTC).

Material and Methods: Using structure-from-motion, we used the perspective shift of a colonoscopic video camera to build a 3D image; using the relative translation and rotation of the camera from different projections we triangulated 3D points to reconstruct the endoluminal surface via a dense 3D reconstruction algorithm (plane sweep approach) to extract surface point clouds in 3D. Validation used a 3D printed colon model generated from 25cm of real CTC data that contained two polyps (8mm, 15mm). The 3D model was then painted to resemble human colon, examined using an endoscope (1920x539 resolution), and the 15-mm polyp used as the input sequence for the reconstruction algorithm. We then used a point set registration algorithm (coherent point drift) to match polyp point clouds between the colonoscopic and CTC images and computed the matching cost to assess the accuracy of registration.

Results: The normalised matching cost was smaller at the correct polyp match between colonoscopy and CTC: 1.0 for the target 15 mm polyp vs. 3.9 for the non-target 8 mm polyp. Matching with 370 other endoluminal structure points (e.g. haustra) also found the global minimum occurred correctly at the surface point cloud corresponding to the 15 mm polyp.

Conclusion: Matching endoluminal images between colonoscopy and CTC is technically feasible and could direct endoscopists to polyps seen previously at CTC.

SS 12.10

Patient experience of CT colonography in a national colorectal cancer screening programme

A. Plumb[1], A. Ghanouni[1], C. Rees[2], S. Halligan[1], C. Nickerson[3], S.A. Taylor[1], P. Hewitson[4], R. Bevan[2], H. Miller[2], C. Von Wagner[1]; [1]London/UK, [2]South Shields/UK, [3]Sheffield/UK, [4]Oxford/UK

Purpose: To investigate patient experiences of CT colonography (CTC) in the English national bowel cancer screening programme (BCSP) compares to colonoscopy.

Material and Methods: The English BCSP monitors patient experiences following colonic testing via a post-test questionnaire, inviting responses regarding pre-test assessment (risks/benefits and consent), the test itself (including discomfort) and post-test symptoms. Complications are also recorded by BCSP staff. Screenees tested between 1/1/11 and 31/12/12 and responding to at least one item were included. Multiple imputation of missing data was conducted under the missing-at-random assumption and pooled chi-squared tests of imputed data were used for comparison with colonoscopy.

Results: 79,493 questionnaires were analysed; 61,899 contained at least one response. 2,119 screenees provided data regarding CTC and 60,581 regarding colonoscopy. Understanding of the risks and benefits of CTC (86.9% and 93.6%, respectively) was less than for colonoscopy (95.7% and 98.2%; p<0.001). 25.7% of people found CTC more uncomfortable than expected, more than for colonoscopy (20.8%; p<0.001). Post-procedural pain was relatively infrequent after either test (CTC=14.6%, colonoscopy=14.3%; p=0.91). Direct CTC-related complications were rare (n=16; 0.5%), although a further 20 (0.6%) suffered complications from subsequent procedures provoked by CTC. Colonoscopy complication rates were similar (n=779; 1.0%).

Conclusion: Whilst overall satisfaction with CTC was high, it was judged unexpectedly uncomfortable more frequently than colonoscopy. Understanding of risks was also greater for colonoscopy than CTC. Clear communication of the risks, benefits and procedural experience of CTC is required.

11:00 - 12:30 **Wolf Dietrich**

Scientific Session 13

GI tract - functional imaging and fistula assessment

SS 13.01

Evaluation of a double contrast esophagram instructional video module

B. Kakarala, K. Matsuo, B. Tahir, D.E. Heitkamp; Indianapolis, IN/US

Purpose: Advanced imaging and increasing endoscopy have produced a decline in performed fluorosocpy. However, fluoroscopic skills are necessary for successful practice of radiology. We designed and integrated an instructional video into the first-year radiology resident orientation to evaluate knowledge and competency in performing an esophagram before and after watching the video.

Material and Methods: Prior to any fluoroscopy or instructional video exposure, 15 first-year radiology trainees completed an 11-item written test assessing knowledge and comfort in performing esophagram. One week later, the trainees were provided access to our instructional esophagram video and then asked to complete the same written test. Validity of the exam and statistical significance of the results were analyzed.

Results: Ten objective items were analyzed with the pre and post-test. An average of 6.2 questions were answered correctly per resident on the pre-test while 9.5 questions were answered correctly per resident on the post-test, a 36% improvement ($p<.01$). A 1-5 scale (5 indicating most comfort) was used to assess comfort in performing an esophagram before and after video intervention. Average comfort level rose from 1 to 2.7, a 60% increase ($p<.01$).

Conclusion: Our esophagram video improved the comfort level of novice radiology trainees performing an esophagram. Their knowledge and competency regarding procedural details improved. Other potential audiences benefiting from this video include radiology technology students or practicing radiologists needing fluoroscopy refreshers and continuing education.

SS 13.02

MR fluoroscopy in diagnosis of postoperative complications following laparoscopic Nissen-Fundoplication for GERD

C. Kulinna-Cosentini, W. Schima, A. Ba-Ssalamah, E. Cosentini; Vienna/AT

Purpose: The aim of this study was to determine the feasibility for detecting postoperative complications in symptomatic patients who underwent Nissen Fundoplication for GERD with dynamic magnetic resonance imaging.

Material and Methods: 30 patients (22 patients with recurrent/persistent symptoms and 8 symptomless patients as control group) underwent MRI at 1.5 T. Bolus transit of a buttermilk-spiked gadolinium mixture was evaluated with T2-weighted, half-Fourier acquisition single-shot turbo spin-echo (HASTE) and dynamic gradient echo sequences (B-FFE) in 3 planes. The results of MRI were compared with intraoperative findings, or, if the patients were treated conservatively, with endoscopy, manometry, pH-metry, and barium swallow.

Results: MRI was able to identify the correct location of fundoplication wrap in 28/30 cases (93% overall accuracy) and the malpositions of the fundoplication wraps in 4/6 cases (67%), as well as all wrap disruptions (4/4 cases). All six stenoses in the GEJ were identified and could be confirmed intraoperatively or during dilatation. MRI correctly visualized three cases with motility disorders, which were manometrically confirmed as secondary achalasia. Three patients showed signs of recurrent reflux without anatomical failure.

Conclusion: Our preliminary results demonstrate that dynamic MRI is helpful in diagnosing postoperative complications in patients having undergone antireflux surgery and may be a useful tool in clarifying dysphagia in such patients additional to manometry and ph-metry.

SS 13.03

Morphological and functional evaluation of sleeve gastrectomy: MDCT and cMR imaging

D. De Santis, M. Rengo, L. Bertana, D. Caruso, T. Biondi, A. Laghi; Latina/IT

Purpose: To evaluate morphological and functional changes after laparoscopic sleeve gastrectomy (LSG) using volumetric MDCT, for the evaluation of gastric volumes and thoracic migration, and cine magnetic resonance (cMR) of the esophagus, for the evaluation of motility anomalies and gastroesophageal reflux.

Material and Methods: Thirteen patients, presenting gastroesophageal reflux after LSG, underwent both volumetric MDCT of the stomach and cMR of the esophagus. Gastric volume, stomach length, sleeve length, antrum length thoracic migration and staple-line length were evaluated on MDCT. Motility anomalies of the esophagus and the presence of gastroesophageal reflux were evaluated on cMR.

Results: Gastroesophageal reflux was detected in all patients by cMR. Thoracic migration was found in 50% of patients. Mean gastric volume increase after surgery (initial post-surgical volume 200 ml) was 105.3 ml. Antrum or proximal sleeve dilatation was found in all patients.

Conclusion: Volumetric MDCT and cMR can identify both morphological and functional causes of gastroesophageal reflux and can be helpful in the planning of reintervention.

SS 13.04

Quantitative in vivo analysis of small-bowel motility using MRI examinations in mice: proof of concept study

S. Bickelhaupt[1], M. Wurnig[2], M. Lesurtel[2], M.A. Patak[2], A. Boss[2]; [1]Heidelberg/DE, [2]Zurich/CH

Purpose: Invasive techniques to assess intestinal motility in animal-models should be avoided by application of non- or less-invasive radiological examinations in compliance with the rule of “three-Rs” of humane animal-experimentation (reduction-refinement-replacement). Thus, our aim was to investigate the feasibility of in vivo small-bowel-motility-analyses in mice using dynamic MRI acquisitions.

Material and Methods: All experimental procedures were approved by the institutional animal-care-committee. Six C57BL/6-mice underwent MR-imaging without additional preparation after isoflurane-anaesthetization in prone-position on a 4.7T-small-animal-imager using a birdcage-whole-body-mouse-coil. Motility was assessed using a true-fast imaging in steady-precession-sequence in coronal-orientation (acquisition-time per slice 512ms, in plane resolution 234x234 µm, matrix size 128x128, slice-thickness 1 mm) over 30 s (60 acquisitions). Motility was manually assessed measuring the small-bowel diameter-change over time. The resulting motility curves were analyzed for the following parameters: contraction-frequency-per-minute, maximal contraction-amplitude, luminal diameter and luminal-occlusion-rate.

Results: Mean small bowel contraction frequency was 10.67 contractions-per-minute (SD±3.84), mean amplitude of the contractions was 1.329 mm (SD ±0.43) with a mean luminal diameter of 1.37 mm (SD ±0.42). The mean luminal occlusion rate was 1.044 (SD ±0.45). The mean duration needed for a single motility-assessment was 185 s (SD ±54.02).

Conclusion: Our study demonstrated the feasibility of an easy and time-sparing functional assessment for in vivo small bowel motility analyses in mice. This could improve the development of small animal models of intestinal diseases providing a method similar to clinical MR examinations that is in concordance with the “three Rs” of humane animal experimentation.

SS 13.05

High within-subject variability of segmental small bowel motility as assessed by magnetic resonance enterography

A. Plumb, A. Menys, D. Atkinson, S. Halligan, S.A. Taylor; London/UK

Purpose: To assess variation of small bowel (SB) motility at (a) different enteric segments in the same individual and (b) the same segment at different time points.

Material and Methods: 20 healthy volunteers underwent magnetic resonance enterography following oral 2.5% mannitol. “Cine” BTFE free-breathing (60 second acquisition) volumes were acquired at 3 Tesla with a 1 second/volume temporal resolution. Enteric motility was quantified using the number of contractions per minute (CPM) by measuring luminal diameter on each image: A contraction was defined as a reduction of >10%. Subsequently an optic-flow algorithm was used to generate a deformation field measure (Jacobian standard deviation, JSD), which acts as a surrogate for motility, measured in arbitrary units (AU). Motility was compared in four abdominal quadrants and at two time points (4 weeks apart) using Bland-Altman limits of agreement (LoA).

Results: CPM and JSD showed moderate positive correlation ($r=0.51$, $p<0.001$). Mean motility across all quadrants was 6CPM and 0.34AU. There was substantial variation in motility in the same individual, with the mean difference between the most motile and least motile quadrants being 4.4 CPM and 0.21AU. Temporal variability was even greater, with the Bland-Altman LoA being 6CPM and 0.32AU.

Conclusion: SB motility is highly variable between enteric segments and at different times, irrespective of the quantitative metric used. Segmental SB motility measurements as a disease biomarker may be limited by high spatial and temporal variation.

SS 13.06

Quantitative assessment of global small bowel motility in chronic intestinal pseudo-obstruction and controls: a preliminary study

E.A. Kamalanathan, A. Menys, G. Bhatnagar, S. Butt, N. Zarate, A. Emmanuel, D. Atkinson, S. Taylor; London/UK

Purpose: To compare MRI-quantified small bowel motility in controls and patients with chronic intestinal pseudo-obstruction (CIPO).

Material and Methods: 12 healthy controls (mean age 33) and 5 CIPO patients (mean age 53) underwent enteric MRI after ingesting 1 l of 2.5% mannitol. A 15-slice coronal 3D Balanced Turbo Field Echo motility volume was acquired through the small bowel over a 20-s breath hold (2.5 x 2.5 x 10 in plane resolution, TE=1.7 ms, TR=3.5 ms). Three linear ROIs were placed perpendicular to the central axis of the small bowel and the following were calculated: average contraction rate per minute (CRM) = average number of contractions greater than 10% of mean bowel diameter; average luminal diameter (LD) = average ROI length; average contraction cycle (CC) = average time between maximum contractions. Metrics were compared using the Student t-test on statistical advice.

Results: Mean CRM was 2.2 (±2.5) and 14.1 (±3.06) for CIPO patients and controls respectively; mean difference 11.9 (95% CI 8.6-15.2) p<0.0001. Mean LD was 53.5 mm (±16.5) and 16.7 mm (±2.6), for CIPO patients and controls respectively; mean difference 36.83 mm (95% CI 26.8-46.84) p<0.0001. Mean CC was 8.8 s (±1.6) and 4.0 s (±1.3) for CIPO patients and controls respectively; mean difference 4.8 (95% CI 3.2 to 6.3) p<0.0001.

Conclusion: MRI can quantify reduced contraction magnitude and increased bowel diameter suggesting that it might be useful in CIPO diagnosis.

SS 13.07

Evaluation of bowel motility by means of motility mapping in dynamic MRI improves detection of lesions in inflammatory bowel disease

M.L. Hahnemann, F. Nensa, S. Kinner, S. Maderwald, G. Gerken, T.C. Lauenstein; Essen/DE

Purpose: To evaluate whether additional investigation of motility alterations in bowel magnetic resonance imaging (MRI) of patients with inflammatory bowel disease (IBD) leads to an increased detection rate of inflammatory lesions compared to static MRI alone.

Material and Methods: Thirty consecutive patients with suspected or known IBD underwent bowel MRI using an 1.5 T scanner. In addition to static T2-weighted and contrast-enhanced T1-weighted data, a dynamic coronal T2-weighted sequence (dynamic MRI) was collected. Dynamic sequences were used to automatically generate a map depicting motility of the bowel. These resulting motility maps allow for the detection of bowel motility disorders, e.g. by hypomotilities of the bowel. Two readings of the MRI were performed; first, evaluation of static MRI alone, and second, evaluation of static MRI combined with dynamic MRI (motility mapping). Locations showing motility alterations were analyzed on static MRI for IBD-related lesions.

Results: Detection of inflammatory lesions was increased by additional application of the automated evaluation of bowel motility compared to evaluation of static MRI alone. Eleven of thirty (37%) patients showed additional lesions. Especially, short-distance lesions as well as lesions in incomplete distended bowel sections were found.

Conclusion: Motility assessment of the bowel provides additional information and increases the detection rate of inflammatory lesions in MRI.

SS 13.08

Assessment of fistula activity with diffusion-weighted MR imaging in perianal disease

S. Bakan, D. Cebi Olgun, O. Tutar, F. Kantarci, C. Samanci, I. Adaletli, G. Ogut, I. Mihmanli; Istanbul/TR

Purpose: To determine the activity on diffusion-weighted magnetic resonance imaging (DWMRI) in perianal fistulas with or without abscess.

Material and Methods: 66 patients with 82 perianal fistula and abscess were included. DWMRI was performed (b-factors 50, 400 and 800 s/mm^2) and apparent diffusion coefficient (ADC) values of lesions were measured. The lesions were classified four groups based on radiological findings: only abscess, only fistula, abscess component of abscess associated with fistula and fistula component of abscess associated with fistula. The lesions were classified into two groups based on clinical findings: positive inflammatory activity (PIA) and negative inflammatory activity (NIA). ADCs of both groups were compared using Mann Whitney U and Pearson test.

Results: The mean ADC value (mm^2/s) of PIA lesions was significantly lower than NIA lesions in fistula associated abscess (1.371±0.168 x 10^{-3} vs.1.586±0.136 x 10-3, p=0.036). The mean ADC value of PIA lesions was 1.289±0.256 x 10-3, while the mean ADC of NIA lesions was 1.238±0.217 x 10^{-3} in patients with only perianal fistula. There was no statistically difference in mean ADC values between PIA and NIA fistula in these patients (P=0.507).

Conclusion: The measurement of ADC values in perianal fistula-associated abscess, are helpful in MR diagnosis to detect fistula activity. As a result, DWMRI could play a role in clinical practice and may be an option for surgeons to evaluate fistula activity.

SS 13.09

Diffusion-weighted MR imaging for the diagnosis of abscess complicating fistula-in-ano: preliminary experience

A. Dohan[1], C. Eveno[1], R. Oprea[1], K. Pautrat[1], V. Placé[1], M. Pocard[1], C. Hoeffel[2], M. Boudiaf[1], P. Soyer[1]; [1]Paris/FR, [2]Reims/FR

Purpose: To investigate the role of diffusion-weighted MR imaging (DWMRI) in evaluating fistula-in-ano.

Material and Methods: MRI examinations of 24 patients with fistula-in-ano, including fat-suppressed T2-weighted turbo spin-echo (T2-TSE) MRI and DWMRI were reviewed by two independent readers for presence and number of visible fistulas, conspicuity and apparent diffusion coefficient (ADC) measurement of suspected fistula tracks and pelvic collections. Reference standard was surgical and follow-up findings.

Results: Sensitivity was 91.2% [95% CI: 76%-98%] for T2-weighted TSE MRI and 100% [95% CI: 90%-100%] for DWMRI for detecting fistulas. ADC value was lower in abscesses than in inflammatory masses (P=0.714.10-6). Area under ROC curve was 0.971 and optimal cut-off ADC value was 1.186 x10-3mm²/s, yielding sensitivity of 100% [95% CI: 77%-100%] and specificity of 90% [95% CI: 66%-100%] for the diagnosis of abscess. ADC values of the fistula track did not correlate with inflammation according to Van Assche classification (R^2=0.1084). Fistula conspicuity was greater with DWMRI than with T2-TSE MRI for the two observers (P=0.0034 and P=0.0007).

Conclusion: DWMRI shows high sensitivity and specificity for the diagnosis of perianal abscesses and helps discriminate between abscess and inflammatory mass. Conspicuity of fistulas-in-ano is greater with DWMRI than with T2-weighted TSE MRI. ADC value does not correlate with perineal lesion activity.

SS 13.10

Fluoroscopically guided balloon dilation of strictures of the gastrointestinal tract: review of 2041 procedures performed over 30 years

R. Khot, D.L. Lambert, G. Easley, H.A. Shaffer, E.E. De Lange; Charlottesville, VA/US

Purpose: Fluoroscopically guided balloon dilation (FGBD) is a routine clinical procedure at our institution for treating strictures of the gastrointestinal (GI) tract since 1983. The purpose was to review the indications, the dilating effect on the strictures, and the number and severity of complications encountered with the procedure.

Material and Methods: This study was HIPPA compliant and IRB approved. A total of 2041 FGBDs were performed in 1177 patients (mean age 56.8 years; age range 5 weeks-94 years; M/F 646/531) for strictures of the esophagus (n=1794), stomach/pylorus (n=177), small bowel (n=19), and colon/rectum (n=51). Of the 1177 patients, 785 (66.6%) had one, 211 (17.9%) had two, 120 (10.1%) had 3, and 61 (5.1%) had >3 FGBDs. Change in pre-post stricture diameter and area were calculated, and complications reviewed.

Results: Mean increase in luminal diameter was 3.7x the initial (predilation) diameter (min 1x-max 33x; p<0.01), and mean increase in luminal area was 21.5x the initial area (min1x-max 900x; p<0.01). There were 38 complications in the 2041 procedures. Of these 5/2041 (0.2%) were not related to the GI tract [hypertension (n=1), hypotension (n=1), hypoxia (n=2), tachycardia (n=1)]. Lacerations occurred in the remaining 32 (1.5%) consisting of intramural tear (n=11, 0.5%), contained leak (n=14, 0.7%), and complete, through-and-through perforation (n=7, 0.3%) needing surgery.

Conclusion: FBGD is a highly effective, low-risk procedure for treating GI strictures, with through-and-through perforations requiring surgery occurring in only 0.3% of procedures.

11:00 - 12:30 **Papageno**

Scientific Session 14

Biliary tract and peritoneum

SS 14.01

High-resolution ultrasonography: staging accuracy for gallbladder cancer and differential diagnosis of neoplastic gallbladder polyp comparison with conventional ultrasonography

J.H. Kim, H.W. Eun, J.Y. Lee, J.K. Han, B.I. Choi; Seoul/KR

Purpose: To compare staging accuracy for gallbladder cancer and differential diagnosis of neoplastic gallbladder polyp of high-resolution US (HRUS; combined low- and high-MHz transducers) and conventional US (CUS; low-MHz transducer).

Material and Methods: Our study consisted of 37 surgically proven gallbladder cancer (T1a=7, T1b=2, T2=22, T3=6) and 88 surgically proven gallbladder polyp (malignant polyp=46, benign polyp=42) who underwent preoperative HRUS. Two radiologists independently and retrospectively accessed T-stage and evaluated the presence or absence of predefined findings of the gallbladder polyp on HRUS and CUS. Statistical analyses were performed using Chi-square tests and McNemar test.

Results: Diagnostic accuracy for T-stage was T1a=68%-78%, T1b=76%-81%, T2=57%-59%, T3=81%-89% with moderate agreement (κ=0.569) in CUS and T1a=92%-95%, T1b= 89%-95%, T2=78%-86%, T3=84%-89% with substantial agreement (κ=0.642) in HRUS. Diagnostic accuracy in differentiating T1 and over T1 was 65% and 70% in CUS and 92% and 89% in HRUS. Statistically common US findings for malignant polyp included size >1cm, single, lobular surface, vascular core, hypoechoic polyp, and hypoechoic foci ($p < 0.05$). HRUS was better depicted internal echo foci than CUS (39 and 21). Polyp size >1 cm was independently associated with the malignant polyp (Exp(B)=7.5, p=0.02).

Conclusion: HRUS was useful in accurately depicting T-stage of gallbladder carcinoma and differentiating malignant gallbladder polyp. Combined use of low- and high-MHz transducers would improve the diagnostic performance of ultrasonography in malignant gallbladder diseases.

SS 14.02

Biliary dilation in the presence of a periampullary duodenal diverticulum

J.J. Lee, G. Brahm, S. Bruni, B. Sreeharsha; Toronto, ON/CA

Purpose: Periampullary diverticulum (PAD) often presents as an incidental CT finding. Its significance and its effect on biliary dilation are unclear. The aim of our study was to determine if the presence of a PAD is associated with abnormal dilation of the CBD.

Material and Methods: Patients with PAD were retrospectively identified from the radiology database from November 2011 to November 2012 and those with known pancreaticobiliary pathology were excluded. 150 patients were selected. A control group of 150 patients with no PAD was also chosen. Data with respect to demographics, PAD size and location, ductal diameter, previous cholecystectomy and liver function tests were collected.

Results: 34 patients had cholecystectomy in PAD and 11 in control groups. Statistically significant increase in CBD measurement (at pre ampulla, pancreatic head and distal to confluence) was noted in both the groups only with prior cholecystectomy when compared to non-cholecystectomy (P = <0.01; <0.01; <0.01 for both). There was no statistically significant difference in CBD between PAD and control groups in both without cholecystectomy (P=0.18; 0.85; 0.16) and with (P=0.61; 0.82; 0.56) subcategory. Liver function tests were within normal limits in PAD non-cholecystectomy subcategory. CBD measurements in the non-cholecystectomy category were in concordance with that from previous published studies.

Conclusion: Our study confirms that PAD on its own does not lead to abnormal CBD dilation and has no clinical significance on imaging.

SS 14.03

Feasibility of computed tomography cholangiography using Gd-EOB-DTPA: a phantom study

R. Girometti, L. Cereser, G. Lissandrello, G. Como, M. Bazzocchi, C. Zuiani; Udine/IT

Purpose: To assess the feasibility of computed tomography cholangiography (CTCG) using an hepatobiliary contrast agent for magnetic resonance imaging (Gd-EOB-DTPA).

Material and Methods: We built three CT phantoms including a radiotransparent 2:1 scale representation of the extrahepatic and intrahepatic bile ducts up to the second order branches. By assuming standard contrast pharmacokinetics in an adult male patient of 70 kg, we filled phantoms with water and a volume of 4.05, 3.15 and 2.25 mL of 0.25 mmol/L concentrated Gd-EOB-DTPA, respectively. Volumes corresponded to the expected dose fraction (DF) of Gd-EOB-DTPA in the biliary tree given a i.v. dose to the patient (DP) of 9.0, 7.0 and 5.0 mL, respectively. Phantoms were scanned with a 64-row multidetector CT using a standardized protocol (120 kVp and 200-500 mA). We then performed a quantitative analysis by calculating the signal-to-noise ratio (SNR) of the biliary tree over the phantom background.

Results: On visual analysis, the biliary tree phantoms appeared as hyperattenuating, regardless of contrast DF/DP. On quantitative analysis, the phantom with DF/DP = 3.15/7.0 mL, corresponding to the standard patient dose, showed average SNR (6.51) similar to that of the 2.25/5.0 mL phantom (SNR=6.45), although lower than the DF/DP = 4.05/9.0 mL phantom (SNR=11.56).

Conclusion: In our model, a standard i.v. dose of Gd-EOB-DTPA determines acceptable hyperattenuation of the biliary tree on CT.

SS 14.04

Efficacy of gadoxetic acid-enhanced MRC in the diagnostic work-up of primary sclerosing cholangitis

R. Nolz, U. Asenbaum, A. Wibmer, E. Henrik, C. Kulinna-Cosentini, W.K. Matzek, J. Hodge, A. Ba-Ssalamah; Vienna/AT

Purpose: To evaluate the diagnostic value of gadoxetic acid-enhanced T1w MR cholangiography (T1w MRC) combined with conventional T2w MR cholangiography (T2w MRC), compared to endoscopic retrograde cholangiopancreatography (ERCP) in patients with primary sclerosing cholangitis (PSC).

Material and Methods: In twenty patients with PSC, gadoxetic acid-enhanced T1w MRC and T2w MRC were retrospectively compared to ERCP with regard to morphological features and gradation of central bile duct stenosis. Liver parenchymal impairment was also evaluated by measuring the relative enhancement (RE) of the affected segmental areas in comparison to the adjacent healthy liver parenchyma. Two abdominal radiologists performed all measurements independently.

Results: For direct detection of PSC features in the peripheral bile ducts, T2w MRC demonstrated significantly higher accuracies in both readers, whereas in central bile ducts, study sequences were comparable. Comparing gradation of central bile duct stenoses, T2w MRC showed a significant overestimation ($p < 0.001$) in both readers. Liver parenchymal impairment was detected in eight patients by reader 1, and in nine patients by reader 2 (inter-reader kappa: 0.831).

Conclusion: The combined performance of conventional T2w MRC with gadoxetic acid- enhanced T1w MRC provides a comprehensive diagnosis of PSC, including early morphological features, as well as the gradation of central bile duct stenosis, and can be used as a predictive tool based on liver parenchymal impairment.

SS 14.05

Five-year experience of intraductal photodynamic therapy in hilar cholangiocarcinoma patients

O.N. Sergeeva, V. Panov, A. Kukushkin, E. Virshke, A. Reshetnikov, B. Dolgushin; Moscow/RU

Purpose: Demonstration of early and late intraductal photodynamic therapy (PDT) outcomes in hilar cholangiocarcinoma patients.

Material and Methods: Eighty-eight PDT procedures (from one to ten per patient) have been performed in 27 biopsy confirmed hilar cholangiocarcinoma patients (10 female, 17 male, age range 34-75 years) with previous percutaneous bile duct drainage in N. N. Blokhin Cancer Research Center since February 2008. All patients had Bismuth IV type tumors and were not surgical candidates. The second generation chlorin sensitizers, 0.6-2.0 mg/kg, were administrated intravenously two to four hours prior the procedure with consecutive intraductal laser irradiation (662 nm laser LAHTA-MILON) at low fluence rate pulse mode regimens (20-50 mW/cm^2, up to 1000 J per liver). The follow-up included clinical examination, lab tests and abdomen MRI every three months.

Results: There was no post-procedural mortality. The only patient developed post-procedural liver abscess required percutaneous biliary drainage. The intraductal PDT resulted in bile duct recanalization, cholangitis abatement and improvement of liver function tests. Several MRI findings (post-PDT peritumoral inflammatory infiltration, lymph node reaction, etc.) assumed possible immune system activation. The median survival was 14.9 months (min-max 2-47 months) from the first PDT procedure and 30.2 months (min-max 5-68 months) from the diagnosis. One and two-year survival rates were 71.6% and 25.7% from the first PDT procedure.

Conclusion: The intraductal PDT is safe and an effective strategy in non-surgical hilar cholangiocarcinoma patient management, increasing both survival rate and quality of life.

SS 14.06

Estimation of the malignant potential of gastrointestinal stromal tumors: the value of multislice computed tomography and magnetic resonance imaging

T.V. Bartolotta, A. Tirri, V. Venturella, F. Di Giacomo, A. Taibbi; Palermo/IT

Purpose: To correlate multidetector CT (MDCT) and magnetic resonance imaging (MRI) findings with malignant potential of gastrointestinal stromal tumors (GIST).

Material and Methods: 24 MDCT and 6 MRI studies of 28 patients (15 men and 13 women; mean age 57.9 years; range 30-80 years) with histology-proved GIST were restrospectively evaluated by two experienced radiologists with respect to tumor location, size, grade and enhancing pattern and distant metastasis. MDCT findings were matched with the number of mitosis per high-power fields (50 HPF).

Results: 13/28 GISTs were located in the stomach, 10/28 in the jejunum-ileum, 2/28 in the rectum, 1/28 in the sigmoid colon, 2/28 in the peritoneum; tumor size range was 1.4-21 cm (mean: 7.8 cm). 10/28 GISTs showed a marked contrast-enhancement (c.e.), 16/28 GISTs presented a moderate c.e. and 4/28 GISTs a faint c.e.; 11/28 GISTs showed a markedly inhomogenous c.e., 10/28 GISTs a moderately inhomogenous c.e., whereas 5/28 GISTs homogeneously enhanced; 15/28 patients had distant metastasis: liver (n=12), peritoneum (n=8), lungs (n=2) and spleen (n=1). The number of mitosis per 50 HPF was: <2/50 (n=3), 2-5/50 (n=14), 5-10/50 (n=9), >10/50 (n=2), with a statistically significant correlation with CT and/or MRI grade of contrast-enhancement ($p<0.05$).

Conclusion: In our series, the MDCT and MRI contrast-enhancement grade correlates positively with the malignant potential of GIST as measured by the mitotic count.

SS 14.07

The potential role of F-18 FdG PET-CT in early prediction of malignancy of gastrointestinal stromal tumors, before therapy

E. Biscaldi[1], D. Comandini[1], F. Decian[1], M. Malerba[2], L. Mastracci[1], A. Piccardo[1], G.A. Rollandi[1]; [1]Genoa/IT, [2]Pietra Ligure/IT

Purpose: Gastrointestinal stromal tumors (Gists) tumors may have either c-KIT (exon11) or PDGFRA mutation; a small percentage have none of them. Kit's mutations have a worse prognosis, whereas PDGFRAs have a better one, independent from the therapy. Our purpose is to evaluate if F-18 FdG PET-CT, performed before therapy, as the first diagnosis tool, may reveal what is likely the Gist's genotype.

Material and Methods: We evaluated retrospectively 20 patients (8 women, 12 males, mean age 57). All underwent F-18FdG contrast-enhanced PET-CT, before, after surgery and along the follow-up, between 2008 and 2013. All patients were operated, the molecular analysis showed exon11 mutation (11 cases), Pdgfra mutation (6), and 3 wild type (not considered in statistics). In each case, we evaluated: 1) tumor's maximum diameter, 2) proliferation index, 3) SUV_{max} (standardised uptake value). 11 patients had preoperative $SUV_{max}>3$; 9 had $SUV_{max}<3$. SUV >3 proves that PET registration is pathologic without any clinical doubt. We calculated statistical correlation between: 1) mitotic index and SUV_{max}, 2) SUV_{max} and tumor maximum diameter (Pearson's test), 3) SUV_{max} and genotypic mutation.

Results: The correlation between mitotic index and SUV_{max} was positive (Pearson test 0.26); as between tumor max diameter and SUV_{max} (P=0.72); focusing on prognosis, the stats prove that exon11 mutation correlates to a higher SUV_{max} (4.85±2.26), just as a lower SUV_{max} (1.86 ± 0.63) relates to PDGFRA mutation: as the Test F of Snedecor (F=10.364, $p<0.001$) demonstrates.

Conclusion: The F-18FdG PET-CT, if used preliminary to any therapy, in Gists may help to preview future prognosis, suggesting the genetic pattern.

SS 14.08

Accuracy of MDCT in preoperative definition of peritoneal carcinomatosis of bowel loops in patients with advanced ovarian cancer who underwent peritonectomy and hyperthermic intraperitoneal chemotherapy

S. Guerrini, A. Cirigliano, N. Cioffi Squitieri, G. Bettini, F.G. Mazzei, D. Marrelli, M.A. Mazzei, L. Volterrani; Siena/IT

Purpose: To evaluate the accuracy of MDCT in the preoperative evaluation of peritoneal carcinomatosis (PC) of bowel loops in patients with advanced ovarian cancer who underwent peritonectomy and hyperthermic intraperitoneal chemotherapy (HIPEC) to obtain an optimal cytoreduction surgery.

Material and Methods: Pre-surgery abdominal CT examinations of 24 patients with advanced ovarian cancer after neoadjuvant chemotherapy were blindly and prospectively analysed by a radiologist with expertise in the oncologic field. The peritoneal carcinomatosis index (PCI) was scored according to the Sugarbaker classification, based on lesion size and distribution, with particular attention to the abdomino-pelvic regions refer to small bowel. The results were compared with macroscopic and histologic data after surgery.

Results: Considering the patient-level analysis (the capacity to detect PC), the sensibility, specificity, positive predictive value (PPV), negative predictive value (NPP) and accuracy of MDCT, were 75%, 67%, 69%, 73% and 71%, respectively. Considering the regional level analysis (the capacity to localise PC), a sensitivity, specificity, PPV, NPV and accuracy of 63%, 87%, 55%, 91%, and 82%, respectively were obtained for the correlation between CT and histology.

Conclusion: Our results encourage the use of MDCT as the only technique sufficient to select patients with PC for cytoreductive surgery and HIPEC on the condition that a CT examination will be performed using a dedicated protocol, optimised to detect minimal peritoneal disease and CT images will be analysed by an experienced reader.

SS 14.09

CT-enteroclysis prior to cytoreductive surgery in patients with peritoneal carcinomatosis: the surgical equivalent and the clinical significance of imaging findings in a prospective study of 100 consecutive patients

N. Courcoutsakis[1], A.-A. Tentes[2], E. Astrinakis[1], M. Mantatzis[1], R. Goulimari[3], P. Prassopoulos[1]; [1]Alexandroupolis/GR, [2]Didimotichon/GR, [3]Xanthi/GR

Purpose: To understand the surgical equivalents of abnormalities detected on CT-enteroclysis (CTE) and their clinical impact on cytoreductive surgery in patients with peritoneal carcinomatosis (PC).

Material and Methods: This prospective study enrolled 100 consecutive PC-patients, examined by CTE prior to cytoreductive surgery. The imaging findings on CTE were analyzed, compared and correlated with surgical ones by radiologists and surgeons in consensus.

Results: The "layered"-type of involvement corresponded to myriad cancerous nodules and/or plaques covering the intestinal wall; the stenotic loops with irregular borders to extensive mural infiltration; mural enhancement without stenosis to micronodular superficial infiltration; affixed loops, even distented, to small indolent implants in their curves or angulations; or distensible loops adjacent to an "omental cake" mass to extensively infiltrated intestine requiring partial enterectomy. The stranding appearance of the mesentery on CTE corresponded to superficial nodular infiltration along with thickening and rigidity of the mesentery, requiring local thermocoagulation; the "frozen mesentery" (shortened, distorted, rigid) to extensive malignant infiltration precluding cytoreductive surgery; the thickened, enhanced peritoneal lining to covering malignant plaques requiring extensive peritonectomy.

Conclusion: Lesion-by-lesion correspondence between imaging and surgical findings is important for preoperative assessment of disease burden, for the selection of candidates for cytoreductive surgery and for the development of common terminology and classification systems for use by both radiologists and surgeons.

SS 14.10

Accuracy of MDCT in the preoperative definition of Peritoneal Cancer Index in patients with advanced ovarian cancer who underwent peritonectomy and hyperthermic intraperitoneal chemotherapy: radiological and surgical correlation

C. Cavallini[1], F. Iafrate[1], M. Ciolina[1], D. Bellini[2], A. Laghi[1]; [1]Rome/IT, [2]Latina/IT

Purpose: To evaluate the accuracy of MDCT in the preoperative definition of Peritoneal Cancer Index (PCI) in patients with advanced ovarian cancer who underwent a peritonectomy and hyperthermic intraperitoneal chemotherapy (HIPEC).To compare the radiological PCI with surgical PCI in three readers with different level of experience.

Material and Methods: Pre-HIPEC, CT examinations of 60 patients with advanced ovarian cancer were prospectively analyzed by three radiologists with different levels of experience (Reader1>100 cases, Reader2>25 cases, Reader3 inexperienced). PCI score was evaluated according to Sugarbaker system, based on lesion size and distribution and radiological results were compared with surgical PCI. Sensibility for lesion < 0.5 cm as well as per patient and per anatomic site analysis was evaluated.

Results: Concerning the patient-level analysis, MDCT showed a sensitivity of 75%, 66% and 25%, respectively for the three readers according to surgery. Reader1 and Reader2 overestimated 25% of lesions, Reader3 underestimated 75% of lesions. Concerning lesions < 0.5 cm sensitivity of 66% was observed for Reader1 and Reader2 and sensitivity of 12% was obtserved for Reader3. Reader1 had overestimated 55% of lesion less than 0.5 cm, missing 37%, whilst Reader2 had overestimated 65% of 0.5 cm lesions, missing 25% of the lesions.

Conclusion: Sensitivity of MDCT in detecting peritoneal metastasis appeared to be strongly related to lesion size and location. For more experienced readers overestimation is observed, whilst underestimation is more common in lesser experienced readers.

11:00 - 12:30 **Trakl**

Scientific Session 15

Technical advances and structured reporting

SS 15.01

Performance of pure iterative reconstruction in conventional dose CT imaging

K.P. Murphy[1], L. Crush[1], H. O'Sullivan[1], J. Bye[2], N. Moore[1], O.J. O'Connor[1], F. Shanahan[1], M.M. Maher[1]; [1]Cork/IE, [2]Chalfont St. Giles/UK

Purpose: Pure iterative reconstruction has been utilised to improve diagnostic quality of low-dose CT images. We assess the performance of MBIR (model-based iterative reconstruction) in improving conventional dose CT enterography (CTE) images.

Material and Methods: 43 Crohn's patients (27 female) (38.5±12.98years) referred for CTE were included. Images were reconstructed with MBIR in addition to standard department protocol (60%FBP/40%ASiR, filtered back projection, adaptive statistical iterative reconstruction). Image quality was assessed objectively and subjectively at 6 anatomical levels. Clinical interpretation was undertaken in consensus by 2 blinded radiologists along with 2 non-blinded readers ('gold standard'). Results were analysed using SPSS.

Results: Mean estimated radiation dose was 6.05±2.84 mSv (SSDE 9.25 ± 2.9 mGy). Objective and subjective assessment yielded 6106 datapoints. MBIR images significantly outperformed those using standard reconstruction techniques across all subjective ($p<0.001$ for all comparisons) (noise, contrast resolution, spatial resolution, streak artefact, axial diagnostic acceptability, coronal diagnostic acceptability) and objective ($p<0.004$) (noise, signal-to-noise ratio) parameters. Clinical reads of the MBIR images agreed more closely with the gold standard reads than the standard 40% ASiR image reads in terms of overall Crohn's activity score ($\kappa=0.630, 0.308$) and detection of acute complications ($\kappa=1.0, 0.896$). Results were comparable for bowel wall disease severity assessment ($\kappa=0.523, 0.593$).

Conclusion: MBIR considerably improves image quality of conventional dose CTE images and therefore should be considered for routine use in CT imaging.

SS 15.02

Comparison of different iterative reconstruction algorithms in dedicated CT of the liver and pancreas

A.J. Ruppert-Kohlmayr, M. Fauster, T. Maier, M. Uggowitzer; Leoben/AT

Purpose: To compare diagnostic impact of two different iterative reconstruction algorithms, iDose4® and iMR®, compared with standard-CT of liver and pancreas using filter back projection (FBP). Will iterative reconstruction improve diagnostic impact and which algorithm proves to be better?

Material and Methods: In a prospective clinical study, 30 patients with jaundice or liver lesions were examined with liver or pancreatic CT. The used 256-slice CT-scanner (iCT-Elite®, Philips) enabled routine and simultaneous use of different iterative reconstruction algorithms, iDose4 and iMR. Two experienced staff-radiologists and two residents independently evaluated in a blinded manner CT-exams with two different algorithms with standard slice thickness of 1 mm for lesion conspicuity, lesion margins, and signal-to-noise. Density measurements in lesions were performed and densities and standard deviations were compared.

Results: In 30 patients, 52 liver lesions and 8 pancreatic tumors were found. Lesion conspicuity was significantly better, lesions had sharper margins and density measurements showed significantly lower standard deviations in iMR than in iDose4 and in standard-CT for all 4 radiologists. With iMR reconstruction examination with slice thickness of 1 mm had much less noise than with iDose4 or standard-CT.

Conclusion: Iterative reconstruction of modern CT-scanners are responsible for better image quality with less noise and more accurate density measurements. In comparison to iDose4 the recently available reconstruction algorithm iMR delivers images without significant noise. This might improve exam quality with better lesion detection and conspicuity.

SS 15.03

Role of model-based iterative reconstruction in CT enterography

K.P. Murphy[1], L. Crush[1], P.D. Mclaughlin[1], C. Page[1], I. Mildenberger[1], O.J. O'Connor[1], J. Bye[2], N. Moore[1], S. Mcsweeney[1], F. Shanahan[1], M.M. Maher[1]; [1]Cork/IE, [2]Chalfont St. Giles/UK

Purpose: We analyse the performance of pure model-based iterative reconstruction (MBIR) in the setting of low-dose CT enterography (CTE).
Material and Methods: 44 Crohn's patients (27 female) (38.5±12.98 years) referred for CTE were included. Low-dose modified-protocol (MP) and conventional-protocol (CP) CT datasets were contemporaneously acquired. CP-ASiR image formation used 40% adaptive statistical iterative reconstruction. MP data were reconstructed with 100% MBIR (MP-MBIR) and 40% ASiR (MP-ASiR). Image quality was assessed objectively and subjectively at 6 levels. Clinical interpretation was undertaken independently by 2 blinded radiologists along with 2 non-blinded readers in consensus ('gold-standard').
Results: A 75% average radiation dose reduction was seen: MP effective-dose (ED) 1.61±1.18mSv (size-specific-dose-estimate (SSDE) 2.47±1.21mGy); CP ED 6.05±2.84mSv (SSDE 9.25±2.9mGy). Image-quality assessment yielded 9372 datapoints. Objective noise in MP-MBIR images was superior ($p<0.05$) at 3/6 levels and comparable in the remainder. MP images were superior to CP-ASiR ($p<0.05$ in all cases) for subjective noise, spatial resolution, contrast resolution, streak artefact and coronal diagnostic acceptability. CP-ASiR axial diagnostic acceptability was superior ($p=0.76$). MP-MBIR clinical reads agreed more closely with gold-standard reads than CP-ASiR reads regarding bowel wall disease assessment ($\kappa=0.589/0.700$ vs 0.583/0.564) for both readers whereas overall Crohn's activity score ($\kappa=0.549/0.441$ vs 0.315/0.596) and detection of acute complications ($\kappa=1.0/0.689$ vs 0.896/0.896) were comparable.
Conclusion: Low-dose CTE with MBIR yields images that are superior or comparable to conventional images.

SS 15.04

CT enterography: a comparison of image quality and dose reduction between routine-standard radiation dose with filtered back projection and low-dose with iterative reconstruction in a 128-channel MDCT

L. Costa-Silva, M.D.C. Silveira; Belo Horizonte/BR

Purpose: To evaluate image quality and radiation dose (RD) of CT enterography (CTE) with iterative reconstruction (IR)-SAFARE, in comparison with standard dose with Filtered Back Projection (FBP) in the evaluation of small bowel.
Material and Methods: 202 patients (mean age, 43.3 years) underwent CTE between March and December 2013 were included in the study. 101 patients were scanned with standard-dose protocol (group 2) and 101 with low-dose protocol with IR (group 1). MDCT includes a weight-based i.v. contrast protocol and mAs Modulation dose (Care Dose) for all patients. Group 1 used the following parameters: 120 kVp, mAs reference: 210, 2-mm thickness, 128×0.6 mm detector configuration. Group 2 used 100 kVp, mAs: 140, 0,6-mm thickness, 128×0.6 mm detector configuration. One blinded reader reviewed the randomized CTE scans of all patients to assess image quality.
Results: In group 1, average RD parameters were: kVp: 120.39; effective mAs at enteric phase: 187.58; CTDIvol: 12.70 mGy and DLP: 594.60 mGy/cm. The mean effective dose considering the enteric phase: 8.91 mSv (range: 1.79-26.67mSv). In group 2, the following average parameters were: kVp: 104.60; effective mAs: 144.92, CTDIvol: 6.86 mGy and DLP: 334.45 mGy/cm. The mean effective dose was 5.01mSv (range: 2.19-13.85mSv). Group 2 had optimal image quality and were rated comparable to or better than Group 1 images (mean score, 4.62vs4.33; $p=0.909$).
Conclusion: Low-dose CTE studies with IR were of appropriate quality for confident evaluation of the small bowel while allowing approximately 44% DR in comparison with FBP technique.

SS 15.05

Accurate tissue characterisation with low-dose CT imaging with hybrid and pure iterative reconstruction

K.P. Murphy, P.D. Mclaughlin, V. Chan, O.J. O'Connor, M.M. Maher; Cork/IE

Purpose: Low-dose CT protocols that employ pure iterative reconstructive techniques such as model-based iterative reconstruction (MBIR) have recently been developed. We assess the ability of low-dose images to maintain accurate tissue and lesion characterisation.
Material and Methods: Standard protocol (SP) and low-dose modified protocol (MP) CTs were contemporaneously acquired in 34 Crohn's disease patients referred for CT. The SP images were reconstructed using manufacturer recommendations (60% FBP, filtered back projection; 40% ASiR, Adaptive Statistical iterative Reconstruction, SP-ASiR40). The MP datasets were reconstructed in 4 ways (100% FBP; 40% ASiR; 70% ASiR; 100% MBIR). 3 observers measured tissue volumes using Hounsfield unit thresholds for fat, soft tissue and bone and contrast via Osirix (Ver 4.1.1) on each dataset. Data analysis was performed with SPSS.
Results: Inter-observer agreement for tissue volume measurement was very strong for the 1530 datapoints ($rs>0.9$ for all comparisons). Tissue volume measurement on the MP-MBIR images was significantly superior to all other MP reconstructions and closely correlated with the 'gold standard' SP-ASiR40 images for all tissue types. The superiority of MP-MBIR was most marked in fat volume calculation where Bland-Altman plots showed closest correlation between SP-ASIR40 and MP-MBIR with the lowest average difference (336 cm^3) when compared with other MP reconstructions.
Conclusion: Low-dose CT images reconstructed with MBIR maintain accurate tissue and hence lesion characterisation is superior to other reconstruction techniques when compared with conventional dose images.

SS 15.06

Multi-arterial phase for achieving optimal arterial phase imaging on Gd-EOB-DTPA enhanced magnetic resonance imaging

J.H. Yoon, J.M. Lee, J.H. Baek, E.J. Kim, J.K. Han, B.I. Choi; Seoul/KR

Purpose: To determine whether multi-arterial phase imaging can improve arterial phase (AP) image quality on Gd-EOB-DTPA enhanced-magnetic resonance imaging (MRI).
Material and Methods: Total 169 consecutive patients underwent Gd-EOB-DTPA liver MRI at 3.0T scanner. In liver MRI, AP was obtained using four-dimensional (4D) contrast-enhanced timing robust acquisition order (CENTRA)-keyhole technique. Gd-EOB-DTPA was injected at a rate of 1.5 mL/sec followed by 20 mL saline chaser, using a real-time MR fluoroscopy technique. Three phases of AP (early, middle and late) were obtained in a breath-hold (<25 sec). Two radiologists assessed appropriateness of AP bolus timing and image quality.
Results: At least one optimal AP was achieved in 95.9% (162/169). Twelve of 169 patients did not hold their breaths (n=11) or vomited (n=1) during AP. In 9 of 12 patients, at least one AP with optimal bolus timing and diagnostic acceptable quality was obtained among the three phases: one optimal AP (n=6); two optimal AP (n=1); and three optimal AP (n=2). The remaining three patients showed unacceptable APs due to severe motion artifact (n=2) or too delayed AP timing (n=1). In remaining 158 patients, two patients (1.2%) showed diagnostically unacceptable image quality due to severe ringing artifacts. In six patients (3.8%), all of three APs were either too late (n=3) or too early (n=3).
Conclusion: Multi-arterial phase acquisition using 4D-CENTRA-keyhole technique could improve AP bolus timing and provided diagnostic acceptable AP images.

SS 15.07

Innovative fast scan techniques for abdominal MR imaging in paediatric patients: evaluating image quality

H. Neubauer, T. Pabst, T. Bley; Wuerzburg/DE

Purpose: Scan time and image quality are the key factors in paediatric abdominal MR imaging. We assessed image quality of ultra-fast contrast-enhanced T1w imaging with CAIPIRINHA and high-resolution fat-saturated T2 HASTE, compared to standard sequences.
Material and Methods: Fifty consecutive patients (age 10+/-6 years) underwent routine abdominal MRI (1.5 T, Magnetom AERA, Siemens) with contrast-enhanced T1w 3D-FLASH FS (CAIPIRINHA, slice thickness 3-5 mm, one 14s-breathhold for 72 slices). Standard of comparison were T1w 2D-/3D-FLASH FS (6-8 20s-breathholds, scan time 4 min) in non-sedated and navigator-triggered T1w TSE FS (scan time 8 min) in sedated young patients. Twenty patients had both coronal T2w TIRM (scan time 3 min) and high-res T2w HASTE FS (scan time 40s). Image quality was retrospectively assessed on a 5-level Likert scale ranging from 1 (excellent, no artefacts) to 5 (insufficient for diagnosis).
Results: The proportion of excellent to satisfying image quality (level 1-3) of CAIPIRINHA and HASTE imaging did not differ from standard technique (all $p>0.05$). Upper abdominal organs showed fewer artefacts with T2 HASTE FS, compared to T2 TIRM. Navigator-triggered scans resulted in a higher proportion of excellent and good image quality, compared to CAIPRINHA, in sedated patients ($p<0.05$), while the proportion of excellent to satisfying image quality was comparable ($p>0.05$).
Conclusion: Ultra-fast scanning with CAIPIRINHA and HASTE presents a fast and reliable alternative to standard sequences in paediatric abdominal MRI.

SS 15.08

withdrawn by the authors

SS 15.09

Structured reporting based on evidence-based medicine methodology: magnetic resonance enterography in patients with Crohn's disease

D.J. Murphy, D. Gibson, S.H. Mcevoy, A.E. Smyth, G.A. Doherty, D.E. Malone; Dublin/IE

Purpose: Magnetic resonance enterography (MRE) has an expanding role in triaging small bowel Crohn's disease (SBCD) patients to medical or surgical therapy. We evaluated the MRE signs that best classify SBCD and created a structured MRE report.

Material and Methods: A literature search was performed using the PIO format and relevant MESH terms. The abstracts were reviewed and publications meeting inclusion criteria were chosen and assigned an Oxford Centre for EBM 'Level of Evidence'. The validity and strength of the best evidence was assessed and raw data extracted for calculation of test properties. The MRE signs that best classify SBCD into acute inflammatory versus fibrostenosing/perforating subtypes requiring surgery were identified.

Results: 9 of 36 retrieved abstracts were relevant. Statistics are reported as (sensitivity {95% CI}, specificity {95% CI}, positive and negative likelihood ratios). Level 3 evidence showed MRE reliably identifies fibrostenosing (0.92 [1-0.81],0.9 [1-0.80], 9.2, 0.09) and perforating SBCD (0.81 [1-0.62], 0.96 [1-0.91], 20, 0.2). For acute inflammatory SBCD, level 2 evidence identified 3 useful, weaker signs: bowel wall thickening >4 mm (0.87 [0.98-.75}, 0.42 [0.76-.08], 1.5, 0.4), mural T2 hyperintensity (0.84 [0.96-.7], 0.67 [0.96-.37], 2.5, 0.3) and layered mural post-contrast enhancement (test properties could not be calculated). These results were then incorporated into a structured MRE report, which will be presented.

Conclusion: The MRE signs that most usefully classify SBCD can be used to create a structured report.

SS 15.10

Structured reporting of hepatic CT and MRI: initial experience

L. Van Hoe[1], B. Pilet[1], V. De Grove[1], S. T'Seyen[1], P. Dewachter[1], L. Hermie[1], L. Braeye[2], A. Vanhoyweghen[1], A.-S. Vanhoenacker[3]; [1]Aalst/BE, [2]Halle/BE, [3]Leuven/BE

Purpose: To assess the results obtained with a software system designed for structured reporting of hepatic CT and MRI.

Material and Methods: An electronic platform for structured reporting in radiology was designed and applied to the evaluation of liver disease using CT and/or MRI. The system contained both a structured approach towards the evaluation of liver lesions and specific information guiding the user towards a correct diagnosis in individual patient cases. Ten observers (five radiologists and five radiology residents) used the platform for reporting in 10 randomly assigned cases. Diagnostic accuracy and reporting times were measured. Subjective assessment of user friendliness and report quality (evaluation by reporting and referring physicians) was obtained using a five-point scoring system.

Results: Diagnostic accuracy was 92%, without significant difference between both groups of observers. Average reporting time was 3.5 min. Average score for user friendliness was 4.4. Referring physicians liked the structured reports (average score 4.6).

Conclusion: The system tested in this study showed promising results for structured reporting of hepatic CT and MRI.

SS 15.11

Development of templates in gastrointestinal and abdominal imaging in the framework of the RSNA/ESR structured reporting initiative

P. Scalise, E. Guidi, A. Mantarro, D.L. Lauretti, F. Pancrazi, E. Neri, C. Bartolozzi; Pisa/IT

Purpose: The RSNA/ESR structured reporting initiative was launched at ECR2013 to promote clinical use and development of the reporting templates available online at RSNA website. National radiological and ECR subspecialties societies were involved to implement new templates by modifying and translating the existing ones, considering differences in language, reporting content and format.

Material and Methods: Our Radiology Department started elaborating new templates in the field of gastrointestinal and abdominal imaging. Three working groups (liver and biliary tract, pancreas and GI tract) modified RSNA templates content and structure accordingly to local practice. Templates composition was realized during internal meetings through a consensus process (first by the working groups, then by the entire panel in plenary session). Staff radiologists rated independently each template on a 5-point Likert scale. All ratings for each template were analysed with descriptive statistics. A mean score >4 indicated good agreement between staff radiologists, while 5 indicated complete agreement.

Results: 16 structured reports were elaborated in the following applications: cirrhotic liver CT/MR, MR-cholangiopancreatography, CT/MR enterography, MR in rectal tumors and fistulas, CT in acute/chronic pancreatitis and pancreatic cancer, defecography, US in TIPS placement. The mean level of agreement between the staff radiologists was 4.2.

Conclusion: We achieved to compose a first group of templates usable in the clinical practice. Further new structured reports will be produced and uploaded on the RSNA website making them available to the radiological community.


European Society
ESGAR
Gastrointestinal and Abdominal Radiology

M

N

O

P

European Society
ESGAR
Gastrointestinal and Abdominal Radiology

ESGAR 2015

JUNE 9-12

PARIS
FRANCE

European Society of Gastrointestinal and Abdominal Radiology

www.esgar.org